# Controls and impact of Agulhas leakage

Dissertation
in fulfilment of the requirements for the degree “Dr. rer. nat.”
of the Faculty of Mathematics and Natural Sciences
at Kiel University

submitted by

Jonathan V. Durgadoo

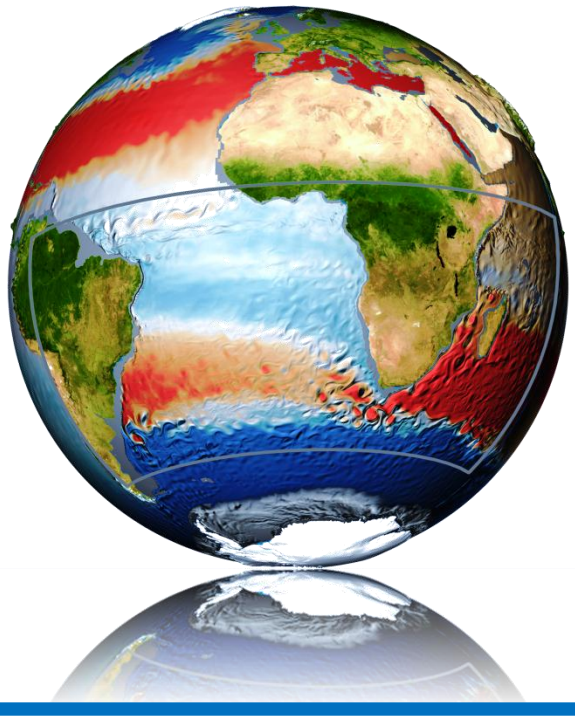

Kiel, 2013

| | | |
|---|---|---|
| First referee | : | Prof. Dr. Arne Biastoch |
| Second referee | : | Prof. Dr. Martin Visbeck |
| Date of the oral examination | : | 23 Sep. 2013 |
| Approved for publication | : | 23 Sep. 2013 |

| | | |
|---|---|---|
| Signed | : | Prof. Dr. W.J. Duschl, Dean |

# Declaration

Hiermit erkläre ich, dass ich die vorliegende Dissertation, abgesehen von der Beratung durch meine akademischen Lehrer, selbstständig verfasst habe und keine weiteren Quellen und Hilfsmittel als die hier angegebenen verwendet habe. Diese Arbeit hat weder ganz, noch in Teilen, bereits an anderer Stelle einer Prüfungskommission zur Erlangung des Doktorgrades vorgelegen. Ich erkläre, dass die vorliegende Arbeit gemäß der Grundsätze zur Sicherung guter wissenschaftlicher Praxis der Deutschen Forschungsgemeinschaft erstellt wurde.

Kiel, September 2013.

Jonathan V. Durgadoo.

# Publications

The following publications resulted from the work presented in this thesis. They are classified below according to the chapters they adhere to the most.

## Chapter 2

Durgadoo J.V., A. Biastoch (2013) – The Agulhas System as a Key Region of the Global Oceanic Circulation, in W. E. Nagel et al. (Eds.), High Performance Computing in Science and Engineering '12, Springer, 407–414, doi:10.1007/978-3-642-33374-3_30

Cronin M.F., T. Tozuka, A. Biastoch, J.V. Durgadoo, L.M. Beal (2013) – Prevalence of Strong bottom currents in the Greater Agulhas System. *Geophysical Research Letters*, 40, 1772–1776, doi:10.1002/grl. 50400.

## Chapter 3

Loveday B.R., J.V. Durgadoo, C.J.C. Reason, A. Biastoch, P. Penven (2013) – Decoupling of the Agulhas leakage from the Agulhas Current. *Journal of Physical Oceanography*, under review.

## Chapter 4

Durgadoo J.V, B.R. Loveday, C.J.C. Reason, P. Penven, A. Biastoch (2013) – Agulhas Leakage predominantly responds to the Southern Hemisphere westerlies. *Journal of Physical Oceanography*, in press, doi:10.1175/JPO-D-13-047.1

## Chapter 5

Rühs S., J.V. Durgadoo, E. Behrens, A. Biastoch (2013) – Advective timescales and pathways of Agulhas Leakage. *Geophysical Research Letters*, 40, 3997–4000, doi:10.1002/grl.50782

Scussolini P., E. van Sebille, J.V. Durgadoo (2013) – Paleo Agulhas Rings enter the subtropical gyre during the penultimate deglaciation. *Climate of the Past*, under review.

## Chapter 6

Le Bars D., J.V. Durgadoo, W.P.M. de Ruijter, H.A. Dijkstra, A. Biastoch – Agulhas leakage estimated from sea surface height, in prep.

(Status: 23 Sep. 2013)

# Abstract

Agulhas leakage is a collective term that refers to water exported by the Agulhas Current system into the South Atlantic Ocean. It is postulated that the injection of this warm and salty water into the South Atlantic has the ability to alter the overall Atlantic circulation on decadal to millennial timescales. The Agulhas Current system sits at the nexus between the Indian, South Atlantic and Southern Oceans. The system also lies in a zone of transition between the easterly trade winds and the Southern Hemisphere westerlies. This dissertation investigates how the Southern Hemisphere winds control the magnitude of Agulhas leakage and assesses the impact of a leakage increase on the South Atlantic.

The analysis was performed within two global (ORCA05 & INALT01) and two regional (AGIO & ARC) model configurations. These configurations were constructed to represent adequately both the large-scale circulation and the intricacies of the mesoscale dynamics of the Agulhas Current system. A series of sensitivity experiments were designed and performed within the four configurations with the aim to disentangle systematically the influence of the winds on Agulhas leakage. In the first series of simulations, the intensity of Indian Ocean trade winds was modified. The second set of experiments imposed changes to position and intensity of the westerlies. The magnitude of the changes applied was representative of past, present and future climate scenarios. Through the multi-model approach and the identical definition of Agulhas leakage within all configurations, robust results were achieved.

The easterly trade winds substantially affect the horizontal circulation of the Indian Ocean, including the strength of the Agulhas Current. Changes to the current are communicated downstream to latitudes where wind changes were not applied. Therefore, the inertia of the current at separation is altered. Despite large changes in mesoscale variability of the retroflection, its position is maintained by topography. Consequently, Agulhas leakage is unaffected. This implies that Agulhas leakage is decoupled from upstream dynamics. Instead, leakage is controlled by the Southern Hemisphere westerlies, in particular their intensity. Changes in wind stress curl over the southern portion of the Indian Ocean subtropical gyre yield a westward transport south of Africa. This is manifested as changes in leakage, which responds proportionally to the intensity of the westerlies up to a certain point. Beyond this, through the adjustment of the large-scale circulation, energetic interactions occur between the Agulhas Return Current and the Antarctic Circumpolar Current that result in a state where leakage no longer increases. This adjustment takes place within one or two decades. Results further show that an equatorward (poleward) displacement of the westerlies increases (decreases) leakage. This occurs because of the redistribution of momentum input by the winds. In the South Atlantic, the advection of Agulhas leakage follows the mean horizontal circulation. Along the South American coast, a bifurcation occurs and two pathways emanate: via the North Brazil Current across the Equator, and a re-circulatory route via the Brazil Current. A simulated wind-driven increase in Agulhas leakage in the South Atlantic results in a favoured re-circulatory route, since the subtropical gyre of the South Atlantic is enhanced.

# Zusammenfassung

Agulhas Leakage ist ein Sammelbegriff, der sich auf die Wassermassen bezieht, die durch das Agulhasstromsystem in den Südatlantik transportiert werden. Bisherige Arbeiten postulieren, dass der Eintrag dieses warmen und salzigen Wassers in den Südatlantik die Fähigkeit besitzt, die gesamte Zirkulation des Atlantiks auf dekadischen und tausendjährigen Zeitskalen zu verändern. Das Agulhasstromsystem sitzt am Nexus zwischen dem Indischen, dem Südatlantischen und dem Südpolarmeer. Das System liegt außerdem in der Übergangszone zwischen den östlichen Passatwinden und den Westwinden der südlichen Hemisphäre. Diese Dissertation untersucht, wie die Winde der Südlichen Hemisphäre die Intensität der Agulhas Leakage kontrollieren und beurteilt die Auswirkungen einer Zunahme der Agulhas Leakage auf den Südatlantik.

Die Analyse wurde anhand von zwei globalen (ORCA05 & INALT01) und zwei regionalen (AGIO & ARC) Modellkonfigurationen durchgeführt. Diese Konfigurationen wurden entwickelt, um sowohl die großskalige Zirkulation als auch die Feinheiten der mesoskaligen Dynamik des Agulhasstromsystem adäquat zu repräsentieren. Innerhalb der vier Konfigurationen wurde eine Reihe von Sensitivitätsexperimenten entworfen und durchgeführt, um den Einfluss der Winde auf die Agulhas Leakage systematisch zu untersuchen. In der ersten Serie von Simulationen wurde die Intensität der Passatwinde des Indischen Ozeans modifiziert. In der zweiten Serie wurden Änderungen der Position und Intensität der Westwinde vorgenommen. Die Größe der angewandten Veränderungen spiegelte dabei die vergangenen, gegenwärtigen, und zukünftigen Klimaverhältnisse wieder. Durch den Multi-Modellansatz und identische Definition der Agulhas Leakage in allen Konfigurationen, wurden robuste und vergleichbare Ergebnisse gewährleitet.

Die östlichen Passatwinde beeinflussen die horizontale Zirkulation des Indischen Ozeans substantiell, einschließlich der Stärke des Agulhasstroms. Änderungen der Strömung werden stromabwärts, in Breiten, in denen keine Windänderungen angewendet wurden, propagiert. Dies beeinflußt die Trägheit an der Ablösungsstelle des Agulhasstromes vom Kontinentalsockel. Hingegen der großen Veränderungen in der mesoskaligen Variabilität der Retroflektion, bleibt die Position des Stromes aufgrund der Topographie unverändert. Entsprechend bleibt die Agulhas Leakage unbeeinflusst. Dies bedeutet, dass die Agulhas Leakage von der stromaufwärtigen Dynamik entkoppelt ist. Stattdessen kontrollieren die Westwinde der südlichen Hemisphäre, insbesondere deren Intensität, die Agulhas Leakage. Positive Änderungen der Rotation des Windschubs über dem südlichen Teil des subtropischen Wirbels des Indischen Ozeans verursachen einen Transport nach Westen, südlich von Afrika. Dies erklärt die Änderungen in der Agulhas Leakage, die bis zu einem bestimmten Punkt proportional zu der Intensität der Westwinde ist. Darüber hinaus kommt es durch die Adaption der großskaligen Zirkulation zu energetischen Wechselwirkungen zwischen dem Agulhasrückstrom und dem antarktischen Zirkumpolarstrom und führt zu einem Zustand, in dem die Agulhas Leakage nicht weiter zunimmt. Diese Adaption erfolgt innerhalb von ein bis zwei Dekaden. Die Ergebnisse zeigen außerdem, dass eine Verlagerung der Westwinde äquatorwärts (polwärts) zu einer Zunahme (Abnahme) der Agulhas Leakage führt. Dies geschieht aufgrund der Neuverteilung des Impulseintrages durch die Winde. Die Advektion der Agulhas Leakage folgt der mittleren horizontalen Zirkulation im Südatlantik. Entlang der südamerikanischen Küste kommt es zu einer Aufspaltung in zwei Pfade: durch den Nordbrasilstrom über den Äquator hinweg und eine Rückströmung durch den Brasilstrom. Durch einen simulierter wind-getriebener Anstieg der Agulhas Leakage in den südlichen Atlantik, kommt es zu einer verstärkten Rückströmungsroute, da der Südatlantische subtropische Wirbel verstärkt wird.

GEOMAR Helmholtz Centre for Ocean Research Kiel

# Controls and impact of Agulhas leakage

Kontrollmechanismen und Auswirkungen der Agulhas Leakage

**Jonathan V. Durgadoo**

Agulhas leakage is a collective term that refers to the warm salty waters entering the South Atlantic from the Indian Ocean, south of the African continent, through the Agulhas Current system.

# Content

# 1. Introduction

Upper ocean transport at all latitudes of the Atlantic Ocean is generally northward. This flow in the upper 1500 m constitutes waters originating from the Southern Ocean as well as from the Indian-Pacific Oceans (Figure 1.1). These two sources are referred to respectively as the Atlantic cold- and warm-water routes (Speich et al. 2001). Ultimately, waters from both routes penetrate the subpolar North Atlantic and the Nordic Seas, where deep convection occurs (Marshall and Schott 1999). While the cold route can be regarded as the direct inflow of water from Drake Passage (Friocourt et al. 2005), the warm route is more complex (Figure 1.1). This warm pathway, south of the African continent, consists of water masses from very different origins: from the Pacific in the form of the Indonesian through-flow (Sprintall et al. 2009) and the Tasman leakage (Speich et al. 2002); from the Southern Ocean as the indirect flow from Drake Passage (Friocourt et al. 2005; Speich et al. 2001); and recirculation within the Indian-Atlantic portion of the supergyre (Ridgway and Dunn 2007; Speich et al. 2007). South of Africa, the Agulhas Current system (Lutjeharms 2006; Beal et al. 2011) is at the centre of this complex warm-water conduit (Figure 1.2). It negotiates the bulk of the exchange between the Indian and Atlantic Oceans (Gordon 1986; Gordon et al. 1992).

Much of the warm-water exchange occurs in the Cape Basin (Figure 1.3). Thermocline and intermediate waters of various origins interact vigorously (Donners et al. 2004; Rimaud et al. 2012; Roman and Lutjeharms 2007, 2010; Stramma and England 1999). Roman and Lutjeharms (2010), Rimaud et al. (2012) and Rusciano et al. (2012) diagnosed two variants of Antarctic Intermediate Water in the Cape Basin: one of Indian Ocean origin and one of Atlantic origin. The latter constitutes the indirect flow from Drake Passage (Friocourt et al. 2005; Speich et al. 2001). This thesis focussed and examined the portion of the Indian-Atlantic warm-water exchange that is mediated by the Agulhas Current. This is referred to as Agulhas leakage.

## 1.1. What is Agulhas leakage?

Agulhas leakage refers to waters exported into the Atlantic Ocean by the Agulhas Current system. These waters primarily consist of upper and intermediate waters of Indian Ocean origin (de Ruijter et al. 1999). Here, the terms Indo-Atlantic flux/transport/transfer/exchange are employed as synonyms for Agulhas leakage. Furthermore, Agulhas leakage is a collective term used to encapsulate the different oceanic features that enable the westward water transfer between the two oceans

(illustrated by the extension of warm water across the South Atlantic in Figure 1.2). These features carry water of Agulhas Current origin.

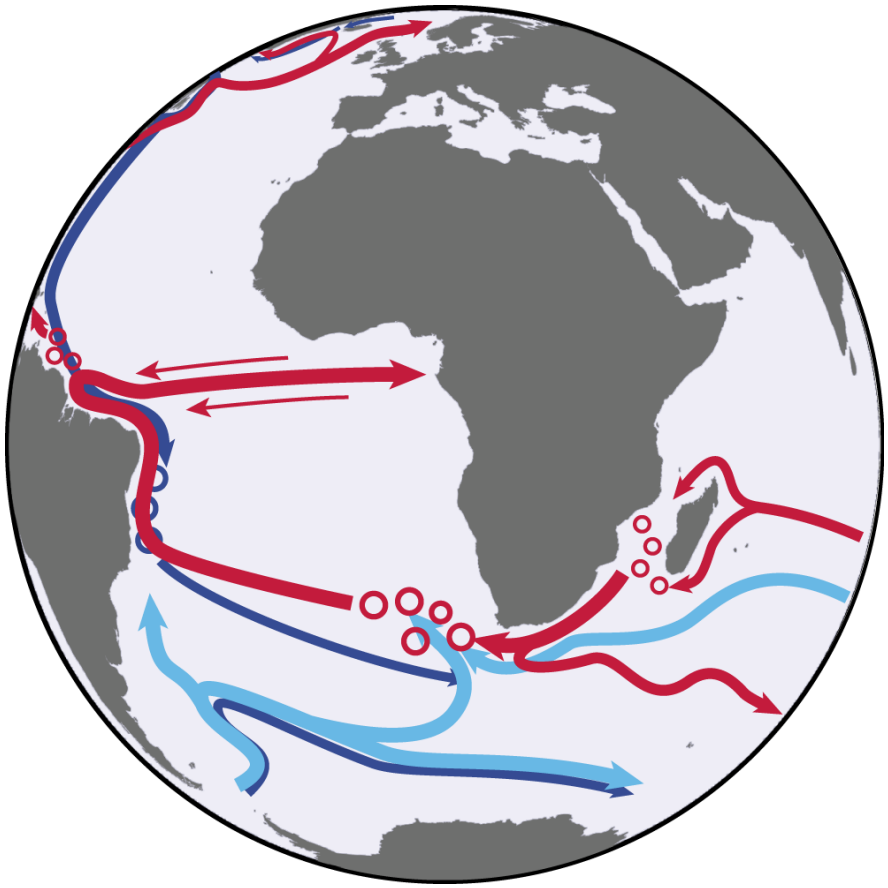

**FIGURE 1.1:** Schematic of the ocean circulation south of Africa. Colours indicate surface (0 – 1000 m, red), intermediate (1000 – 1500 m, light blue) and deep (1500 – 4000 m, dark blue) pathways. In the South Atlantic, two northward flowing routes exist: the cold-water route which is the direct inflow from Drake Passage, and the warm-water route south west of South Africa.

The Agulhas Current (Figure 1.4) flows along the southeastern coast of South Africa. At the southern tip of the continent, about 70 to 75 % of the current retroflects back into the Indian Ocean, forming the Agulhas Return Current. The remaining portion enters the Cape Basin in the form of large anti-cyclonic Agulhas Rings (Gordon 1986; Goni et al. 1997; Lutjeharms and Gordon 1987; Duncombe Rae et al. 1996; Duncombe Rae 1991; Tréguier et al. 2003), cyclones (Boebel et al. 2003a; Hall and Lutjeharms 2011; Matano and Beier 2003), and other filaments and plumes (Lutjeharms and Cooper 1996; Stramma and Peterson 1990; Tréguier et al. 2003).

Attempts to estimate Agulhas leakage from observed datasets have focussed mainly on either the quantification of water being transported by the above-mentioned features or on geostrophic transports across hydrographic sections occupied in the Cape Basin (de Ruijter et al. 1999). Agulhas

Rings are typically 150 – 250 km in diameter (Boebel et al. 2003a; Dencausse et al. 2010a) and extend down to the sea-floor (van Aken et al. 2003). These large rings drift into the South Atlantic with a velocity of about 3 – 4 km/day and have a lifespan of less than a year (Dencausse et al. 2010a; Donners and Drijfhout 2004; Schonten et al. 2000). Transport estimates obtained per Agulhas Ring range between 0.4 and 3 Sv[1] (Byrne et al. 1995; Garzoli et al. 1999; Gordon and Haxby 1990; McCartney and Woodgate-Jones 1991; Olson and Evans 1986). Assuming that approximately 4 – 6 rings are formed per year (Byrne et al. 1995; Feron et al. 1992; Goni et al. 1997; Schonten et al. 2000), this would give an average of ~8.5 Sv per annum of leakage solely through rings (Dencausse et al. 2010a; Garzoli et al. 1999; Richardson 2007). More recently, using altimetry data to locate and track rings in combination with subsurface floats to resolve their vertical structure, Souza et al. (2011) estimated 9 ± 8 Sv of Indo-Atlantic transfer through rings. The large standard deviation reflects the inter-annual variation in ring shedding events. Eulerian-based estimations of leakage could potentially capture the host of features found in the Cape Basin. However, the challenge lies in the need to define adequate boundaries for integration (van Sebille et al. 2010a), in addition to the fact that these estimates only represent temporal snapshots. Estimates of the Indo-Atlantic flux using such methods yielded between 2.8 and 10 Sv (de Ruijter et al. 1999). The most recent observed measurement of Agulhas leakage, employing a decade of modern surface drifters and subsurface floats, gives approximately 15 Sv in the upper 1000 m (Richardson 2007). This value is the most widely accepted measurement of Agulhas leakage to-date. In order to address the lack of sustained observation of leakage, the deployment of a series of moorings between Cape Town and Tristan da Cunha is planned in 2013[2] (Ansorge, pers. comm.). This promises new estimates of Agulhas leakage as well as insights into its variability (Garzoli and Matano 2011).

Given the temporal scarcity and poor spatial coverage of observed datasets, several attempts of estimating Agulhas leakage have also been made within numerical models. Here, despite the availability of consistent and contiguous datasets, difficulties (*i.e*. source of disagreement in leakage estimates) lie in the correct representation of the Agulhas dynamics within models (*e.g.* mesoscale variability). This is in addition to the lack of a proper method of assessing Agulhas leakage. At low horizontal resolution (greater than the first baroclinic Rossby radius), the Agulhas Current is typically represented as a laminar current without variability. Such models tend to overestimate the Indo-Atlantic flux (Biastoch et al. 2008c; Weijer et al. 2012). At high resolution (where the first baroclinic Rossby radius is resolved), with exception of the results presented by Speich et al. (2006), models converge towards the Richardson (2007) estimate, yielding between 10 and 20 Sv of leakage

[1] 1 Sv = $10^6$ $m^3$ $s^{-1}$

[2] http://www.coriolis.eu.org/Science/Research-Activities2/Atlantic-Ocean/GOODHOPE-SAMOC

(Biastoch et al. 2008c; Doglioli et al. 2006; van Sebille et al. 2009b,c). These model studies assessed leakage in a Lagrangian framework. It should be noted that within models, horizontal resolution is not the only determining factor; parameterisation of unrepresented processes, choices in advection schemes and lateral boundary conditions among others also play important roles (Backeberg et al. 2012; Barnier et al. 2006; Quartly et al. 2013).

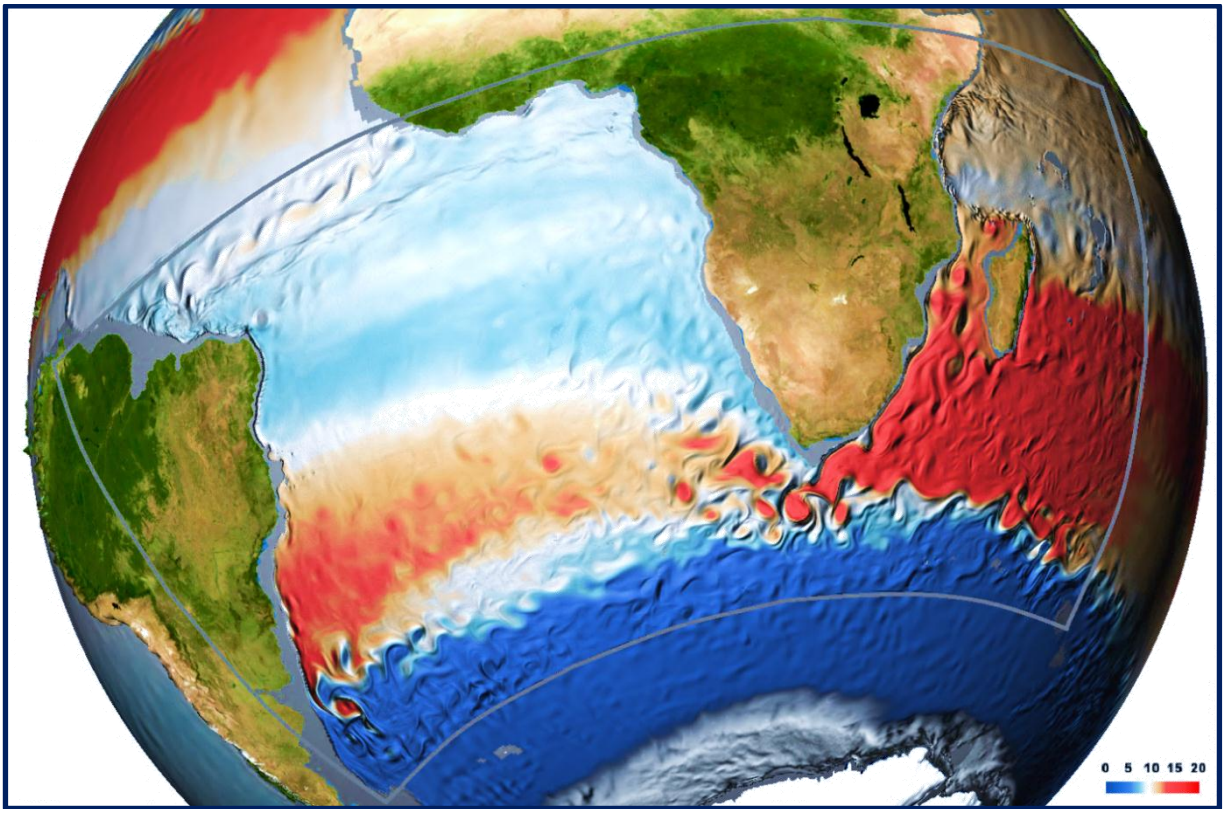


**FIGURE 1.2:** The greater Agulhas Current system. Snapshot from the INALT01 model configuration (described in chapter 2) illustrating the warm-water route south of the African continent. Colours indicate temperature (°C) at 450 m depth. A global version of this illustration is shown on the cover page.

Of current importance, hind-cast ocean simulations suggest that since the late 1960s, the magnitude of water exported from the Indian Ocean to the Atlantic Ocean is on the rise (Biastoch et al. 2009b; Rouault et al. 2009). Naturally, given this reported contemporary increase in leakage, the pertinent question that follows concerns the overall implication of the increase on the Atlantic circulation.

## 1.2. What is the importance of Agulhas leakage?

The impact of Agulhas leakage on the Atlantic circulation is binary: through radiation of planetary waves and through advection. Leakage waters entering the Cape Basin, being warmer and saltier

than the surroundings, depress the isotherms and isohalines in the thermocline (Giulivi and Gordon 2006). The resulting undulations in isopycnals radiate dynamic disturbances that slowly propagate across the South Atlantic as Rossby waves (Biastoch et al. 2008b; van Sebille and van Leeuwen 2007). These waves, carrier of the dynamical imprint of Agulhas leakage, reach the South American coast within 4 – 6 years and are subsequently rapidly communicated across the Equator by coastal Kelvin waves (Biastoch et al. 2008b; Weijer et al. 2002). As such, leakage impacts the zonally-integrated flow of the Atlantic, that is, the so-called Atlantic Meridional Overturning Circulation (AMOC, Cunningham and Marsh 2010), within a decade.

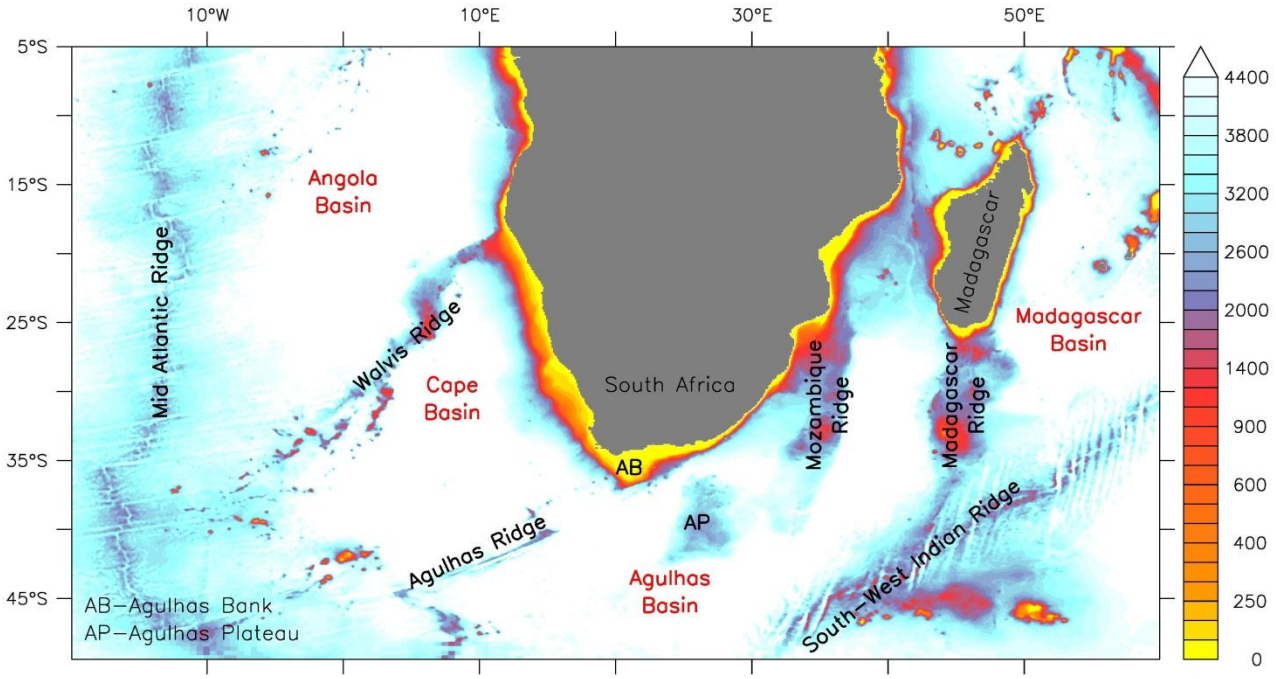


**FIGURE 1.3:** Main features of the bathymetry (m) around Southern Africa. Bathymetry dataset is derived from ETOPO2 and interpolated on a 0.1° x 0.1° grid (section 2.1).

Agulhas Rings, the principal carrier of Agulhas leakage, decay rapidly in the Cape Basin (Schmid et al. 2003; Schonten et al. 2000; van Sebille et al. 2010b). In particular, they lose their anomalous surface thermal content fairly quickly to the atmosphere (van Aken et al. 2003). The remaining salt content anomaly persists for longer and contributes to an overall densification of the South Atlantic (Biastoch et al. 2008b; Biastoch and Böning 2013). In this respect, Agulhas leakage impacts the Atlantic thermohaline circulation through the advection of salt. Advective timescales being slower, this effect is communicated north within 2 – 4 decades (Rühs et al. 2013; van Sebille et al. 2011; Weijer et al. 2002).

Therefore, through the radiative and advective mechanisms described above, the recently reported upward trend in leakage, diagnosed from hind-cast simulations (Biastoch et al. 2009b; Rouault et al.

2009), may translate into profound alteration of the delicate structure of the Atlantic. This is particularly relevant in the course of global warming and climate change (Biastoch and Böning 2013). One might further hypothesise that the slow export of additional salt from the Agulhas could eventually compensate or even thwart the impact of an increasing freshwater inflow that result from the melting of Arctic sea-ice (Walsh 2013) and of Greenland ice-sheets (Bamber et al. 2012). This hypothesis draws some support in the fact that Agulhas leakage has also been shown to be a key process in past climate changes.

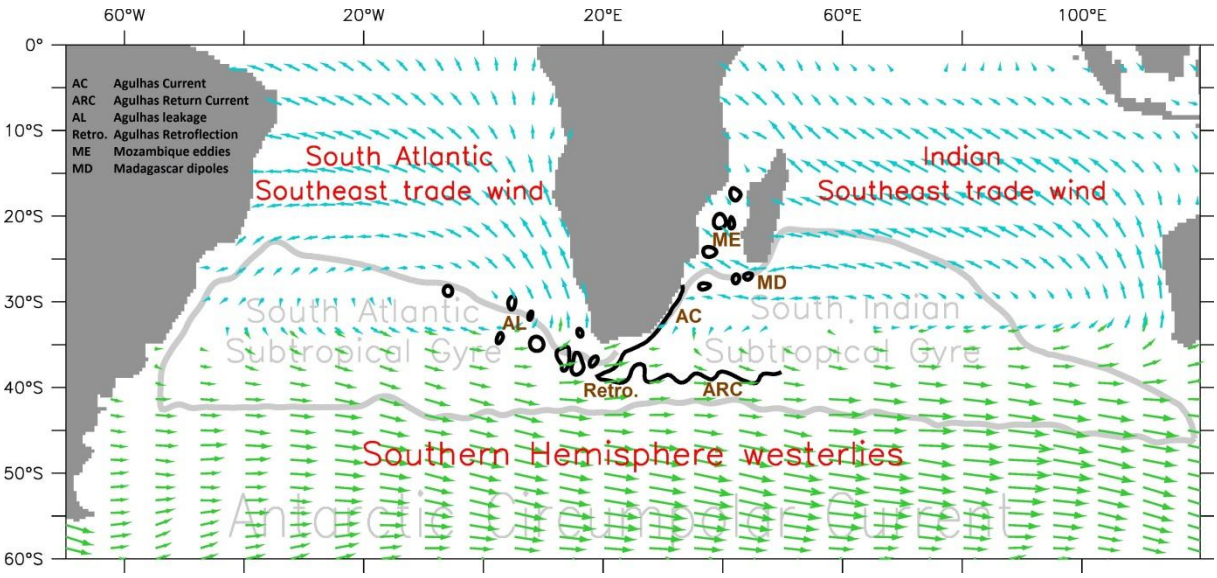


**FIGURE 1.4:** The Agulhas Current system (schematically drawn, dark black lines) sandwiched between the Southern Hemisphere westerlies (green arrows) and the Southeast trade winds (blue arrows), as well as embedded within the large-scale circulation (light grey). Wind stress derived from the Common Ocean-ice Reference Experiment (CORE) dataset (described in chapter 2).

The Atlantic circulation of the past has responded to changes in both the cold- and warm-water routes (Knorr and Lohmann 2003). While the behaviour of the paleo-AMOC has been highly variable (Srokosz et al. 2012), distinct instances of increased leakage during glacial terminations (Peeters et al. 2004) have been linked to reinvigorations of the AMOC (Chiessi et al. 2008). Changes in leakage between glacial and inter-glacial periods may have been prompted by the Southern Ocean (Bard and Rickaby 2009) and/or changes in the wind pattern of the Southern Hemisphere (Kohfeld et al. 2013; Sime et al. 2013; Toggweiler et al. 2006). Furthermore, it has been suggested that the present-day increase in leakage is in one way or another related to anthropogenic modifications of the Southern Hemisphere winds (Biastoch and Böning 2013; Son et al. 2010; Toggweiler 2009). Given the importance and relevance of Agulhas leakage for climate, it is of great interest to understand its controlling factors.

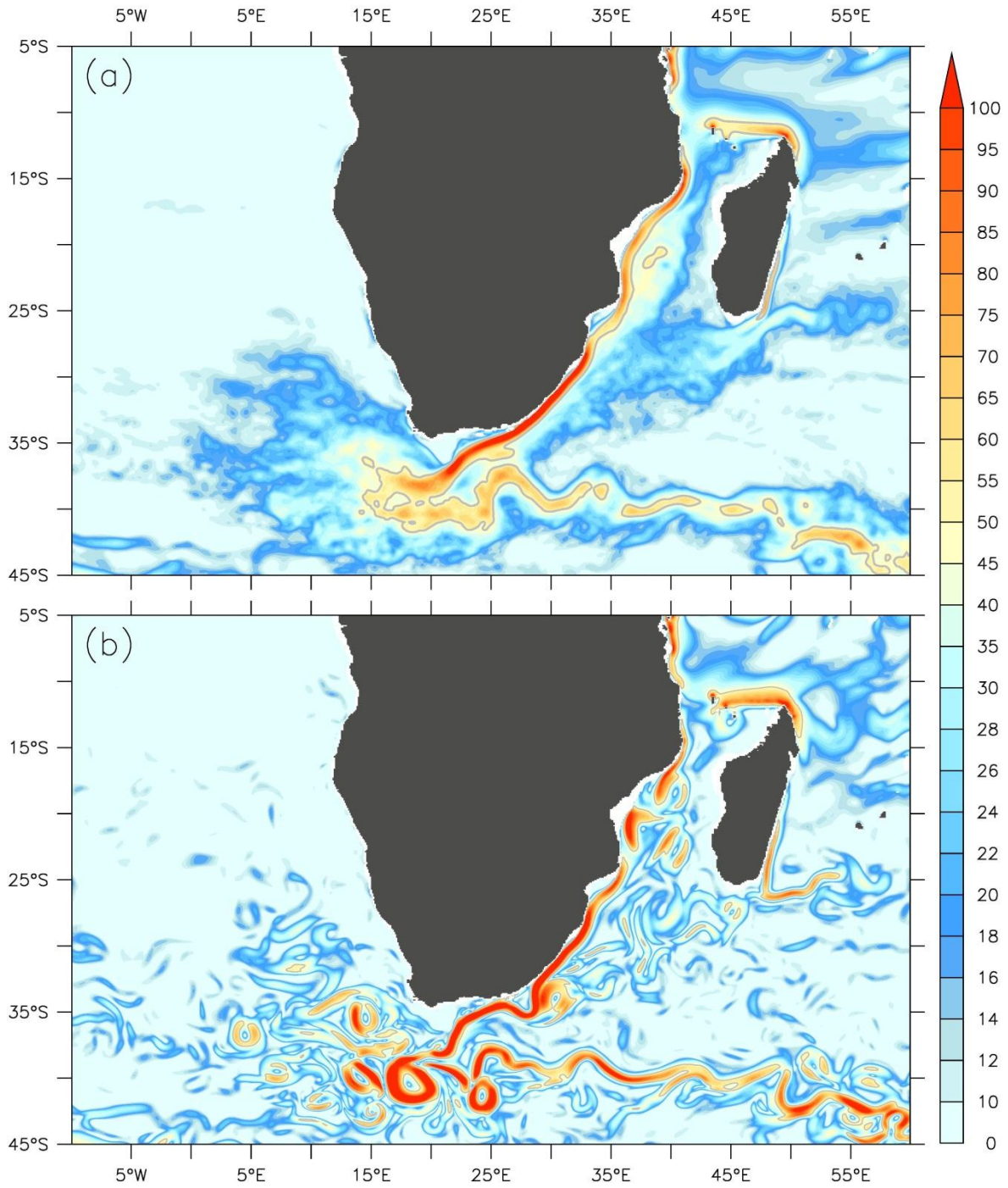


**FIGURE 1.5**: Upper 100 m speed (shading, cm $s^{-1}$; 50 cm $s^{-1}$ contour in light grey) of the greater Agulhas Current system from the INALT01 model configuration (described in chapter 2) illustrating the complexity of the flow around southern Africa; (a) annual mean and (b) instantaneous view.

## 1.3. What determines Agulhas leakage?

Agulhas leakage can be regarded as a by-product of the Agulhas Current. The Agulhas Current is the western boundary current of the South Indian Ocean (Lutjeharms 2006). Unique to the Agulhas Current is the fact that it redistributes heat and salt not only poleward, as it is usually the case for

this family of currents, but also equatorward. The current system is schematically shown in Figure 1.4. The current flows along the continental slope of the east coast of South Africa. Between about 25°S and 33°S, the current is on average fairly stable (Gründlingh 1983), flowing approximately 30 to 50 km offshore. Upper ocean speed within the core of the current typically exceeds 1 m $s^{-1}$ (Figure 1.5; Beal and Bryden 1999; Bryden et al. 2005). Having a width of about 100 – 150 km, and extending to about 1500 m in depth, the current transport is estimated to be in the order of 70 Sv. On its course poleward, the current intensifies, drawing water from recirculations (Stramma and Lutjeharms 1997), and at 34°S it encounters the eastern flank of the Agulhas Bank (Figure 1.3), where the steepness of the continental slope becomes more gradual. The current, therefore, becomes less stable and eventually, at about 37°S, it leaves the continent as a free-jet into the South Atlantic (de Ruijter 1982). An interplay between its inertia and the wind field of the Southern Hemisphere (also shown schematically in Figure 1.4) leads to its retroflection at around 19°E (Ou and de Ruijter 1986). The return current of the Agulhas display a large meander around the Agulhas Plateau (Figure 1.3). Downstream, the Agulhas Return Current flows eastward on average along 40°S, and deflects gradually poleward east of 50°E (Boebel et al. 2003b; Lutjeharms and Ansorge 2001).

One of the notable characteristics of the Agulhas system is that many of its components are highly variable both in space and time. This is particularly true for the source regions of the Agulhas Current, namely the Mozambique Channel and south of Madagascar. The time-mean flow through the Mozambique Channel portrays a continuous current beginning at around 12°S and subsequently joining the Agulhas Current (Figure 1.5a; Lutjeharms et al. 2012). However, snapshots of the circulation in the Mozambique Channel reveal that it is most of the time laden with cyclonic and anti-cyclonic vortices that propagate poleward (Figure 1.5b; Harlander et al. 2009; Lutjeharms et al. 2012; Quartly and Srokosz 2004; Schouten et al. 2003). These vortices, known as Mozambique eddies, have been shown to induce large displacements of the Agulhas Current. Natal Pulses, alias solitary meanders, occur when anticyclonic eddies from the Mozambique Channel flow adjacent and interact with the mean flow of the current (Lutjeharms and van Ballegooyen 1988; Rouault and Penven 2011; Schouten 2002; Tsugawa and Hasumi 2010), leading to its temporary offshore excursion. An example of a Natal Pulse accompanied by a Mozambique eddy is shown in Figure 1.5b, centred at 28°E, 34°S. Furthermore, Natal pulses have been shown to affect Agulhas Ring shedding events (Schouten 2002; van Leeuwen et al. 2000), thereby rendering the mesoscale variability of the Mozambique Channel relevant in determining the variability of the exchange of water between the Indian and Atlantic Oceans (Biastoch et al. 2008c).

The variability south of Madagascar is equally important. The South East Madagascar Current, also a western boundary current, is relatively less imposing than the Agulhas Current. Carrying approximately 30 Sv of water poleward (Lutjeharms et al. 1981; Nauw et al. 2008), the South East Madagascar Current at times also exhibits a retroflection (Quartly et al. 2006). Approximately half of the current's waters, carried by means of cyclonic eddies (Quartly and Srokosz 2004), proceed into the Agulhas Current (Siedler et al. 2009). It has been shown recently that dipoles (adjacent cyclonic and anti-cyclonic eddies) originating from south of Madagascar, combined with Mozambique eddies, have the potential to short-circuit the retroflection (de Ruijter et al. 2004; Ridderinkhof et al. 2013). Two such events have been observed in the last two decades, in 2001 (van Aken et al. 2013) and in 2008 (Rouault et al. 2010). The downstream consequence of early retroflections is a temporary discontinuation of Agulhas leakage.

Variability of the Agulhas Current system does not only impact the global circulation by influencing the pathway (Biastoch et al. 2008c) and timing (Schouten 2002) of Agulhas Rings. The Agulhas Current also has profound regional consequences. Some indications of seasonality in the current have been observed. The current appears to have a peak in geostrophic velocity during Southern Hemisphere summers (Krug and Tournadre 2012), possibly modulated by the Indian Ocean trade winds (Figure 1.4; Biastoch et al. 1999; Matano et al. 2002). It is conceivable that variability of the current on both seasonal and intra-seasonal timescales may influence the regional weather pattern through air-sea interactions (de Boer et al. 2013a; Liu et al. 2007; Nakamura 2012; Rouault et al. 2002). The current is also important for cross-shelf physical-biological interactions (Jackson et al. 2012) as well as for the replenishment of nutrients along the southeast coast of South Africa through impulses of kinematically-driven upwelling (Lutjeharms and Stockton 1987; Lutjeharms et al. 2000). Furthermore, immotile fish larvae spawned over the Agulhas Bank take advantage of by-products of the Agulhas Currents to reach the Benguela upwelling region (Lutjeharms et al. 2007).

The Agulhas retroflection negotiates the exchange of waters between the Indian and Atlantic Oceans (Figures 1.4 & 1.5). Establishment of a retroflection south of Africa hinges upon various factors; most notably inertia (Boudra and Chassignet 1988; Boudra and De Ruijter 1986; de Ruijter 1982) and the accumulation of anti-cyclonic vorticity (de Ruijter and Boudra 1985) that is reinforced by the beta-effect (Ou and de Ruijter 1986). Retroflection is maintained by the locking effect of topography (Dencausse et al. 2010b; Matano 1996). Also of crucial importance is the wind pattern of the Southern Hemisphere. Depicted in Figure 1.4, the Agulhas system is sandwiched between the easterly trade winds and the Southern Hemisphere westerlies. The Agulhas Current acquires its inertia from the positive wind stress curl prevailing between the maximum easterlies (~15°S) and

maximum westerlies (~50°S). At separation (~37°S), the current runs out of coastline but remains under the influence of the positive wind stress curl. Its large inertia hinders it from completely leaking into the South Atlantic, but instead promotes its veering back into the Indian Ocean (Beal et al. 2011; de Ruijter 1982). Therefore, the controls of Agulhas leakage are linked to the wind pattern of the Southern Hemisphere.

## 1.4. What is unknown about the controls of Agulhas leakage?

Before identifying the gap in knowledge that this thesis addressed, it would be instructive to summarise the status-quo in the understanding of the controls of Agulhas leakage. In addition to the wealth of theoretical studies that used simple models to determine the governing factors behind the establishment of a retroflection south of Africa (summarised in de Ruijter et al. 1999), in 2009, several noteworthy milestones were reached in the understanding of the controls Agulhas leakage. These works employed realistic state-of-the-art ocean models. The following highlights the achievements and lays the basis on which this thesis was constructed.

- Biastoch et al. (2009b) – Using a high-resolution global-nested model (AG01; Biastoch et al. 2009a) forced by inter-annually varying fields (1958 – 2004) from the Coordinated Ocean-ice Reference Experiment dataset (CORE version 1; Large and Yeager 2004), the authors diagnosed a positive trend in Agulhas leakage for the period 1968 – 2001 (1.2 Sv / decade). Concomitant, they showed a poleward expansion of the supergyre (Ridgway and Dunn 2007) by about 2°. The resulting increase in leakage was shown to contribute to an overall salinification of the South Atlantic subtropical gyre and of the North Brazil Current. The authors claimed that these contemporary changes were intimately linked to the anthropogenically-driven (Cai 2006) poleward shift of the Southern Hemisphere westerlies (Toggweiler 2009).

- van Sebille et al. (2009b) – The authors, employing the AG01 model of Biastoch et al. (2009a), reported an anti-correlation between Agulhas Current and leakage. Within the range of biennial-average values simulated by AG01 for the period 1968 – 2001, they found a significant negative correlation, where a 1 Sv decrease in Agulhas Current leads to a 0.7 ± 0.2 Sv increase in leakage. They went on to explain their results based on the theoretical arguments proposed by Ou and de Ruijter (1986). Due to a reduced outcropping and less accumulation of anti-cyclonic (de Ruijter and Boudra 1985), a weaker Agulhas Current leads to a more westward retroflection and hence more chance of leakage. Therefore, over the 34-year period analysed by Biastoch et al. (2009b)

and van Sebille et al. (2009b), synchronous to the 1.2 Sv / decade increase in Agulhas leakage, the Agulhas Current exhibits a negative trend of -1.4 Sv / decade.

- Rouault et al. (2009) – From an observed sea surface temperature dataset, Rouault et al. (2009) reported that the greater Agulhas Current system has been experiencing a warming trend since the 1980s. Their subsequent analysis of a regional model (SAfE; Penven et al. 2006), forced at the surface by the National Centres for Environmental Prediction (NCEP) reanalysis dataset and along the lateral boundaries by SODA outputs (Simple Ocean Data Assimilation, Carton et al. 2000), revealed the warming to be linked to an increased Agulhas Current over the same period. They further examined the implications on Agulhas leakage and, in contrast to van Sebille et al. (2009b), noted a positive correlation. They concluded that these observed and modelled results are due to an increase in easterly winds over the subtropical Indian Ocean since the 1980s.

The above-mentioned model studies agree on two things: firstly, Agulhas leakage has been increasing over the last 4 decades; and secondly, the trends in Agulhas Current and leakage are somehow related to the wind pattern of the Southern Hemisphere. The obvious disagreement however point to the need for more systematic studies.

Biastoch et al. (2009b) and Rouault et al. (2009) respectively attributed the present-day increase in leakage to a poleward shift of the westerlies and to increased trade winds. However, Biastoch et al. (2009b) also noticed a decreased Agulhas Current transport which contradictorily point to a possible decrease in trade winds. This discrepancy could be ostensibly due to the different forcing fields employed for hind-cast experiments. These fields bear inherent trends and their influences on leakage are, firstly, difficult to disentangle and, secondly, individually poorly understood. It is, therefore, not clear how the wind field affect Agulhas leakage. The importance of understanding the control exerted by the wind on leakage is not only relevant for present-day climate.

Hypotheses put forward regarding the role of the Agulhas system in the past have been based on various assumptions related to the wind field (Zahn 2009; Zahn et al. 2010). Bard and Rickaby (2009) reconstructed sea surface temperatures of the Agulhas Current and noted that, in comparison to inter-glacial periods, the current was several degrees cooler during glacial times. They associated this fluctuation in temperatures to displacements of the subtropical front south of Africa. Zahn (2009) conjectured that such displacements would be caused by the adjustment of the large-scale circulation to altered Southern Hemisphere wind patterns. From these inferences, and in combination with results of Peeters et al. (2004), the common assumption is that shifts of the

Southern Hemisphere wind belts (easterly trades and/or westerlies) would lead to the widening/narrowing of the gap between Africa and the subtropical front, thereby controlling the amount of warm salty Indian Ocean waters leaking into the South Atlantic. Zharkov and Nof (2008) analytically tested this hypothesis by assuming an extreme equatorward retroflection (at ~27°S), and found that the angle of the coastline at that latitude inhibits ring formations. Nof et al. (2011) also noted suppressed ring formations for very large wind stresses (about 4 times present-day values). While it is not possible to ascertain whether or not these extreme scenarios occurred during ice-ages, it is evident that the wind patterns of the Southern Hemisphere have profound impact on Agulhas leakage. The need to deconstruct the effect of the winds on leakage is called for.

## 1.5. What does this thesis reveal about Agulhas leakage?

In this introductory chapter, Agulhas leakage has been presented as an important component of the ocean circulation. Leakage provides a crucial connection between the Pacific/Indian and the Atlantic Oceans. From the previous section, it has become clear that what determines leakage is for the most part thought to be linked to the wind patterns of the Southern Hemisphere. This thesis investigated the precise control of the Southern Hemisphere winds on leakage. The overarching aim was to deconstruct the influence of the trade winds and of the westerlies on Agulhas leakage. In addition, the impact of leakage on the Atlantic circulation was explored.

A modelling strategy was favoured for two reasons: firstly, the notorious inadequacy in sustained observations in the Southern Hemisphere hampered a full assessment of the controls of leakage; and secondly, a modelling approach provided a unique platform to explore and isolate the dynamical mechanisms behind the controls of Agulhas leakage by means of a suite of dedicated sensitivity experiments.

For this purpose, two new global model configurations were set up as part of this thesis. The configurations, described in chapter 2, are integral outcomes of the work presented in this dissertation. In addition, two regional configurations, developed at the University of Cape Town, were used to supplement the arguments made. Agulhas leakage was defined identically within all four configurations, enabling inter-model comparison.

Three specific questions were addressed:

- **How is Agulhas leakage influenced by upstream dynamics?**

  A series of experiments were designed with the intention to alter only the magnitude of the Indian Ocean trade winds, thereby producing significant changes in the Agulhas Current transport. No modifications in the wind field were applied elsewhere. The basin-wide effects of the changes in Indian Ocean easterlies were explored and the downstream connection was assessed. This question is addressed in chapter 3.

  Results show that changes to the Indian Ocean trade winds significantly induce changes in Agulhas Current transport and energetics. Despite the unaltered wind forcing further downstream (at the retroflection), the inertia at separation is modified. The retroflection position is stable but exhibits large changes in kinetic energy. The Atlantic circulation shows no significant change. It is, therefore, concluded that isolated changes to the upstream dynamics of the Agulhas Current, induced by changes in trade winds, does not impact leakage.

- **How is Agulhas leakage influenced by the Southern Hemisphere westerlies?**

  Given the decoupling between Agulhas Current and leakage, the influence of the Southern Hemisphere westerlies on leakage was investigated and is presented in chapter 4. The position and intensity of the westerly wind belt were systematically and individually altered in a series of sensitivity experiments. These changes were applied only to the winds south of the African continent, and thereby had no direct influence on the Agulhas Current.

  Results show that modulations of westerlies produce large and significant responses in leakage. Shifts of the westerlies produce results that are contrary to popular beliefs. Intensity changes of the westerlies give rise to proportional responses in leakage. However, at strong wind stress, the response is transient and dependent on the evolution of the large-scale circulation, in particular that of the Antarctic Circumpolar Current.

- **How does an increase in Agulhas leakage impact the South Atlantic circulation?**

From chapter 4, it was concluded that the reported increase in leakage over the last four decades results predominantly from the contemporary strengthening of the Southern Hemisphere westerlies. The westerlies act over the southern portion of the subtropical gyres, the Agulhas Current system, as well as over the Southern Ocean (Figure 1.4). As such, it is difficult to distinguish the direct effect of a leakage increase on the Atlantic circulation from the indirect consequences of the large-scale adjustment. An experiment was designed to study the impact of Agulhas leakage increase in isolation and the changes in the South Atlantic circulation were examined. Some first insights are presented in chapter 5.

Results show that an isolated increase in leakage yields changes in both the velocity and the buoyancy fields of the South Atlantic. Leakage waters advected across the South Atlantic follow a preferred pathway and approximately 40 % and 30 % of Agulhas Leakage feeds into the North Brazil Current and the Brazil Current respectively within 2 decades. Furthermore, the thermohaline characteristics of the North Brazil Current show a densification in the upper 100 m, but a lightening between 100 m and 900 m.

# 2. Model description

A modelling approach was adopted for this thesis since direct hydrographic observations, covering the entire Agulhas system and the large-scale circulation within which the system is embedded, are not available for a sufficiently long time. The scientific community rely on accurate modelling simulations to be able to understand the Agulhas Current system. Designing a suitable Agulhas model configuration presents various challenges that are to some extent dependent on the research questions. In order to address the questions outlined in section 1.5 of chapter 1, three major concerns of equal importance were identified. Firstly, the large-scale circulation had to be adequately represented. This includes features such as western boundary currents, equatorial regimes, the Antarctic Circumpolar Current and the meridional overturning circulation. Secondly, representation of the Agulhas Current, its source region, and its leakage needed to be realistic. The broad range of the known variability of the Agulhas system is to be represented. Finally, the model configuration should lend itself to the possibility of running multiple sensitivity experiments, each resulting in at least 3 – 6 decades of integration, with output fields having at least 5-daily temporal resolution.

On the one side of the spectrum, a high-resolution global configuration would be ideal. For the Agulhas, a model requires at least a 10-degrees spacing in the horizontal to be considered as high-resolution (Beal et al. 2011). Such configurations already exist (*e.g.* OFES, HYCOM12, and ORCA12[1]) and have been shown to perform relatively well in representing both the large-scale and the details of the Agulhas system (Chassignet et al. 2007; Deshayes et al. 2013; Masumoto et al. 2004). Unfortunately, given the limited computing capabilities available, a global high-resolution configuration would be limited by the number of possible realisations. This option was therefore not suitable for this study. On the other side of the spectrum, a high-resolution regional model setup could be used. This has been proven to be satisfactory both in terms of the running cost and in the representation of the Agulhas system (Biastoch and Krauss 1999; Biastoch et al. 1999; Penven et al. 2006; Doglioli et al. 2006). This approach, however, suffers from an inadequate representation of the large-scale circulation, which is typically prescribed by open-boundary conditions and therefore lacks flexibility.

[1] OFES: Ocean general circulation model For the Earth Simulator; HYCOM: HYbrid Coordinate Ocean Model; ORCA bears no expansion

| Configuration | Horizontal Resolution | Domain |
|---|---|---|
| ORCA05 | 1/2°; 43 km at 30°S | Global |
| AGIO | 1/4°; 22 km at 30°S | Regional: 29°W – 115°E; 48°S – 7°N |
| INALT01 | 1/2° & 1/10°; 9 km at 30°S | Global with nest: 70°W – 70°E; 50°S – 8°N |
| ARC | 1/4° & 1/12°; 7 km at 30°S | Regional with nest: 0° – 40°E; 45°S – 30°S |

**TABLE 2.1:** Basic details of the model configurations.

As a trade-off between resolution and number of realisations, two global (ORCA05 & INALT01[1]) and two regional (AGIO & ARC[2]) configurations were used in this thesis (Table 2.1). Using a nesting technique (Debreu and Blayo 2008), a compromise was reached between sufficient horizontal resolution (a least tenth-degree) and the need for multiple realisations. ORCA05 and INALT01 are based on the ocean/sea-ice Nucleus for European Modelling of the Ocean code (NEMO v3.1.1, Madec 2008) and were developed under the DRAKKAR framework (The DRAKKAR Group 2007). AGIO and ARC are based on the Regional Ocean Modelling System (ROMS, Shchepetkin and McWilliams 2005).

The development of the two global configurations was integral to this thesis and they are presented as outcomes of this project. Significant effort was made to establish (*i*) a stand-alone global configuration (ORCA05) that adequately represents the large-scale circulation and (*ii*) a global-nested configuration (INALT01) that simulates the broad spectrum of the mesoscale features present in the Agulhas system. ORCA05 and INALT01 are described in section 2.1 and a detailed verification is carried out in section 2.4.

The regional configurations (AGIO & ARC) were developed at the University of Cape Town, South Africa (Loveday et al. 2013). These model outputs emanated from collaborative work established within the EU-ITN GATEWAYS[3] project (Zahn et al. 2010). The description of these configurations are summarised in section 2.2 and partly verified in section 2.4. For a complete description and verification, the interested reader is referred to Loveday et al. (2013).

## 2.1. The ORCA05 and INALT01 global configurations

Both ORCA05 (global stand-alone configuration) and INALT01 (global-nested configuration) follow an ORCA setup (Barnier et al. 2006; Madec and Imbard 1996). In this setup a tri-polar horizontal grid is

[1] ORCA bears no expansion; INALT: origin of the name is found in the acknowledgements.
[2] AGIO: AGulhas Indian Ocean configuration; ARC: Agulhas Regional Configuration.
[3] European Union's Initial Training Network, www.gateways-itn.eu

used with poles over Antarctica, Russia and Canada to avoid singularity in the Arctic Ocean. South of 20°N, the grid is Mercator. Variables are staggered following an Arakawa-C arrangement. In the vertical, the model uses z-coordinates with a total of 46 levels (10 levels in the top 100 m and a maximum of 250 m resolution at depth). In order to improve flows constrained by $f/H$ contours, the deepest grid box is allowed to be partially filled, with the minimum thickness set to either 25 m or 20 % of the box (Barnier et al. 2006). Additionally, non-linear bottom friction is used (Tréguier 1992). The lateral momentum boundary condition is 'free-slip'. The treatment of tracers is implemented using a Laplacian operator for the lateral diffusion and the Total Variance Dissipation (Zalesak 1979) scheme in vector form for advection. Lateral diffusion on momentum uses a bi-Laplacian operator and a vector form advection scheme that conserves energy and enstrophy (Arakawa and Hsu 1990). Sub-grid scale vertical mixing is stipulated explicitly through the turbulent eddy kinetic dependent diffusion scheme (Blanke and Delecluse 1993).

| Parameter | | ORCA05 / INALT01 Base | INALT01 Nest |
|---|---|---|---|
| Nominal horizontal resolution | km | 50 | 10 |
| Number of grid points ($i$ x $j$ x $k$) | $x10^6$ | 16.97 | 45.34 |
| Integration time-step | s | 2160 | 540 |
| Lateral mixing coefficient in the bottom boundary layer | $m^2\ s^{-1}$ | 1000 | 500 |
| Horizontal eddy diffusivity | $m^2\ s^{-1}$ | 600 | 200 |
| Horizontal eddy viscosity | $m^2\ s^{-1}$ | $-12x10^{11}$ | $-2.125x10^{10}$ |
| Frequency of surface boundary condition update | | 5 | 4 |
| Viscosity coefficient for tracer sponge layer † | s | 2160 | 2160 |
| Viscosity coefficient for dynamics sponge layer † | s | 2160 | 2160 |
| Vertical eddy viscosity | $m^2\ s^{-1}$ | $1.2x10^{-4}$ | $1.2x10^{-4}$ |
| Vertical eddy diffusivity | $m^2\ s^{-1}$ | $1.2x10^{-5}$ | $1.2x10^{-5}$ |

**TABLE 2.2:** Parameterisation values for ORCA05/INALT01-base and INALT01-nest. INALT01 base model is identical to the stand-alone ORCA05 configuration. † Sponge layer is only applicable for the nested configuration.

ORCA05, with half-degree nominal horizontal resolution, which in the Agulhas region is ~43 km, is an established configuration (Biastoch et al. 2008a) and successfully reproduces the large-scale global circulation (Section 2.4.1). INALT01 consists of a base global model (that is identical in configuration to ORCA05) and a nest embedded within between 70°W – 70°E and 50°S – 8°N (Figure 2.1a). The nest refines the horizontal model grid over the greater Agulhas Current system and South Atlantic 5-folds to a tenth-degree (~9 km over the Agulhas region). This also implies a 4-fold time-stepping refinement from 36 (base) to 9 (nest) minutes. Bathymetry within the nest region is interpolated

from ETOPO2[1] with a smoothing factor of 0.75. Specifics of the parameterisation used for the two global configurations are outlined in Table 2.2.

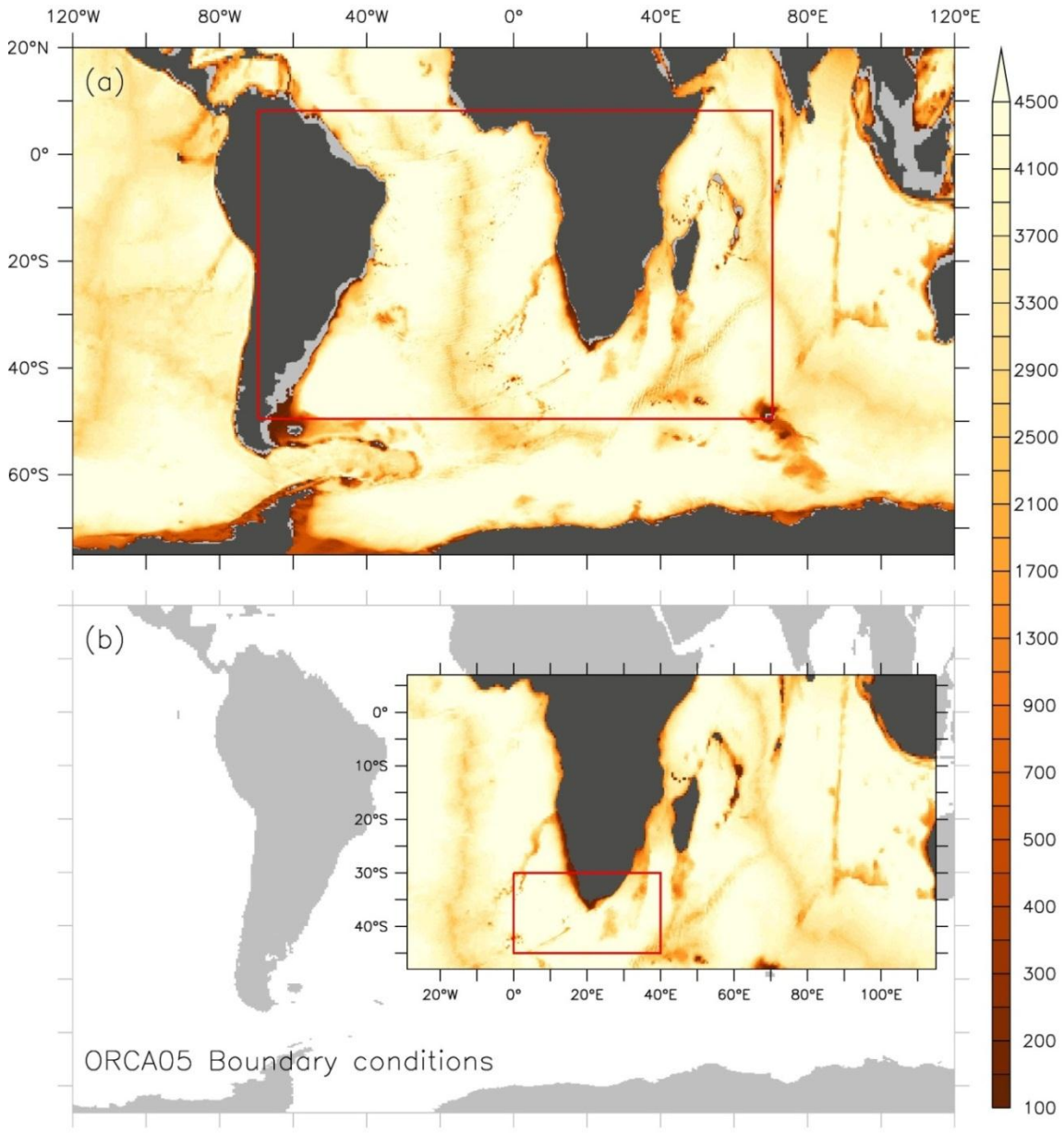


**FIGURE 2.1:** Domain of the (a) INALT01 and (b) ARC configurations. Shading shows the bathymetry (m) used in the respective configurations. INALT01 is a global-nested configuration; the global base is partly shown, nested domain between 70°W – 70°E and 50°S – 8°N (red box). ARC is a regional-nested configuration; regional domain between 29°W – 115°E and 48°S – 7°N, nest between 0° – 40°E and 45°S – 30°S (red box); Indonesian archipelago is masked; the regional configuration receives lateral boundary conditions from ORCA05.

[1] U.S. Department of Commerce, National Oceanic and Atmospheric Administration, National Geophysical Data Center, 2006. *2-minute Gridded Global Relief Data (ETOPO2)* http://www.ngdc.noaa.gov/mgg/fliers/06mgg01.html

The horizontal refinement is achieved by adopting the AGRiF (Adaptive Grid Refinement in Fortran, Debreu and Blayo 2008) approach, whereby both grids are coupled in a 2-way mode at every base model time-step to provide the nest with open boundary conditions from the base but also enabling the mesoscale dynamics of the nest to permeate into the base. For this reason, neither INALT01's base nor ORCA05 have parameterised mesoscale eddies, a practice that is usually common for models of such resolution class. Eddy parameterisation, such as the Gent and McWilliams (1990) scheme or derivations thereof (*e.g.* Tréguier et al. 1997; Visbeck et al. 1997), typically mimics the impact of eddies on tracer fluxes as isopycnal diffusion and eddy advection. This has an overall effect of reducing isopycnal steepness. Such parameterisation is believed to dampen the influence of the mesoscale dynamics of the nest onto the base. ORCA05 was also run without eddy parameterization in order to allow consistent comparison between both global configurations.

INALT01 is an update of AG01 (Biastoch et al. 2009a). The latter has been demonstrated to represent the dynamics of the Agulhas Current and its large-scale impact successfully (Biastoch et al. 2008c,b, 2009b; van Sebille et al. 2009b,a, 2010b). With its wider high-resolution domain encompassing the South Atlantic basin as well as the tropical Atlantic, INALT01 better lends itself to the investigation of the hypothesised impact of Agulhas leakage on the Atlantic circulation, including the heat and freshwater balances. In addition, the advective pathways between the Agulhas system and the North Atlantic can be further explored (Rühs et al. 2013), owing to the longer hind-cast simulation (section 2.3) and improved representation of the Atlantic circulation (section 2.4.1). The new configuration successfully simulates two major western boundary currents of the Southern Hemisphere: the Agulhas Current and the Brazil Current.

ORCA05 and INALT01 were run using a preconditioned conjugate gradient elliptic solver. Laterally decomposing the ORCA05 (INALT01) domain along the *j*-direction (*i*-direction) allow for the model code to run with 4 (16) processors on a vector NEC SX-9 supercomputer. ORCA05, with approximately 17 million grid points, requires ~2 hours / model year computing time. With over 62 million combined grid points, INALT01 takes ~10 hours / model year. Post-processing time is of the order of 2 – 5 hours / model year, depending on time resolution of the output fields. A typical INALT01 model year with 5-daily output fields generate about 150 GB of raw data per annum; a full 60-year simulation requiring up to 9 TB. Simulations of the global configurations were performed on the high-performance supercomputer in Stuttgart (Durgadoo and Biastoch 2013) and on the CAU-Kiel NESH system[1].

[1] http://www.rz.uni-kiel.de/hpc/nec.html

## 2.2. The AGIO and ARC regional configurations

The AGIO configuration (Loveday et al. 2013) is a quarter-degree resolution eddy-permitting implementation of ROMS, constructed using ROMSTOOLS[1] (Penven et al. 2008). ROMS is a split-explicit, free-surface, ocean-only model discretised in coastline and terrain-following curvilinear coordinates (Shchepetkin and McWilliams 2005). The regional domain spans the Indian and South East Atlantic Ocean basins, from 29°W to 115°E and 48°S to 7°N and is expressed on an Arakawa-C Mercator grid (Figure 2.1b, Table 2.1). AGIO is an extension of the SAfE configuration (Southern Africa Experiment, Penven et al. 2006; Rouault et al. 2009). The average grid spacing over the southern Agulhas region is ~22 km. The vertical in AGIO is described by 32 σ-coordinate levels following the GEBCO1[2] derived bathymetry and stretched towards the surface. The regional bathymetry is selectively smoothed to reduce pressure gradient errors (Haidvogel and Beckmann 1999). Higher order numerics and a third-order, upstream-biased advection scheme reduce dispersion, allowing steep density gradients to be preserved, and enhancing precision for a given resolution (Shchepetkin and McWilliams 1998). The splitting of diffusion and advection via the RSUP3 (Rotated, Split-UPstream 3$^{rd}$ order) scheme minimizes spurious diapcynal mixing (Marchesiello et al. 2009). Western boundary currents are selectively damped via a parameterization of horizontal viscosity (Smagorinsky 1963) and sub-grid scale vertical mixing follows a non-local K-Profile parameterisation (Large et al. 1994). The lateral viscosity and diffusion are zero in the domain interior and increase to 1000 $m^2 s^{-1}$ in the sponge layer within ~200 km from the domain boundaries. The Indonesian archipelago is partially masked due to numerical instabilities in the shelf seas within the sponge layer (Figure 2.1b). Prognostic variables are connected to the external conditions by an active radiation scheme (Marchesiello et al. 2001).

Using AGRiF (Debreu and Blayo 2008), the ARC configuration enhances the grid spacing to a twelfth-degree between the region 0° to 40°E and 45°S to 30°S (Figure 2.1b; Loveday et al. 2013). ARC base model is identical to AGIO and variables between base and nest are exchanged using a 2-way approach.

## 2.3. Atmospheric forcing and integration strategy

Prescribing an appropriate atmospheric forcing is crucial for ocean modelling. The CORE (Common Ocean-ice Reference Experiment version 2b, Large and Yeager 2009) project provides the necessary

[1] ROMSTOOLS bears no expansion.
[2] General Bathymetric Charts of the Ocean, http://www.gebco.net/data_and_products/gridded_bathymetry_data/

coherent and globally balanced dataset to drive the model. The CORE project uses the atmospheric state from the National Centres for Environmental Prediction (NCEP) reanalysis dataset and attempts to correct its biases (Smith et al. 2001) by blending in observational datasets (such as the satellite QuickScat[1] wind product, in-situ measurements and other reanalyses). The advantage of using the CORE dataset is that it inherits from the space and time resolution of the NCEP reanalysis, and after addressing its deficits, provides a close dataset with globally balanced fluxes.

The dataset consists of six decades of inter-annually varying fluxes (1948 – 2007):

- Wind components, temperature and humidity at 10 m; 6-hourly, inter-annually varying fields between 1948 and 2007.
- Long and short wave radiation; daily, inter-annually varying fields between 1984 and 2007.
- Precipitation (rain and snow); monthly, inter-annually varying fields between 1979 and 2007.

These fields are also available as climatological 6-hourly averages. In addition, climatological monthly-varying river run-off fields constructed by The DRAKKAR Group (2007) were used. The forcing fields, originally gridded on a Mercator 2° x 2° grid, were interpolated onto the respective model grids, and in conjunction with surface ocean temperatures and velocities (global configurations only), turbulent fluxes were calculated through bulk formulation (Large and Yeager 2009). This effectively allows some feedback between ocean and atmosphere.

Despite the best efforts to close the fresh water budget, minor errors can lead to large drifts in properties (Behrens et al. 2013; Griffies et al. 2009). In order to constrain such artificial drifts within the two global configurations, ORCA05 and INALT01, a 10 % precipitation reduction (which falls well within the CORE dataset uncertainty range; Large and Yeager 2009) north of 55°N was implemented in addition to a sea surface salinity restoring over the top 50 m with a timescale of 8.3 years. Restoring is unphysical and therefore, this “very weak” salt flux damping (Griffies et al. 2009) was further capped at 0.5 kg $m^{-1}$ $s^{-1}$ to prevent regions of strong gradients from being excessively damped (Behrens et al. 2013). Sea surface salinity damping was not applied to regions covered by sea-ice and the temperature field was not constrained. Restoring was not implemented within the regional configurations.

The coarsest resolution configuration, ORCA05, was initialised using thermohaline fields from a combined dataset of Levitus World Ocean Atlas 1998[2] and of the Polar Science Centre Hydrographic Climatology (Steele et al. 2001). Starting from rest, ORCA05 was spun for 20 years (Figure 2.2), forced

[1] http://winds.jpl.nasa.gov/missions/quikscat/
[2] http://www.esrl.noaa.gov/psd/

with inter-annually (1978-1997) varying CORE fields. Dynamic equilibrium is reached within the 20 years spin-up. The output data were then interpolated onto AGIO/ARC and INALT01 grids and used to warm-start these configurations. A fast adjustment is noted following the change in resolution (Figure 2.2).

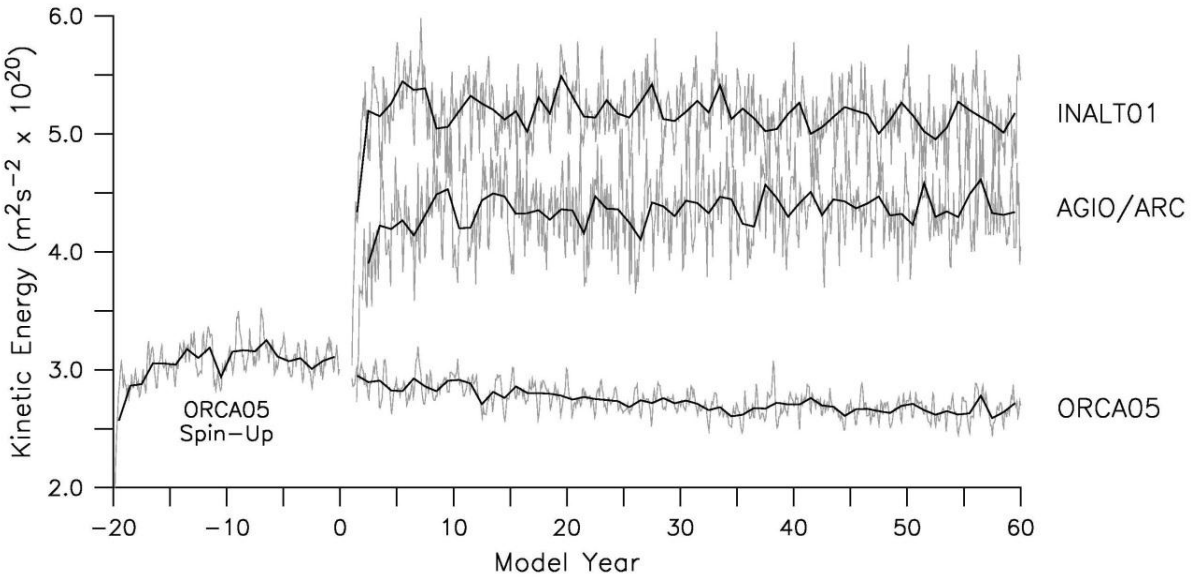


**FIGURE 2.2:** Volume integrated (10°W – 60°E; 10°S – 45°S) kinetic energy per unit mass ($m^2$ $s^{-2}$) with annual values (thick lines) overlaying monthly values (grey). Following a 20 year spin-up, reference experiments were performed for all configurations. Adapted from Durgadoo et al. (2013).

For AGIO and ARC, lateral boundary conditions are derived from the ORCA05 reference experiments (inter-annually varying and annually-repeated climatology). Since the same atmospheric fields are used to drive all configurations, this strategy ensures that the regional setups "feel" an outside world that is dynamically consistent.

In addition to several sensitivity experiments, details of which can be found in the subsequent chapters, all four configurations were integrated for 60 years, forced by the CORE inter-annually varying fields (1948 – 2007). Climatological simulations (annually repeated forcing) were performed in parallel. Pair-wise analysis of these simulations enables the distinction between forced and intrinsic (numerical artefact) oceanic responses.

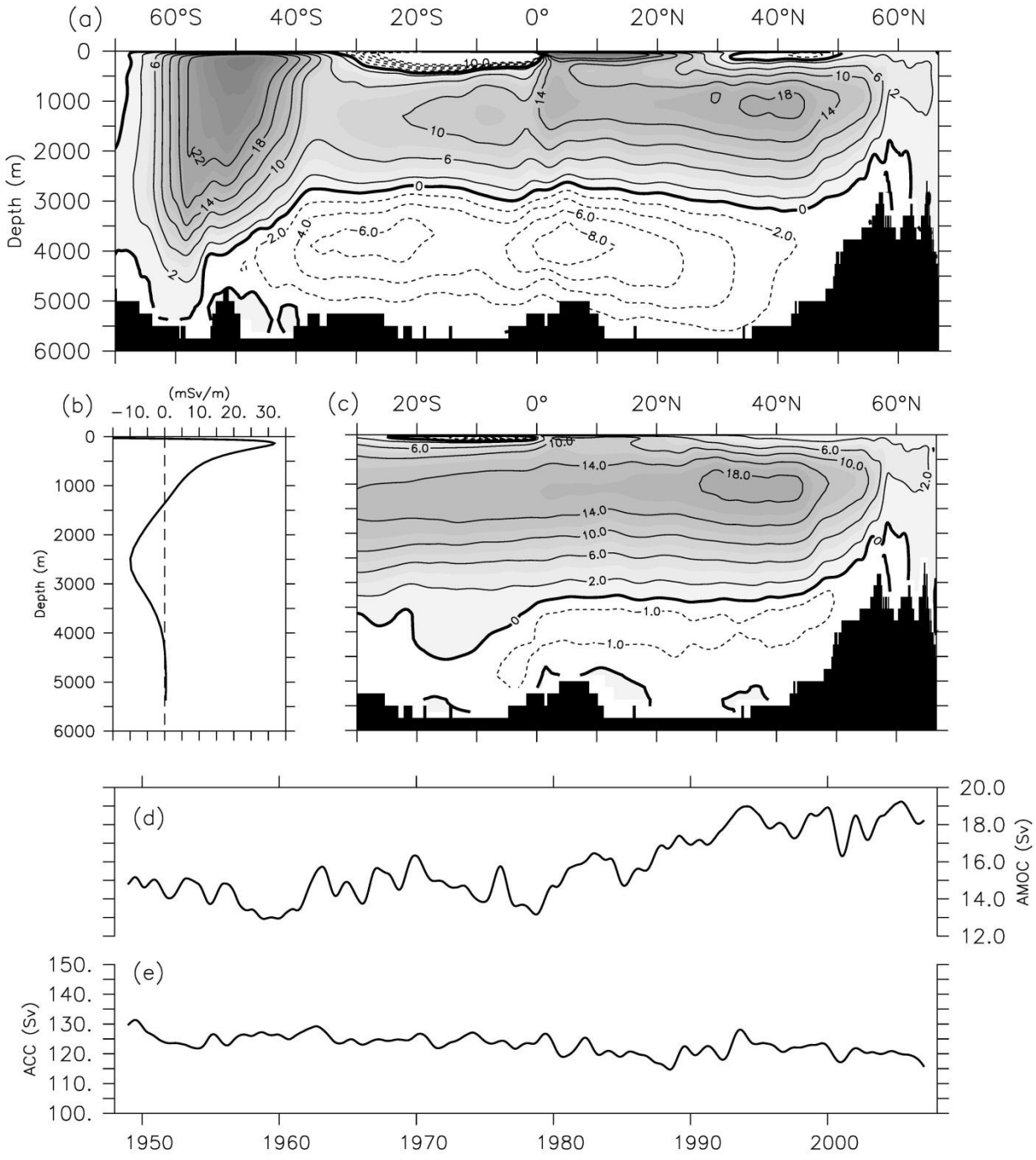


**FIGURE 2.3:** Average (1988 – 2007) (a) global and (c) Atlantic meridional overturning circulation (Sv, shading indicates clockwise circulation). (b) Northward transport per unit depth in the Atlantic averaged between 20°S – 30°S. (d) Atlantic meridional overturning (AMOC) strength (maximum at 36°N). (e) Antarctic Circumpolar Current (ACC) measured across Drake Passage. Data extracted from the ORCA05 simulation forced using the inter-annual CORE dataset.

## 2.4. Model verification

Given the dominance of mesoscale variability in the Agulhas, direct one-to-one comparison with features observed during oceanographic expeditions cannot be expected, even though a high-frequency, inter-annually varying forcing was used. However, time-mean properties and statistical representation of the variability ought to be comparable. ORCA05 is an established configuration of NEMO (Biastoch et al. 2008a). Both AGIO/ARC and INALT01 are updates of previously thoroughly tested configurations; SAfE (Penven et al. 2006; Rouault et al. 2009) and AG01 (Biastoch et al. 2008c,b, 2009b; van Sebille et al. 2009b,a, 2010b) respectively. Since the global configurations form part of the outcome of this thesis, more attention will be paid here to their validation. For an in-depth validation of the regional configurations, the reader is referred to Loveday et al. (2013).

### 2.4.1. The large-scale circulation: ORCA05 and INALT01 (base)

In the design of ORCA05, keeping in mind that it would subsequently be used as base model for INALT01, emphasis was placed in constructing a configuration that is representative of the large-scale circulation and not constrained by salinity restoring (Behrens et al. 2013). The choice of the 20-year period used to spin-up ORCA05 (1978 – 1997) promoted a stable Atlantic meridional overturning circulation. This occurred as a result of the positive North Atlantic oscillation phase during that period that enhanced the formation of intermediate and deep water masses (Lohmann et al. 2008). The stable overturning was then maintained under “very weak” salinity restoring by implementing a 10 % rain reduction over the high latitudes of the Northern Hemisphere.

The average global (Figure 2.3a) and Atlantic overturning (Figures 2.3b-c) circulations of the last two decades of the inter-annually varying ORCA05 simulation show that the four branches of the clockwise circulation are well established. Below the Ekman layer, the surface flow of light waters is northward roughly between 100 and 1300 m. In northern high latitudes, in particular in the Atlantic, convective sinking occurs and the return flow of the North Atlantic Deep Water between 1300 and 4000 m is equatorward (Figures 2.3b-c). In the Southern Ocean, the deep water is subsequently upwelled (Figure 2.3a). At depth, bottom water originating from the Antarctic fills the abyssal plains. The creeping bottom anti-clockwise cell below 4000 m has magnitude of about 1 Sv and penetrates the subpolar North Atlantic (Figure 2.3c). It should be noted that given the length of the simulation (80 model years, including spin-up, Figure 2.2), the abyssal cell is not fully developed. The mean strength of the Atlantic overturning cell is ~17 Sv (Figure 2.3d) for the period 1948 - 2007,

comparable to observations of 14 – 18 Sv from the RAPID[1] array (Cunningham and Marsh 2010). As a measure of the Southern Ocean circulation, the mean transport of the Antarctic Circumpolar Current, measured through Drake Passage, is ~120 Sv (Figure 2.3e), which also lies within observed range (Meredith et al. 2011; Whitworth 1983).

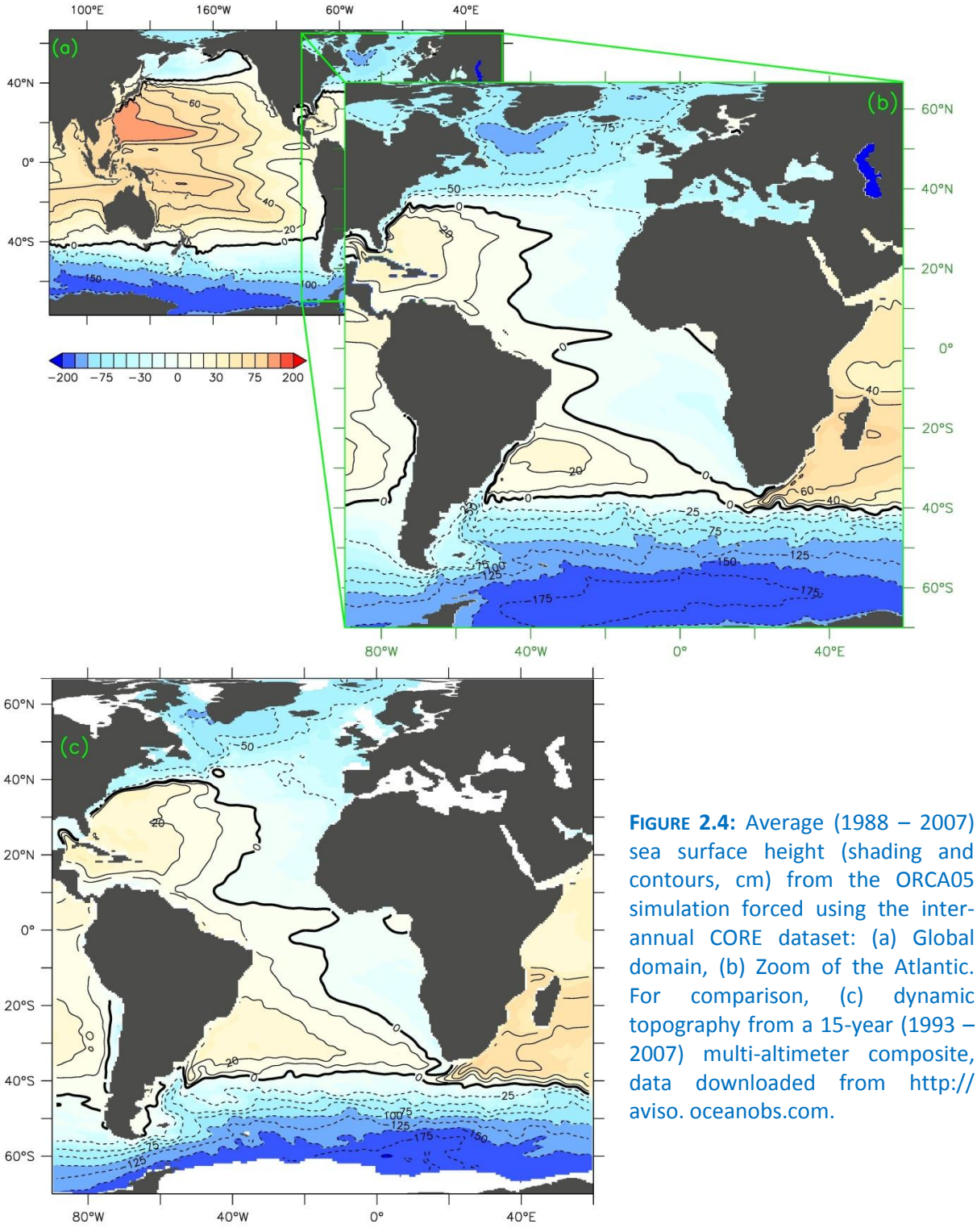


**FIGURE 2.4:** Average (1988 – 2007) sea surface height (shading and contours, cm) from the ORCA05 simulation forced using the inter-annual CORE dataset: (a) Global domain, (b) Zoom of the Atlantic. For comparison, (c) dynamic topography from a 15-year (1993 – 2007) multi-altimeter composite, data downloaded from http:// aviso. oceanobs.com.

[1] RAPID bears no expansion; http://www.rapid.ac.uk/rw/

Figure 2.4 depicts the large-scale ocean circulation within ORCA05. For comparison, the observed mean dynamic topography from altimetry is also displayed. All the known horizontal features of the ocean are satisfactorily represented within ORCA05: the subtropical gyres and their associated western boundary currents; and the subpolar gyres, most notably south of Greenland and east of the Antarctic Peninsula. It is expected that at half-degree horizontal resolution, some aspects of the circulation would be poorly resolved. For instance, the separation of the Gulf Stream from the North American coast occurs abruptly within ORCA05 (Chassignet and Marshall 2008).

Outputs from the ORCA05 configuration were used as boundary condition for AGIO and ARC. Thus, they inherited an adequately represented large-scale circulation.

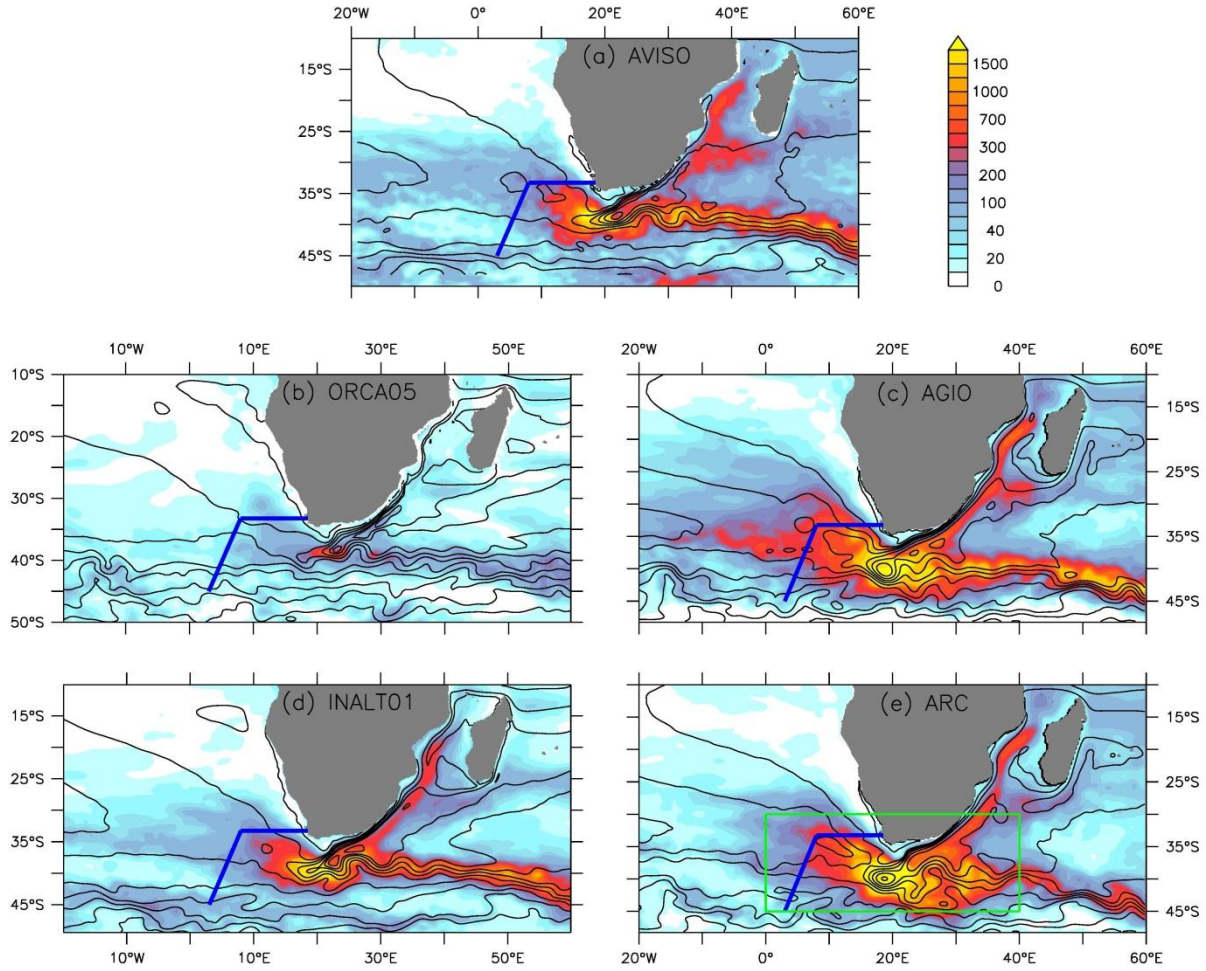


**FIGURE 2.5:** Representation of the mean circulation (contours of sea surface height (SSH) averaged for period 1992 – 2007, 20 cm contour interval) and mesoscale variability (shading of SSH variance, $cm^2$) of the Agulhas system from (a) altimetric observations, AVISO (http://aviso.oceanobs.com), (b) ORCA05, (c) AGIO, (d) INALT01 and (e) ARC (nested region, green box). Agulhas leakage is measured across the Good-Hope line (blue section). Adapted from Durgadoo et al. (2013).

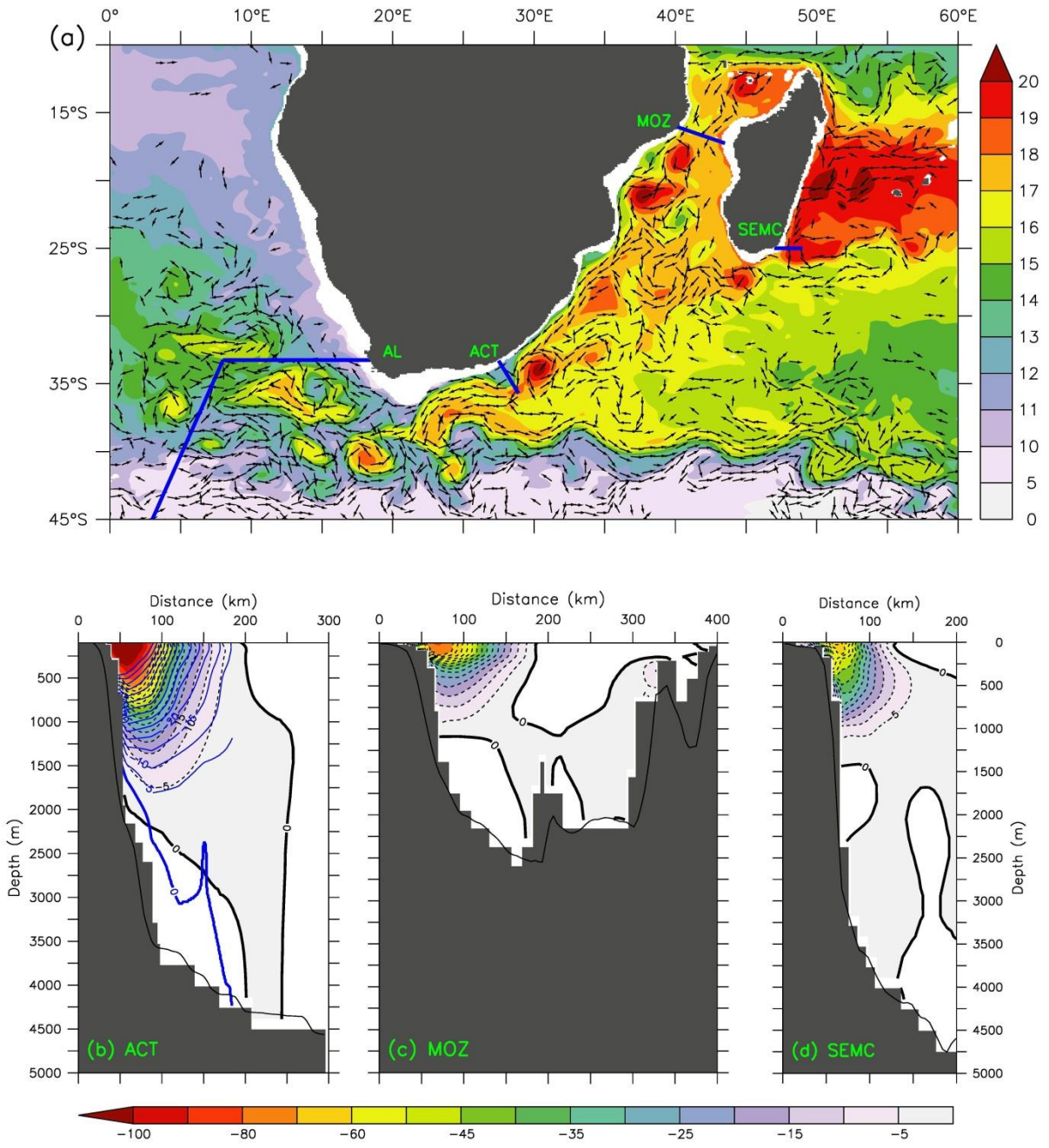


**FIGURE 2.6:** (a) Snapshot of temperature (shading, °C) and velocity (every 8th vector are plotted and capped for clarity) at 250 m centred at 17 Jun 2006 from the hind-cast realisation of INALT01 and vertical sections of cross-stream velocity (shading and contour, cm $s^{-1}$, 5 cm $s^{-1}$ contour interval) taken across the (b) Agulhas Current (ACT, averaged over 1968 – 1970), (c) the Mozambique Channel (MOZ, averaged over 1995 – 2003) and (d) the South East Madagascar Current (SEMC, averaged over 2000 – 2003). These sections are shown in (a), in addition to the Good-Hope line used for Agulhas leakage (AL) measurement (blue lines). Representation of bottom bathymetry (thin black lines) by partially-filled cells is additionally shown (b – d). Overlaid on (b) is an average cross-stream velocity profile derived from an 18-months deployment of moorings along the ACT array (data courtesy Lisa Beal).

### 2.4.2. The Agulhas system

Figure 2.5 portrays the reproduction of the mean circulation as well as the mesoscale variability of the Agulhas system within the four configurations compared to that observed from satellite altimetry. Within ORCA05, the Agulhas Current is represented by a continuous flow that begins in the northern Mozambique Channel with the only source of variability originating south of Madagascar. The current retroflects and occasionally produces some large unrealistic rings. In contrast, within AGIO, INALT01, and ARC, where the first baroclinic Rossby radius of deformation is resolved (20 – 50 km in this region, Chelton et al. 1998), a broad spectrum of mesoscale activity is observed in the known source regions of the Agulhas Current as well as a more realistic representation of the diverse range of features typically found in the Cape Basin, namely Agulhas Rings, cyclones and filaments among others (Boebel et al. 2003a).

An exemplary snapshot taken from INALT01 shows these above-mentioned features (Figure 2.6a), in addition to a Natal Pulse (centred at 28°E, 34°S), the poleward propagation of anticyclonic eddies (centred at 38°E, 22°S, and 30°E, 34°S) from the Mozambique channel and from southern Madagascar (centred at 45°E, 27°S). In Figure 2.6a, the Agulhas Current retroflection occurs at about 21°E and a newly occluded Agulhas Ring is observed centred at 41°E, 18°S. The retroflection connects the Agulhas Current with the meandering Agulhas Return Current, along 40°S. Recirculations along the Agulhas Return Current are further evident. The range of features depicted in Figure 2.6a all form part of the known and observed variability of the Agulhas system (Lutjeharms 2006). Eddies from the Mozambique Channel (Biastoch et al. 2008c; Ridderinkhof et al. 2010) and south of Madagascar (Quartly and Srokosz 2004; Ridderinkhof et al. 2013) drifting poleward occasionally cause the displacement of the Agulhas Current (Natal Pulses, Lutjeharms and Roberts 1988) and result in enhanced variability offshore of the current (Figure 2.5d,e). Downstream, this leads to large variation in ring characteristics, yielding to a realistically variable pathway of ring spreading (*c.f.* Figure 2.5a and 2.5d).

The depth expression within INALT01 of the Agulhas Current across the Agulhas Current Transport array (ACT[1]) at 33°S, of the Mozambique through-flow across the narrows of the channel, and of the South East Madagascar Current at 25°S are shown in Figures 2.6b, c and d respectively. The structure of the Agulhas Current is compared with a recently measured average cross-stream velocity profile derived from an 18-months deployment of moorings along the ACT array (April 2010 – November 2011). The current at that latitude is relatively broad (160 – 180 km) and reaches a depth of about

[1] http://act.rsmas.miami.edu

1500 – 1600 m (bounded by the 10 cm $s^{-1}$ isotach). A weak poleward flow is also noticed extending down to the sea-floor. Hugging the continental slope, an equatorward flowing cell, extending about 50 – 100 km offshore between 1700 and 4000 m, carries the Agulhas Under-Current. Z-coordinate model configurations typically suffer from poor bottom flow representation. While adopting partially filled bottom cells within INALT01 (grey shading on Figure 2.5b-d) may enhance flows along topographic slopes (Barnier et al. 2006), other discrepancies, such as, vertical resolution and parameterisation, still exist. Notwithstanding, a comparison between bottom currents of the Agulhas system within INALT01 and current meter measurements show relatively good agreement (Cronin et al. 2013; Figure 2.7).

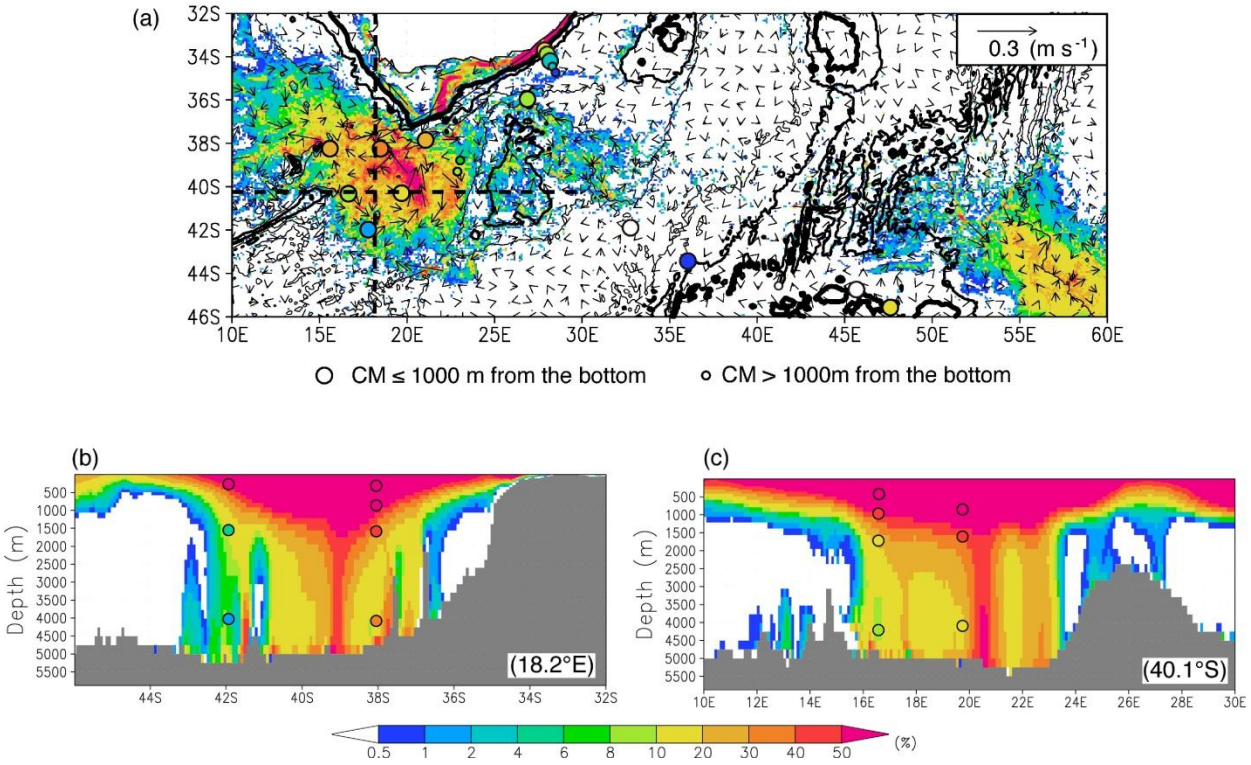


**FIGURE 2.7:** (a) Map of percentage of record (1980 – 2006) within INALT01 with bottom currents greater than 20 cm $s^{-1}$. Arrows show the mean velocity in the bottom-most cell. Vertical sections along (b) 18.2°E and (c) 40.1°S are shown on (a) with black dashed line. Historical current meters (CM) measurements are additionally shown for comparison (circle sizes only applicable for (a)). Adapted from Cronin et al. (2013).

Bryden et al. (2005) estimated a transport of 69.7 ± 21.5 Sv at 31°S (about 200 km upstream of the ACT array) from daily-average current meter measurements collected over 9 months. The range of observed transport was between 9 and 121 Sv poleward. Within INALT01, the current transport is commensurate at 31°S; 67.9 ± 16.7 Sv; range: 12 – 114 Sv poleward (calculated from 1-daily data for period 2001 – 2002). The Agulhas Current transport augments on as it flows along the coast due to recirculations (Stramma and Lutjeharms 1997). For the 18-months average mooring data along the

ACT array at 33°S (blue contours, Figure 2.5b), the mean Agulhas Current and Under-Current transports are 74.7 and 2.1 Sv respectively. Within INALT01, the average magnitude of the Agulhas Current transport along the ACT array is 77.1 Sv, with a 5-daily standard-deviation of 19.7 Sv (Figure 2.8). The Agulhas Under-Current transport within INALT01 at 33°S is 4.7 ± 4.9 Sv, and is very close to the observed estimates of 4.2 ± 2.9 Sv (Bryden et al. 2005) and 4.2 ± 5.2 Sv (Beal 2009). INALT01's predecessor, AG01, simulated a weak under-current; a deficit that was suspected to be linked to the under-representation of the North Atlantic Deep Water inflow into the Cape Basin (Biastoch et al. 2009a). Within the global configurations used here, the Atlantic overturning circulation exports a reasonable amount of deep waters across the Equator (section 2.4.1), which subsequently feeds into the Agulhas Under-Current (Arhan et al. 2003; Beal and Bryden 1997; Beal 2009).

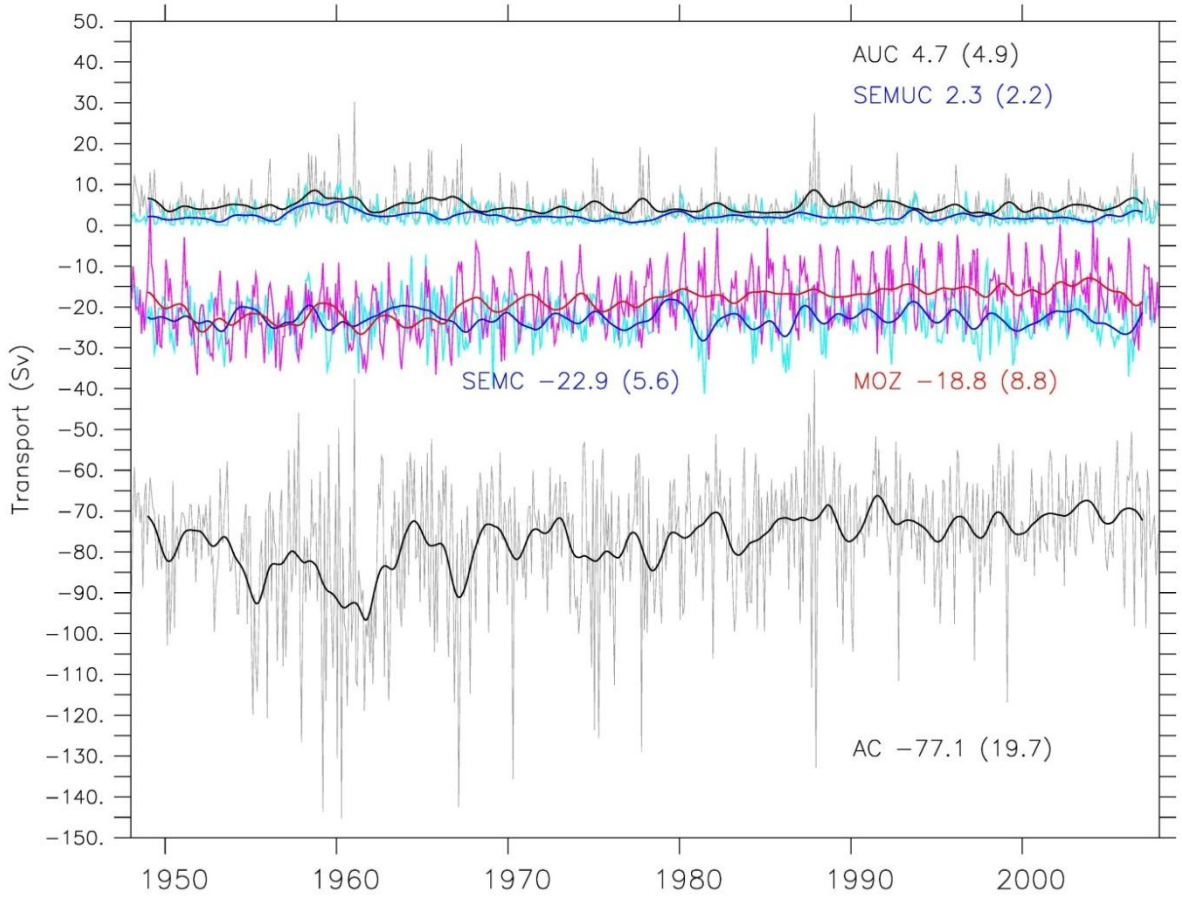


**FIGURE 2.8:** Transport time-series (Sv, positive equatorward) from the hind-cast realisation of INALT01 with monthly (inter-annually filtered) values shown in light (dark) colours. Time-means and 5-daily standard-deviations (in brackets) are also given. Sections shown in Figure 2.6: Agulhas Current (AC, poleward flow across section; black and grey lines) and Under-Current (AUC, equatorward flow integrated for region up to 200 km offshore; black and grey lines) measured across the ACT-line; Mozambique through-flow (MOZ, full-depth flow; red and pink lines); South East Madagascar Current (SEMEC, poleward flow integrated for region up to 200 km offshore, upper 1500 m; blue and cyan lines) and Under-Current (SEMUC, equatorward flow integrated for region up to 150 km offshore; blue and cyan lines).

The source regions of the Agulhas Current are known for their rich eddy activity (Figure 2.5). The surface flow across the Mozambique Channel (Figure 2.6c) is characterised by cells of opposing sign. These cells reflect the poleward propagation of Mozambique eddies (Harlander et al. 2009). In rough accordance with measured estimates of 16.7 ± 13.5 (from daily-average mooring data; Ridderinkhof et al. 2010; van der Werf et al. 2010), the flow across the channel is 18.8 ± 8.8 Sv poleward (Figure 2.8). The time-series also shows a dominant seasonal cycle. In their analysis of various model outputs (including AG01, forerunner of INALT01), van der Werf et al. (2010) noted that, while models adequately represent the magnitude of the seasonal cycle, they also tend to underestimate higher frequency variability in transport that is related to the formation mechanism of Mozambique eddies.

South of Madagascar, dipoles originating from the South East Madagascar Current are commonly observed (Ridderinkhof et al. 2013), and these have been linked to early retroflection events (van Aken et al. 2013). From four hydrographic snapshots in 2001, Nauw et al. (2008) estimated 37 ± 10 Sv and 2.8 ± 1.4 Sv for the South East Madagascar Current and Under-Current respectively. Within INALT01, the current and its associated under-current have transports of 22.9 ± 5.6 and 2.3 ± 2.2 Sv respectively (Figure 2.8). The variability of the South East Madagascar Current is poorly known. To date, no sustained measurements of the current are available. A series of mooring, recently deployed within the Dutch INATEX[1] project, promises to fill this gap in knowledge.

## 2.5. Quantification of Agulhas leakage

Measuring Agulhas leakage is no simple task. Being highly intermittent, leakage occurs predominantly through Agulhas Rings (van Sebille et al. 2010b). However, other features such as cyclones and filaments also contribute to the Indian-Atlantic transport and possibly also its variability. In addition, cyclones found in the Cape Basin have different origins; they do not all originate from the Agulhas system (Boebel et al. 2003a). Therefore, direct quantification of Agulhas Rings crossing the Cape Basin would likely underestimate leakage magnitude (de Ruijter et al. 1999); while full-depth Eulerian measurements would over estimate it. Attempts at estimating leakage using optimized Eulerian methods have been made (van Sebille et al. 2010a), but the skills of such methods have not been tested across models with different horizontal resolutions and vertical representations. From float and drifter observations, Richardson (2007) estimated leakage to be about 15 Sv. It is worth noting that this value is associated with a rather large uncertainty (recognised but not quantified by Richardson (2007)).

[1] http://www.nwo.nl/en/research-and-results/research-projects/47/2300152347.html

Here, annual values of leakage were estimated using the Ariane-v2.2.6[1] Lagrangian package, following the studies conducted by Speich et al. (2001), Biastoch et al. (2008b, 2009b) and van Sebille et al. (2009b,a). Water parcels were released every 5 days for one year over the full-depth of the poleward-flowing Agulhas Current across a zonal 300 km long segment at 32°S (Figure 2.9a). Each parcel had a defined transport of max. 0.1 Sv, and the total number of parcels released was representative of the magnitude of the Agulhas Current at each time-step. In order to capture a good representation of the variability, at least 5-day-average snapshot was required. The parcels were then advected using the model's velocity fields for a total period of five years and aggregated across predefined sections (Figure 2.9a). Parcels were removed once a section had been reached. The integration period optimally allowed 98 % of the parcels to exit the domain. Using this strategy, Agulhas leakage is defined throughout this thesis as that portion of the Agulhas Current exiting the domain through the Good-Hope section (Ansorge et al. 2005) in the Cape Basin (Figures 2.6a & 2.9a). This ingeniously designed section lies immediately west of the highly energetic retroflection region (Figures 2.5) so as to firstly, not to include water that would return back into the Indian Ocean, and secondly, to capture features (*i.e.* rings) before they dissipate (van Sebille et al. 2010b).The advantage of this method is that it could be applied to all four model configurations without the need for additional model-specific redefinitions, allowing direct inter-model comparisons.

Of the 25 exemplary Lagrangian trajectories shown in Figure 2.9a, a total of 6 make it into the Atlantic, that is, approximately 25 %. The trajectories also illustrate the fast-flowing Agulhas Current, the retroflection position between 18°E and 22°E, and the turbulent nature of the Cape Basin. The annual average and detrended inter-annual standard-deviation of Agulhas leakage, estimated for the period 1948 – 2003 within the four configurations, are additionally shown in Figure 2.9a. The two high-resolution configurations (INALT01 & ARC) have leakage values similar to that estimated by Richardson (2007). The over-estimation of leakage within ORCA05 is anticipated due to the lack mesoscale variability in that configuration. Leakage within the eddy-permitting configuration (AGIO) is about twice that of observation. This can be explained by the representation of the Agulhas Current at separation within AGIO. Smoothed-out topography at that resolution combined with the representation of the vertical lead to an overly westward extent of the retroflection loop (*c.f.* the position of the Good-Hope section with respect to the extension of high variability region in Figure 2.5c). Notwithstanding, these differences in leakage values do not hamper further analysis, as it will be shown in the subsequent chapters. Time-series from all four configurations show the high inter-annual variability of Agulhas leakage (Figure 2.9b). In line with other model studies using

[1] http://www.univ-brest.fr/lpo/ariane/

atmospheric forcing from similar datasets, leakage show an increase of about 1.2 Sv / decade since the late 1960s (Biastoch et al. 2009b; Rouault et al. 2009).

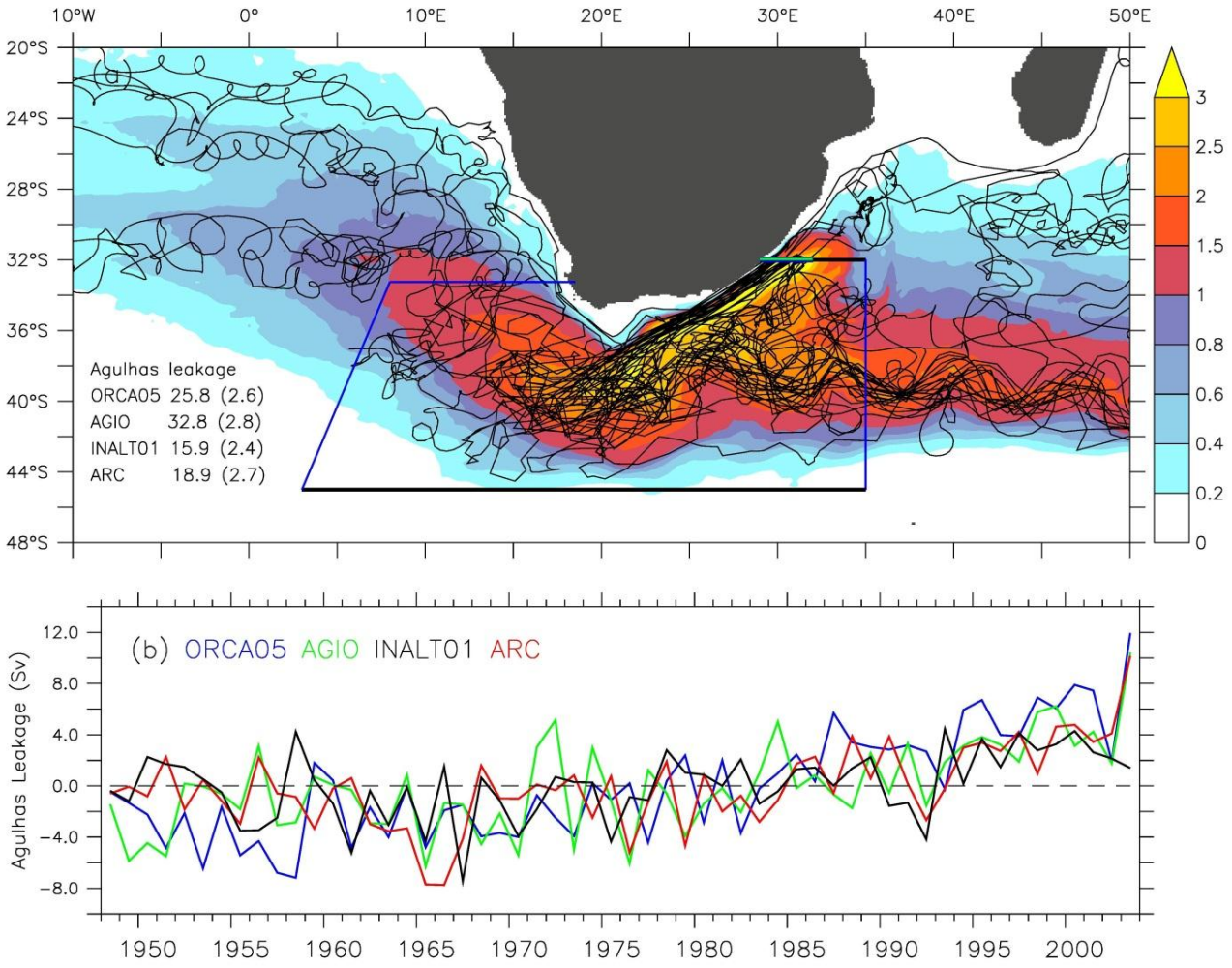


**FIGURE 2.9:** Illustration of the Lagrangian analysis used for Agulhas leakage measurement. (a) Water parcel density (shading, normalised number of occurrences per 0.25° x 0.25° grid box) overlaid by 25 exemplary parcel trajectories. Water parcels were released across the Agulhas Current at 32°S (green section) and integrated forward within all four configurations. The Good-Hope line in the Cape Basin was used to capture parcels exiting the domain as Agulhas leakage. Time-means and annual standard-deviations (in brackets) of leakage for ORCA05, AGIO, INALT01 and ARC hind-cast experiments are also shown. (b) Time-series of Agulhas leakage anomaly (respective mean values removed) within the four model configurations for period 1948 – 2003.

## 2.6. Summary

This chapter introduced two global (NEMO) and two regional (ROMS) model configurations; the global ones being integral outcomes of this thesis. These two classes of models differ in numerics and parameterisation. Yet, the configurations were constructed in such a way that inter-model comparison is possible. Dealing with uncertainty in climate science is of current relevance (van der Sluijs 2012), and the multi-model approach adopted here addresses this issue through robustness.

The four configurations most notably differ in horizontal resolution: half-degree global (ORCA05); quarter-degree regional (AGIO); tenth-degree global-nested (INALT01); and twelfth-degree regional-nested (ARC). The development of the ORCA05 setup was motivated by the necessity to have an adequately represented large-scale circulation within which a high-resolution nest could be embedded (resulting in the INALT01 configuration), as well as providing dynamically consistent boundary for the regional configurations. Within their individual limitations, the four complementary setups were deemed successful, lending themselves to the possibility of exploring the questions outlined at the end of chapter 1 (section 1.5).

# 3. Agulhas leakage is decoupled from the Agulhas Current

The content of this chapter is partly based on the following publication:

Loveday B.R., J.V. Durgadoo, C.J.C. Reason, A. Biastoch, P. Penven (2013) – Decoupling of the Agulhas leakage from the Agulhas Current. *Journal of Physical Oceanography*, under review.

The Agulhas Current forms the return flow of the South Indian subtropical gyre. South of Africa, the current runs out of coastline and retroflects. In principle, the amount of water returning into the Indian Ocean and the amount leaking into the Atlantic should sum up to the volumetric transport of the Agulhas Current at separation (Dijkstra and de Ruijter 2001). This suggests a possible dynamical link between the Agulhas Current and Agulhas leakage. The inertia of the Agulhas Current allows it to overshoot the continent as a free-jet, and this has been argued to be a key player in establishing the retroflection (de Ruijter 1982). The theoretical works of de Ruijter and Boudra (1985), Boudra and de Ruijter (1986), and Ou and de Ruijter (1986) further suggested that with an increased (decreased) inertia, the current's overshoot is enhanced (reduced) resulting in more (less) water feeding the Agulhas Return Current. As consequence, this leads to less (more) leakage. Such an anti-correlation between the Agulhas Current and leakage has been observed in a 34-year hind-cast (1968 – 2002) high-resolution simulation (van Sebille et al. 2009b). This relationship has, however, been challenged by Rouault et al. (2009) who noted an increased in leakage within their model for the period 1982 – 2001, concomitant with an Agulhas Current increase. It is evident that more research effort is needed in order to understand whether or not a dynamic relationship between the Agulhas Current and its leakage exists. The inertia of the current is determined to a large extent by the wind stress curl over the South Indian subtropical gyre.

This chapter explores the possibility of a link between the upstream inertia of the Agulhas Current and the magnitude of Agulhas leakage. The current's transport was varied through the application of wind stress anomalies onto the easterly trade winds that prevail over the South Indian Ocean. Experiments were performed within ORCA05, AGIO, INALT01, and ARC (chapter 2). It is found that despite large variations in Agulhas Current transport, leakage remains relatively unchanged. Within

the high-resolution simulations (INALT01 & ARC), no relationship between the magnitude of Agulhas leakage and the upstream inertia exists.

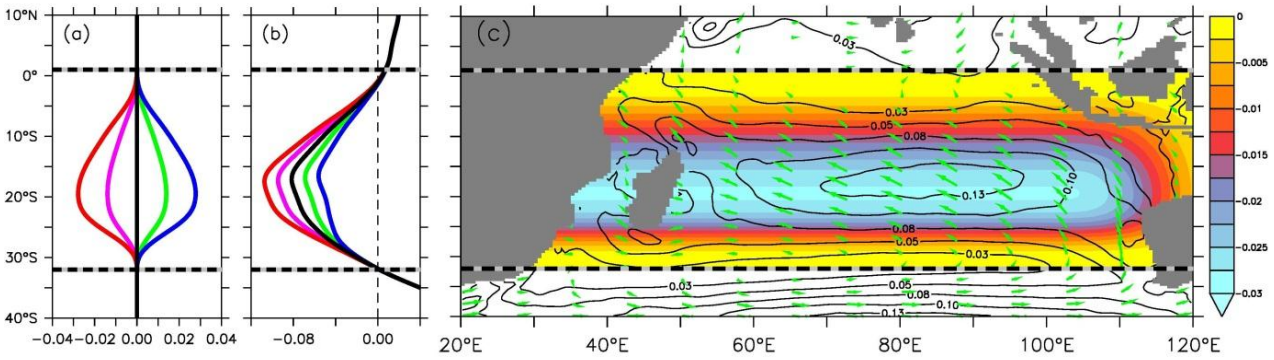


**FIGURE 3.1:** Smooth anomalies (a) are applied to the zonally averaged (20°E – 115°E) reference (thick black line) wind-stress (N $m^{-2}$) altering the easterly trades intensity (b) by -40 % (blue), -20 % (green), +20 % (pink), and +40 % (red). Anomalies are applied within the region 0° – 32.5°S. (c) The region over which the anomalies are applied. Shading shows the STW+40% anomaly (N $m^{-2}$). Overlaid is the mean wind stress magnitude (contours, N $m^{-2}$) and direction (vector) from the ORCA05-REF experiment.

## 3.1. Experiment design

As a working hypothesis, it is presumed here that the conflicting results reported by van Sebille et al. (2009b) and Rouault et al. (2009) may have been related to the fact that the authors employed different ocean models that were forced using different datasets. This is in addition to dissimilar approaches of Agulhas leakage quantification. Therefore, the four model configurations described in chapter 2 were used here and coherently forced using the CORE climatological dataset (section 2.3), and leakage was monitored in a consistent fashion (section 2.5). The climatological (repeated-year) forcing was favoured since it explicitly excludes any inherent long-term trend. It is worth mentioning that the model configurations employed for this study form part of the same family of configurations that were used by van Sebille et al. (2009b) (AG01 is the predecessor of INALT01) and Rouault et al. (2009) (SAfE is the predecessor of AGIO/ARC).

Smooth wind stress anomalies (Figure 3.1a) were designed based on the zonally averaged zonal wind stress across the Indian Ocean (thick black line in Figure 3.1b). When applied, the anomalies effectively altered the magnitude of the trade winds by ±20 % and ±40 %. The meridional component of the wind stress was unchanged. The anomalies were gridded (Figure 3.1c) and added to the wind stress calculated through bulk formula and applied only across the Indian Ocean basin at every model time-step. Thus, the wind anomalies perturbed the momentum flux between the Equator and 32.5°S,

and effects to the buoyancy forcing were ignored. The choice of ±20 % and ±40 % modulation was motivated by the 20$^{th}$ – 21$^{st}$ century observed trends in the trades as well as probable future changes (Backeberg et al. 2012; Han et al. 2010).

| | | Model Configurations | | | |
|---|---|---|---|---|---|
| **Experiment** | **Description** | **ORCA05** | **AGIO** | **INALT01** | **ARC** |
| REF | Climatological Reference | X | X | X | X |
| STW-40% | 40 % Intensity decrease | X | X | X | X |
| STW-20% | 20 % Intensity decrease | X | X | | |
| STW+20% | 20 % Intensity increase | X | X | | |
| STW+40% | 40 % Intensity increase | X | X | X | X |

**TABLE 3.1:** Sensitivity experiments performed using the four model configurations. REF: Reference; STW: Southeast trade wind. All configurations were similarly integrated (Figure 3.2).

In addition to the reference experiment, all sensitivity simulations were run under climatological atmospheric forcing. A list of experiments performed using the four model configurations is given in Table 3.1. All configurations were warm-started using a 20-year spin-up (chapter 2, section 2.3). After 30 years of integration of the reference experiment, the anomalies were applied (Figure 3.2). Starting with a linear ramp-up of the anomalies over model year 31, the configurations were integrated for another 30 years (model years 31 – 60) under the altered forcing. Analysis of the results was performed using an average of the last 20 years (model years 41 – 60, Figure 3.2). This chapter focusses mainly on the results of the two high-resolution configurations, INALT01 and ARC; in particular, the comparison between the REF and the two extreme (STW±40%) experiments (Table 3.1).

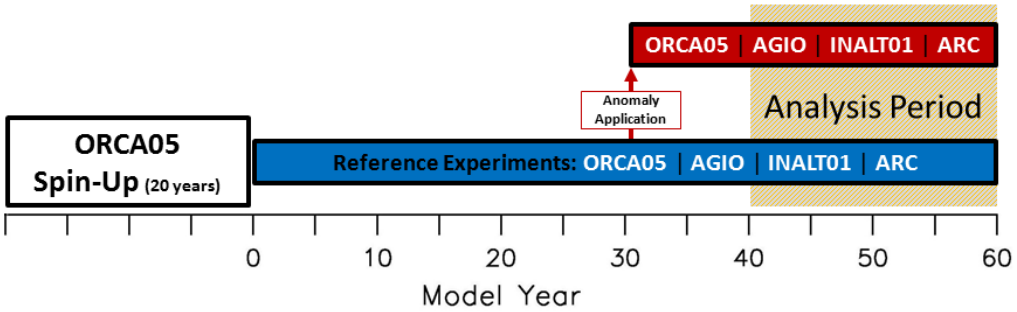


**FIGURE 3.2:** Integration strategy for the four model configurations. Sensitivity experiments were performed with wind stress anomalies (Figure 3.1, Table 3.1) applied from model year 31. Analysis period for all configurations is between model years 41 – 60. All experiments were integrated under climatological repeated-year forcing.

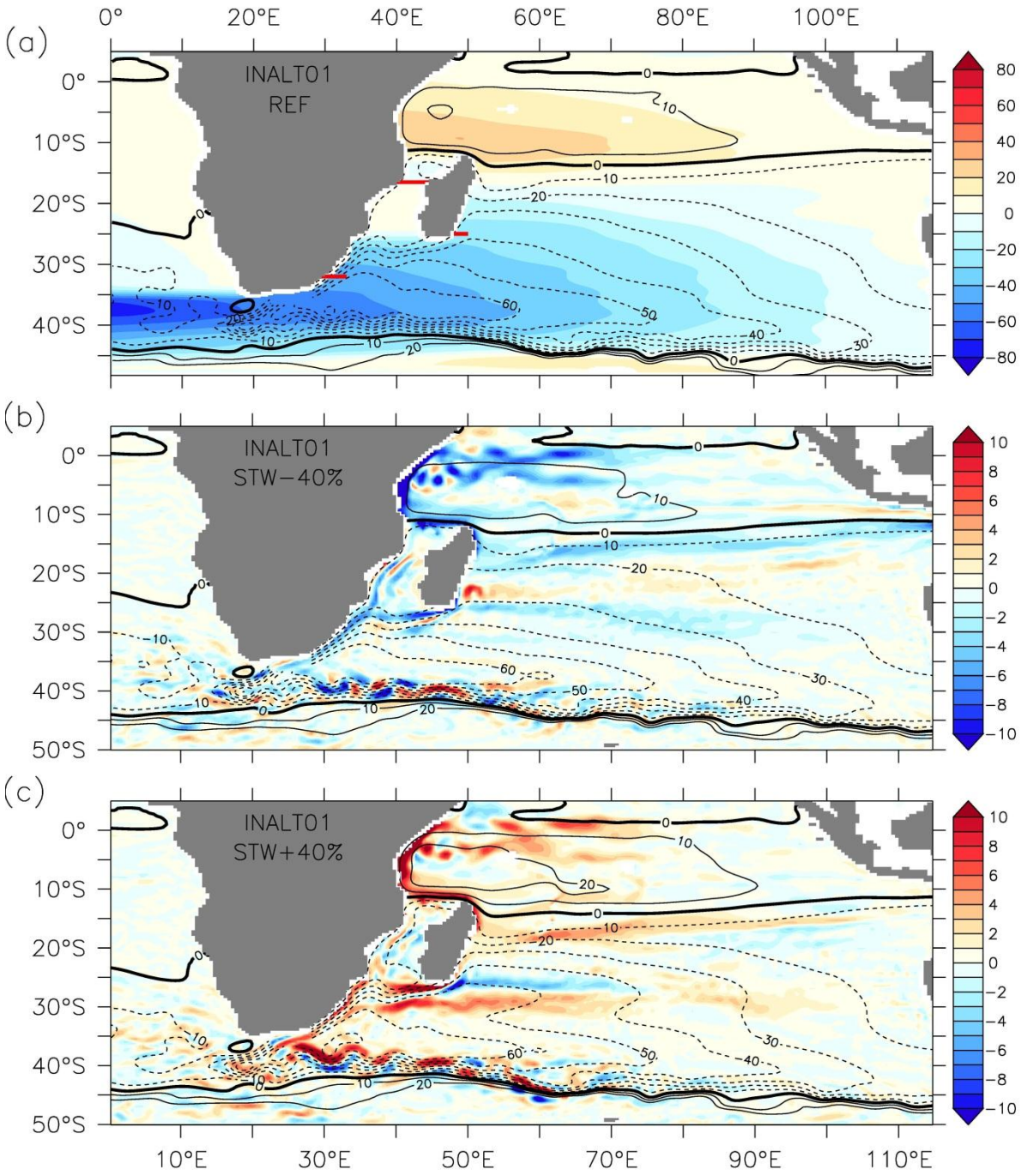


**FIGURE 3.3:** INALT01 time-mean horizontal circulation for model years 41 – 60. (a) REF Barotropic stream-function (contours, Sv) and Sverdrup transport (shading, Sv) calculated from the REF wind stress curl. Sections used to extract the Agulhas Current transport, the Mozambique through-flow and the South East Madagascar Current transport, are shown with red lines. (b) & (c) Barotropic stream-function (contours, Sv) and 100 m speed anomaly (shading, cm $s^{-1}$) for the STW-40% and STW+40% cases respectively. Negative stream-function indicates anti-clockwise circulation.

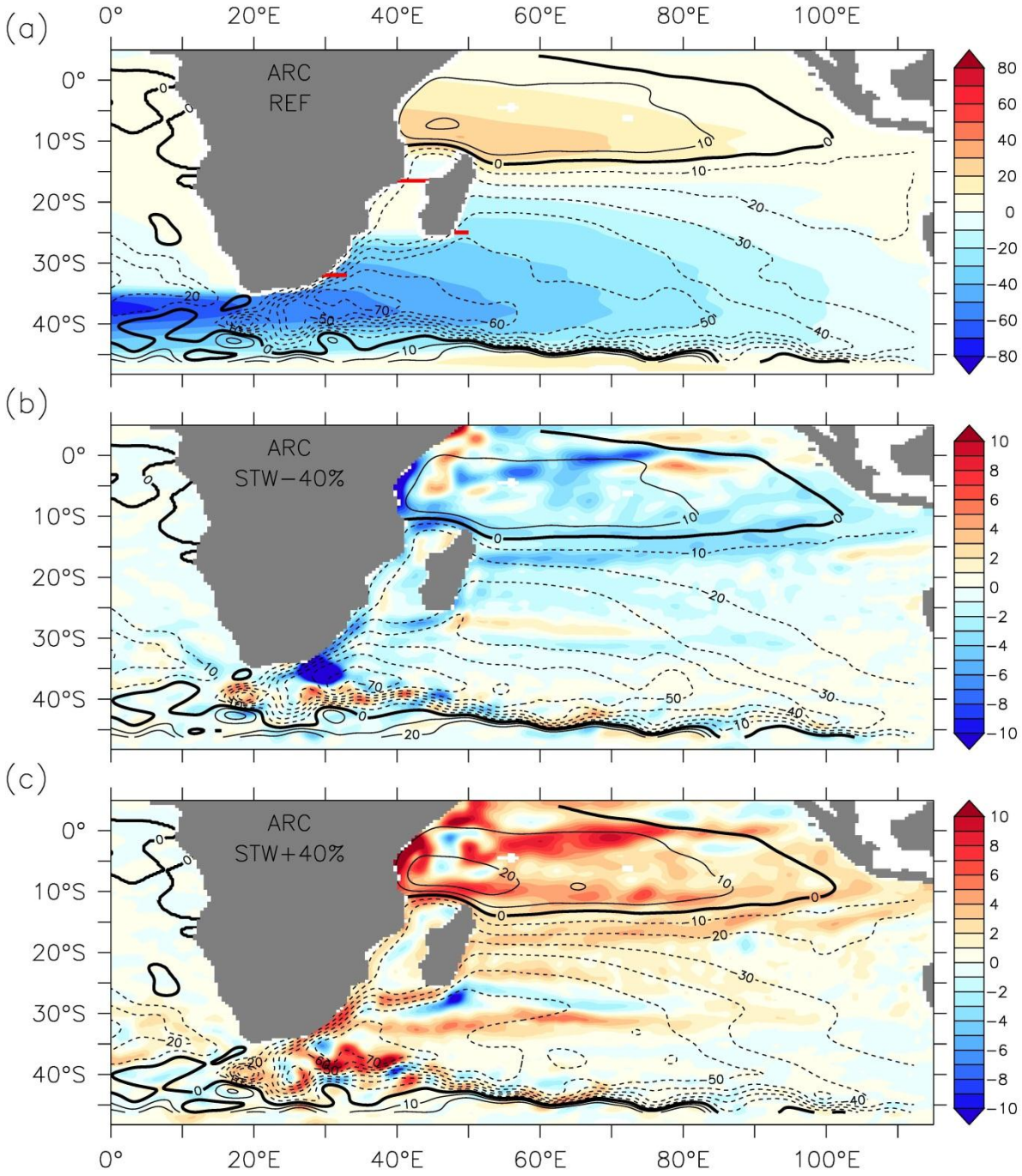


**FIGURE 3.4:** Same as Figure 3.3 for the ARC configuration.

## 3.2. Basin-scale circulation response to altered trade winds

Figures 3.3 & 3.4 show the response of the basin-scale circulation to changes in trade winds within INALT01 and ARC respectively. The general structure of the Indian Ocean circulation is adequately represented within both configurations (Figures 3.3a & 3.4a). Away from the western boundary, Sverdrup theory describes the depth-integrated flow resulting from the surface wind stress. It captures well the general pattern of subtropical gyre circulation of the South Indian Ocean. The

transport values from Sverdrup calculation being lower indicate that the wind only partly contributes to the barotropic flow (Marshall and Plumb 2007). Modifying the intensity of the Indian Ocean trade winds by ±40 % between the Equator and 32.5°S has a significant effect on both the tropical (0° – 12°S) and subtropical (12°S – 32.5°S) circulations (Figures 3.3b,c & 3.4b,c). It is important to note that no disruptions in the horizontal circulation occur as a result of the regional application of the wind stress anomalies. The surface flow of the wind-driven South Equatorial Current, roughly along 15°S (Heywood et al. 1994), is enhanced (weakened) with increasing (decreasing) strength of the trades. This current in turn feeds into the North and South East Madagascar Currents (Swallow et al. 1988), and both respond to the altered wind conditions. Between 22°S and 26°S, the narrow eastward flowing subtropical South Indian Ocean Counter-Current, extending from the island of Madagascar to about 90°E (Siedler et al. 2006), is enhanced at weaker trade winds (Figure 3.3b). Conversely it is somewhat suppressed at stronger winds (Figure 3.3c). Within ARC, this current is represented along 27°S; the slight shift is likely due to the coarse resolution of ARC's base model. Changes in flow speed and transport of the source regions of the Agulhas Current, namely the Mozambique Channel through-flow and the South East Madagascar Current (SEMC), concordantly respond to the altered trade winds. This can be observed within both nested configurations.

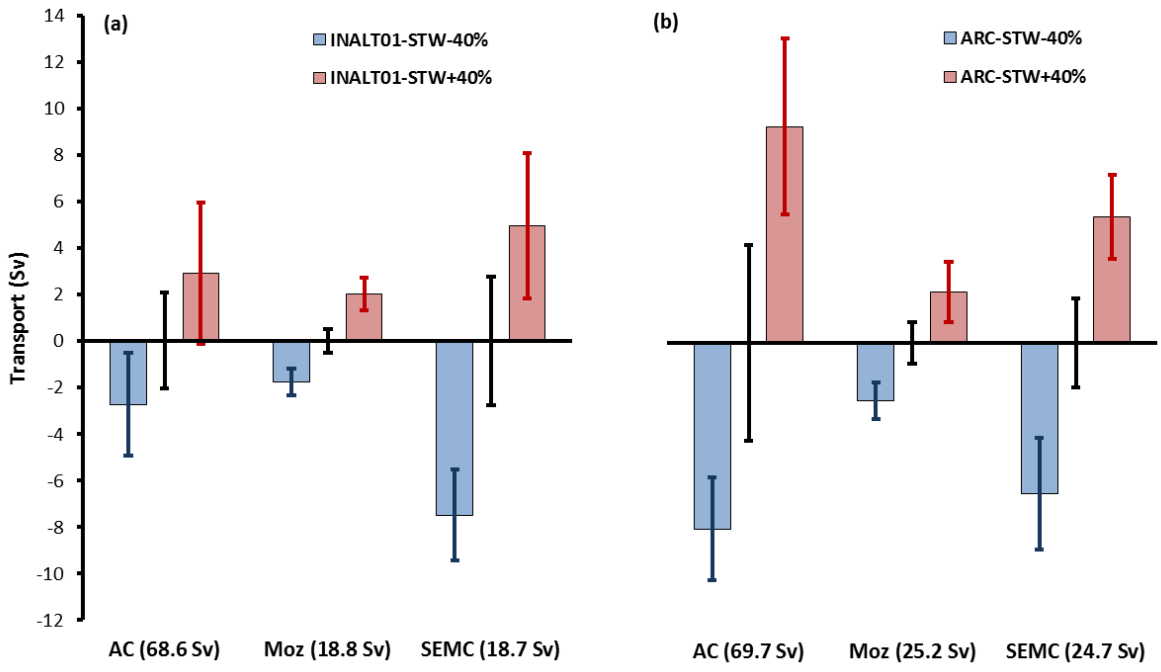


**FIGURE 3.5:** Barotropic transport anomaly (Sv) for (a) INALT01 and (b) ARC. REF experiment set at zero, and time-mean values given in labels. Bars indicate the difference in transport between the STW-40% (blue) and STW+40% (red) experiments respectively. Error bars show the respective inter-annual standard-deviations. Sections used to extract the respective transports are shown in Figure 3.3a & 3.4a.

Slight differences in upper ocean speed between INALT01 and ARC reflect the dissimilarity in bulk formulation employed. Within the NEMO configurations (ORCA05 & INALT01) turbulent fluxes were calculated relative to the ocean surface velocity (Large and Yeager 2009), while within the ROMS configurations (AGIO & ARC) the effect of surface currents were deemed negligible (Fairall et al. 1996). While both strategies have their own merits, pronounced regional differences occur particularly where the wind opposes currents (Zhai et al. 2012). In these instances, when ignoring surface motions (within ARC), the wind imparts more mechanical energy to the currents. Conversely, taking surface motions into account dampens the flow, as it is the case within INALT01. In addition, large-scale gyres are typically strengthened in cases where surface currents are excluded (Duhaut and Straub 2006; Zhai et al. 2012). The choice to whether or not consider ocean surface velocities in wind stress calculation is a matter of current contention in the modelling community (Böning, pers. comm.). Notwithstanding, the general pattern of the response being similar within both configurations provides confidence in the results.

The changes in barotropic transport of the Agulhas Current at 32°S, of the Mozambique Channel through-flow, and of the SEMC are shown in Figure 3.5. These transports were measured along sections shown in Figures 3.3a & 3.4a for the respective model configurations. The mean transports through the Mozambique Channel and of the SEMC are higher within ARC than within INALT01. Nevertheless, altering the intensity of the trade winds by ±40 % consistently produces symmetric responses in transport in the source regions. Both configurations show pronounced changes in SEMC transport; approximately ±33 % and ±24 % for INALT01 and ARC respectively. Due to the shielding effect of Madagascar, where the integrated wind stress curl is interrupted (Penven et al. 2006), changes in the flow through the channel are smaller, about ±10 % within both INALT01 and ARC. Changes in the source regions are communicated downstream. Transport change of the Agulhas Current within ARC is commensurate in magnitude to the combined contributions coming from the Mozambique Channel and South of Madagascar. Within INALT01, however, the response of the Agulhas Current at 32°S is less marked. Recirculation within the subgyre south of Madagascar between 30°E – 50°E and 35°S – 40°S constitutes a third source of Agulhas Current waters (Stramma and Lutjeharms 1997). On average, the subgyre within ARC (Figures 3.4a) is stronger than within INALT01 (Figures 3.3a), explaining the enhanced Agulhas Current transport. The modifications in transport shown in Figure 3.5 are significantly different from the respective reference means at the 99 % confidence level (Welch's t-test[1]). Despite the differences between the global and the regional

[1] Details of the significant tests are in supplementary material S1.1.

configurations, the response of the Agulhas system to changes in trade intensity is consistent, and therefore, robust.

In the South Atlantic, west of 10°E, little to no changes in circulation in neither barotropic nor surface flows are observed (Figures 3.3 & 3.4). This would indicate that, downstream of the Agulhas Current, the inter-ocean transfer is unaffected.

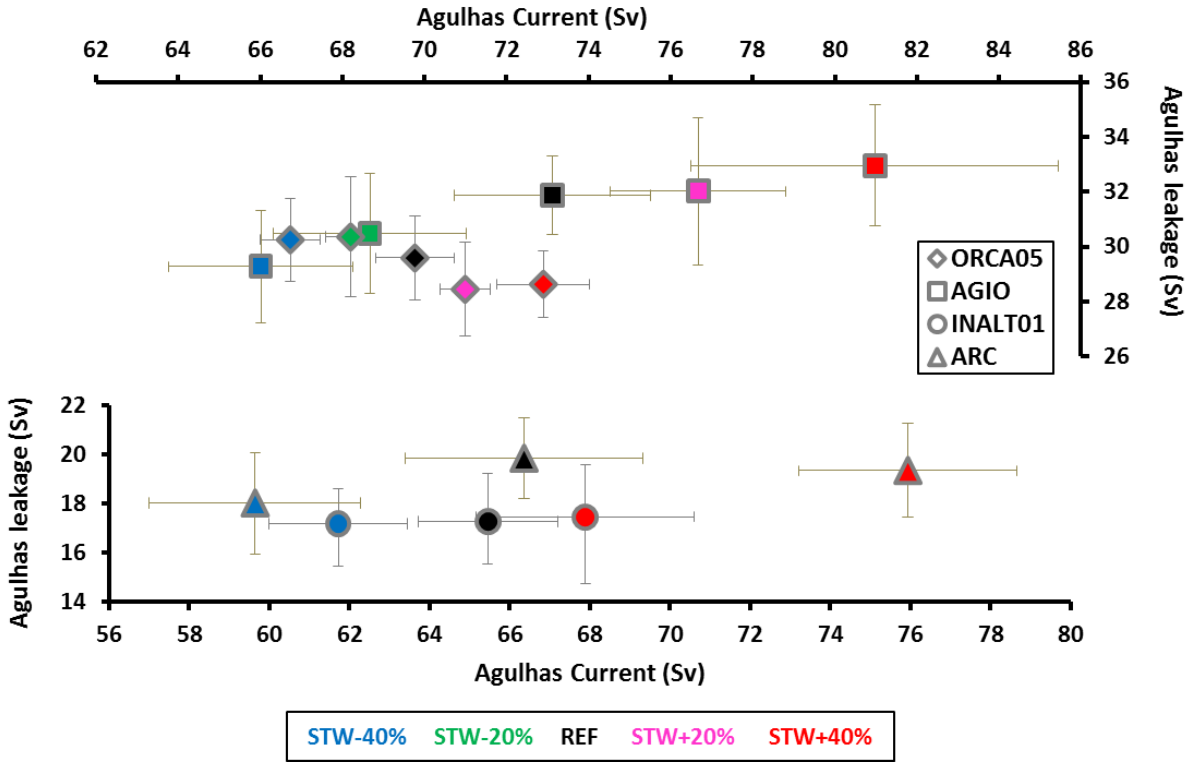


**FIGURE 3.6:** Agulhas leakage versus Agulhas Current transport (Sv) for all configurations. Each point represents a 20 year average (model years 41 – 60), and error bars represent detrended inter-annual standard-deviations.

## 3.3. Agulhas Current and Agulhas leakage decoupling

The response of Agulhas leakage to the Agulhas Current transport changes for all experiments (Table 3.1) within all four configurations is summarised in Figure 3.6. Each data point represents a 20-year average (model years 41 – 60, Figure 3.2) and the error-bars indicate the detrended inter-annual standard-deviation. In general, largest responses are seen within the regional configurations. Modifications of the easterlies intensity result in approximately ±3 to ±9 Sv change from the mean reference Agulhas Current transport. Note that, in contrast to full-depth Agulhas Current transport shown in Figure 3.5, Figure 3.6 considers the poleward-flowing portion of the current (Lagrangian

leakage method described in section 2.5). Despite high inter-annual variability in Agulhas Current transport, within each configuration and for each experiment, the change in transport resulting from the altered trade winds is significantly different from the reference mean at 99 % confidence level[1]. Within the two lower-resolution configurations, ORCA05 and AGIO, Agulhas leakage shows changes ranging between -2 and +1 Sv. At high-resolution, this range decreases. Unlike the response observed in the Agulhas Current transport, the changes in leakage are insignificant at the 99.9 % confidence level[2], and can be accounted for by inter-annual variability (except for the AGIO-STW-40% case).

Figure 3.6, therefore, suggests that leakage is independent from the changes in transport of the incoming Agulhas Current. This confirms the conclusion already observed in Figures 3.3 & 3.4 that the trade winds, which determine the strength of the western boundary current, do not impact the circulation of the southeast Atlantic. In other words, the process behind leakage appears decoupled from the process causing changes in inertia of the current.

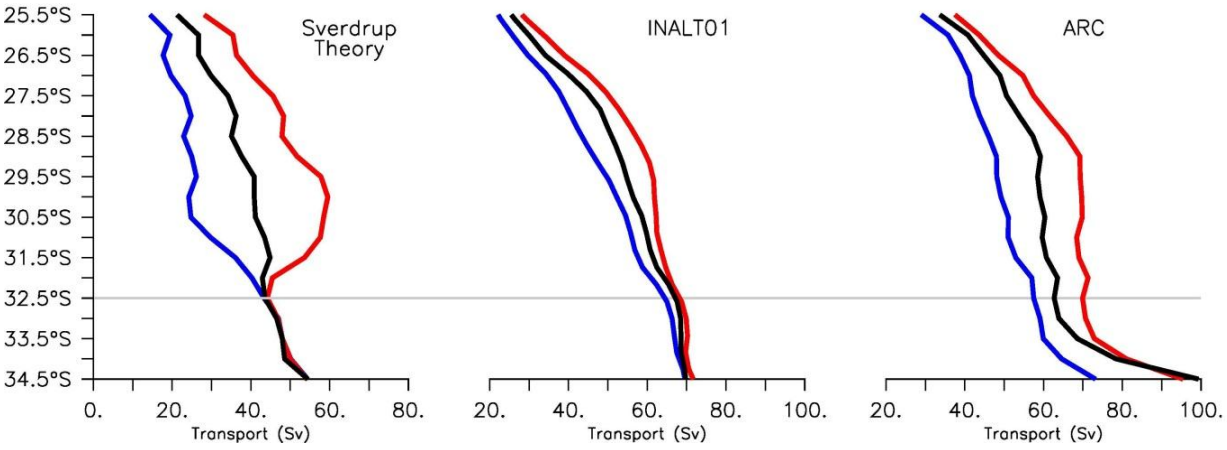


**FIGURE 3.7:** Along-stream Agulhas Current transport predicted by Sverdrup theory (left) and barotropic stream-function within INALT01 (middle) and ARC (right) for the STW-40% (blue), REF (black) and STW+40% (red) experiments. Poleward of 32.5°S, no changes in wind stress were applied.

The magnitude of the Agulhas Current transport, hence, its inertia, increases as it flows along the coast of South Africa (Lutjeharms 2006). This occurs due to the poleward increase in wind stress curl and the beta-effect, recirculation from the southwest Indian subgyre, in addition to non-linear interactions. The portion of the current driven by the wind stress curl and the beta-effect can be predicted from the Sverdrup relation. This is shown in Figure 3.7, and as anticipated, the transport increases with latitude. The application of the STW-40% and STW+40% anomalies linearly and proportionally decreases and increases the transport respectively. Also, by design, the anomalies do

[1] Details of the significant tests are in supplementary material S1.2, Table S1.1.
[2] Details of the significant tests are in supplementary material S1.2, Table S1.2.

not modify the transport of the current poleward of 32.5°S. Additionally shown on Figure 3.7, are the full-depth transports of the western boundary current diagnosed within INALT01 and ARC. It is evident that, due to topographic shielding (Matano et al. 2002) and eddy-mean interactions (Biastoch et al. 2009a), Sverdrup theory under-predict the transport of the Agulhas Current and over-estimate the impact of the applied anomalies on the current's transport. Here again, the effect of the stronger recirculation within ARC is seen. Interestingly, poleward of 32.5°S, where no wind stress anomaly was applied, the change in transport persists. This transmission of inertia along the western boundary is visible within both configurations and could potentially alter the position (Ou and de Ruijter 1986) and/or the energetics (Boudra and De Ruijter 1986; de Ruijter and Boudra 1985) of the retroflection. Figures 3.3 & 3.4 indicate an average retroflection position that is stable. Detailed analysis of the longitudinal position of the retroflection loop for the STW±40% cases within ARC, performed by Loveday et al. (2013), supports this claim further (Figure 3.8). However, Figures 3.9 & 3.10, reveal that downstream momentum transfer plays an important role for the energetics of the greater Agulhas system.

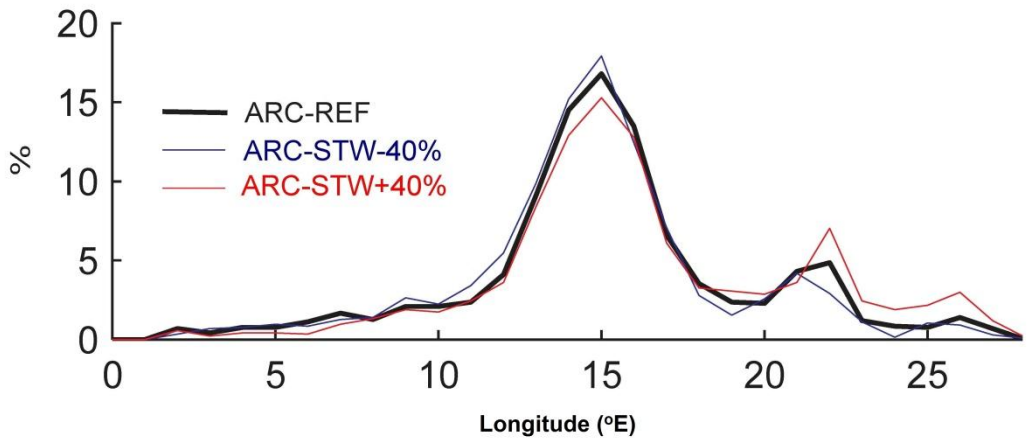


**FIGURE 3.8:** Probability density of retroflection longitude within ARC for the REF and STW±40% cases. Note that despite the fact that retroflection occurs, within this regional model configuration, on average about 4° west of its observed position of ~19°E (Dencausse et al 2010b), altering the Indian Ocean trade winds does not cause a change in retroflection position. Adapted from Loveday et al. (2013).

Mesoscale variability in the Mozambique Channel, induced by modulation of the South Equatorial Current (Backeberg and Reason 2010), is communicated downstream and seen as changes in mean kinetic energy of the northern Agulhas Current between 25°S and 34°S (Figure 3.9a). The retroflection, between 15°E and 30°E, and the Agulhas Return Current, east of 30°E, predominantly respond through changes in eddy kinetic energy (Figure 3.10b,c). It is worth noting the larger responses in eddy energy within ARC than within INALT01 in Figure 3.10. As it was pointed out in

section 3.2, the discrepancy can be attributed to the different methods of calculating turbulent fluxes within the respective configurations. Excluding the effect of ocean surface velocity (as it is the case within ARC) amplifies the wind-driven eddy energy input to the ocean (Hughes and Wilson 2008; Zhai and Greatbatch 2007). However, despite the difference in magnitude, both ARC and INALT01 agree on the sign of the response. Mesoscale variability of the source regions of the Agulhas Current is known to have little impact on the mean leakage into the Atlantic (Biastoch et al. 2008b). It is here shown that large changes in eddy kinetic energy levels of the retroflection region also do not lead to leakage change.

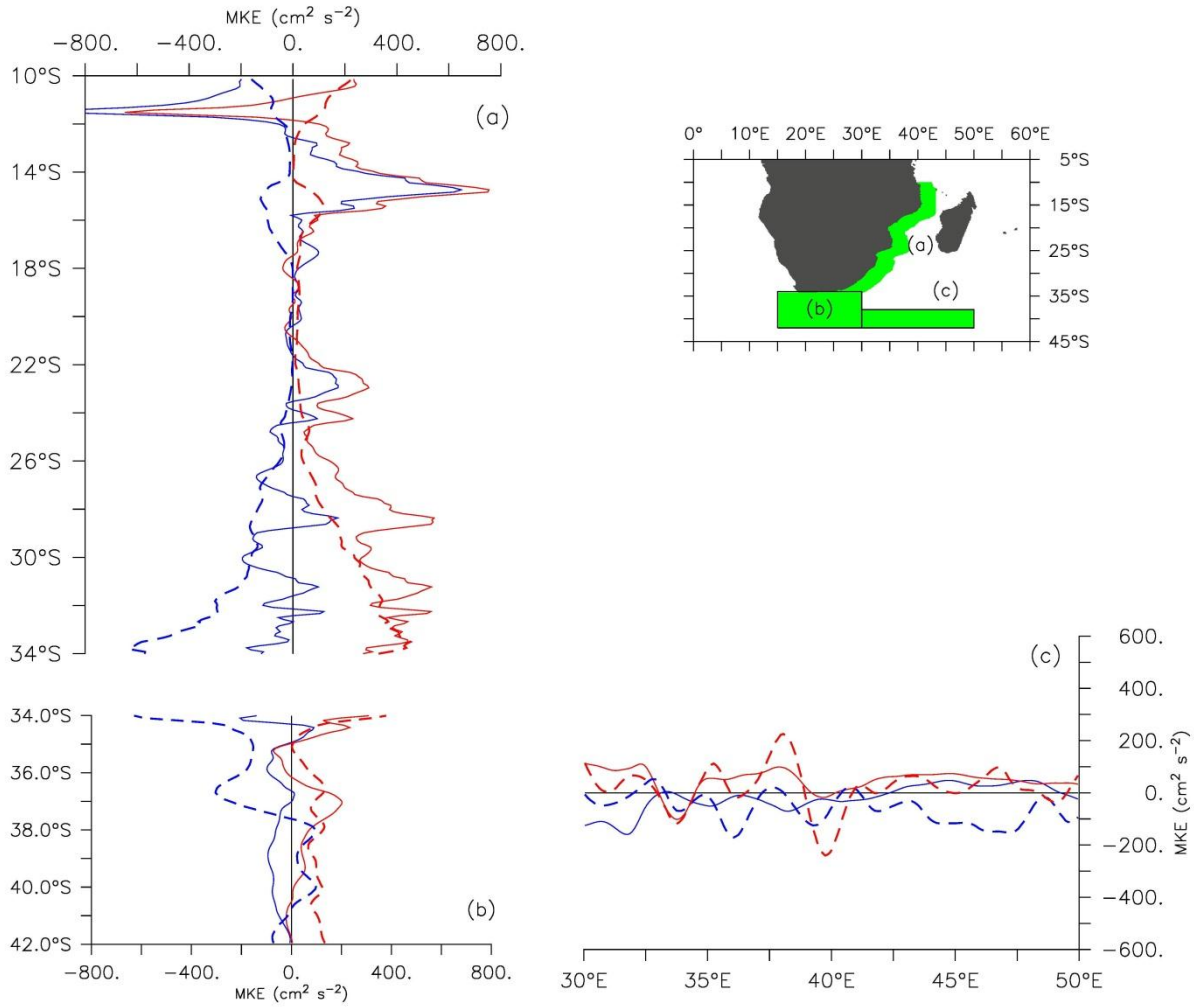


**FIGURE 3.9:** Energy associated with the mean flow of the upper ocean (MKE, $cm^2\ s^{-2}$), along the path of the (a) Agulhas Current, (b) the retroflection and (c) the Agulhas Return Current. MKE anomalies are shown for the STW-40% (blue) and STW+40% (red) experiments with respect to the reference within INALT01 (full lines) and ARC (dashed lines). The inset panel shows the region where spatial averaging was performed.

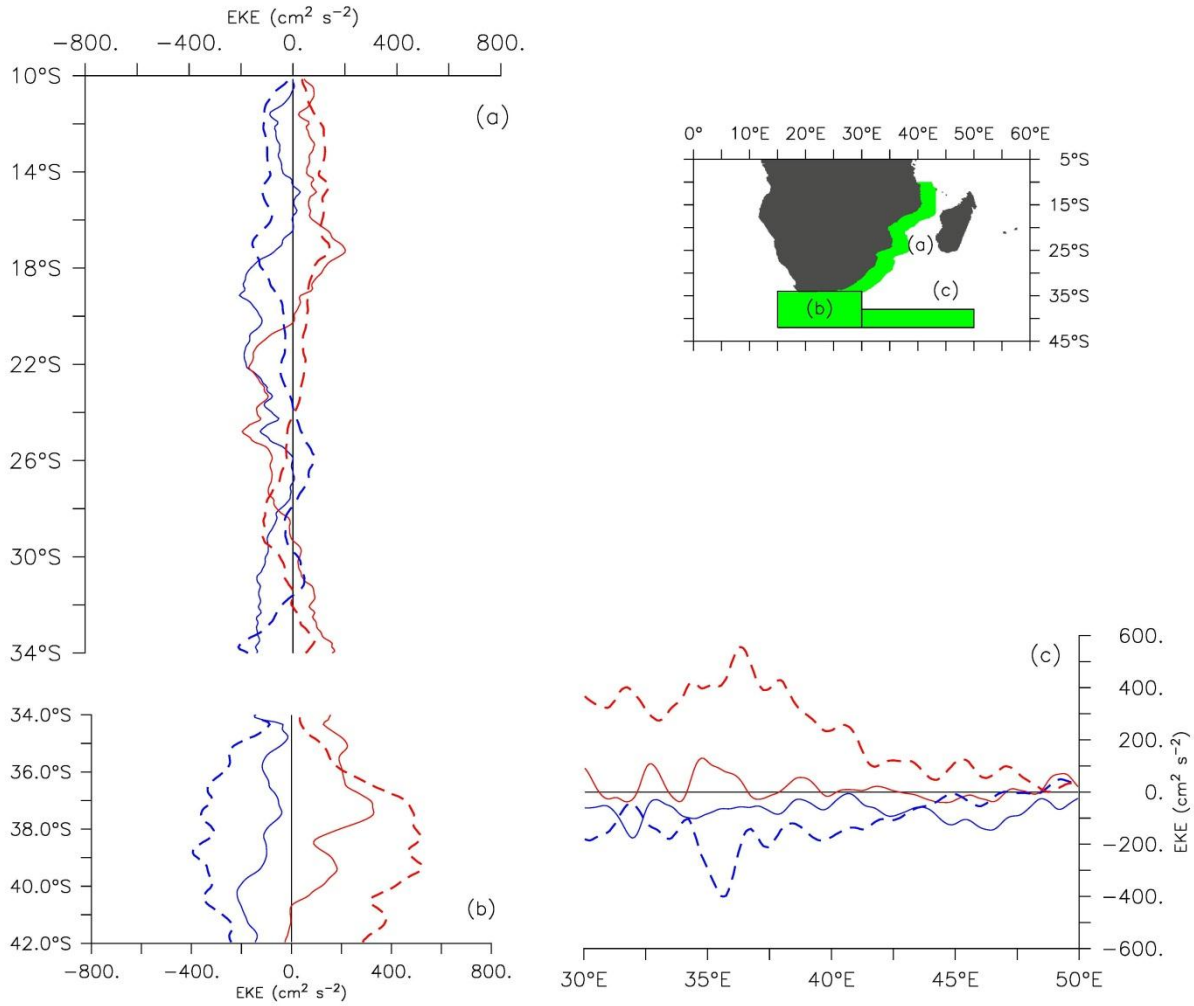


**FIGURE 3.10:** Same as Figure 3.9 but for energy associated with the eddy flow (EKE, $cm^2\ s^{-2}$).

## 3.4. Implications

The results have shown that up to ±40 % changes in the Indian Ocean trade wind intensity give rise to large and significant changes in the Agulhas Current (Figures 3.5 & 3.6), thereby changing its inertia at separation (Figure 3.7). The position of the retroflection loop remains stable (Figures 3.3, 3.4 & 3.8). The stability is believed to be maintained by the locking effect of topography (Dencausse et al. 2010b; Matano 1996). The altered inertia at separation induces large responses in the energetics of the retroflection and of the Agulhas Return Current. Agulhas leakage is unaffected; no significant changes in the Indo-Atlantic transport are noted (Figure 3.6).These results pertain to the steady state (20 year average) response to sustained changes in Indian Ocean trade winds.

Aptly baptised “the Cape Caldron”, the Cape Basin hosts numerous mesoscale features (Boebel et al. 2003a), which have the ability to participate in the thermohaline circulation as Agulhas leakage

(Biastoch et al. 2008b; Weijer et al. 1999, 2002). Given the difficulty in monitoring leakage oceanographically, many attempts have been made to find, so-called, proxy measurement methods. These take advantage of the known behaviour of the Agulhas system and by observing components of the system that are relatively easier to measure. For example, satellite altimetry reveals that the retroflection position abruptly moves east after the expulsion of an Agulhas Ring (Feron et al. 1992; Lutjeharms and van Ballegooyen 1988). Since a large portion of leakage occurs by means of these large rings (van Sebille et al. 2010b), monitoring the displacement of the retroflection loop using satellite measurements may be employed to devise a proxy for Agulhas leakage (van Sebille et al. 2009a). Furthermore, as mentioned at the beginning of this chapter, the source of Agulhas leakage is undisputedly the Agulhas Current. Because it is logistically simpler to measure the current, efforts to relate its transport to the magnitude of Indo-Atlantic flux have been made within model settings (Rouault et al. 2009; van Sebille et al. 2009b). More recently, since model hind-cast studies have revealed a contemporary (over the last 4 decades) increase in Agulhas leakage (Biastoch et al. 2009b; Rouault et al. 2009), attempts have been made to confirm this, using an observed dataset. Backeberg et al. (2012) noted an increase in eddy kinetic energy of the retroflection in the last 17 years (1993 – 2009) from altimetry, and inferred a faster propagation of rings into the Atlantic. How do the results presented in the previous sections relate and compare to these studies? It is of paramount importance to keep in mind the different timescales. In what follows, the distinction is made between the multi-decadal trends noted in the Agulhas Current and leakage from hind-cast model simulations (works of Biastoch et al. (2009b); Rouault et al. (2009) and van Sebille et al. (2009b)) and ~2 decades of observed trends from altimetry (*e.g.* Backeberg et al. (2012); Dencausse et al. (2010a); van Sebille et al. (2009a)).

From 37 years of model output, van Sebille et al. (2009a) studied retroflection events at high-temporal resolutions, and found a linear relationship between retroflection position and leakage. This relationship seems to be valid for the high-frequency (3-months) variability of the retroflection position. The authors subsequently applied the model-derived linear relation to observed sea surface height. With the exception of the early retroflection event of 2001 (de Ruijter et al. 2004; van Aken et al. 2013), they estimated the magnitude of Agulhas leakage to be fairly constant at 13.2 ± 1.5 Sv over the period 1993 – 2009. Furthermore, using the same altimetry dataset over similar periods, Dencausse et al (2010a) reported the retroflection position to be stable, and Backeberg et al. (2012) found an overall increasing eddy kinetic energy trend of the Agulhas system. It can therefore be concluded that, for the observed period 1993 – 2009, it appears that the relationship between leakage and retroflection position and energetics agrees with the results presented here: no change in retroflection mean position, no change in the mean magnitude of Agulhas leakage, but changes in

retroflection energetics. Moreover, the results suggest that for the ~20 year period of observed altimetry measurements, elevated levels of turbulence of the retroflection do not imply increase in leakage. Le Bars et al. (2012) described a retroflection regime whereby increased kinetic energy of the retroflection result in enhanced recirculation and possible loss of water across the discontinuous southern boundary of the Agulhas system (Dencausse et al. 2011). The question that naturally follows is whether or not the relationship is causal and applicable on longer timescales.

On multi-decadal timescales, in particular, the last 40 years, Agulhas leakage has been increasing by about 1.2 Sv / decade (Biastoch et al. 2009b; Rouault et al. 2009; van Sebille et al. 2009b). Such a trend is also reproduced by the inter-annually forced simulations performed using the four model configurations presented in chapter 2 (Figure 2.9). It should be noted that in line with altimetric observations, for the period 1992 – 2003, a flattening trend in leakage is also observed in Figure 2.9. This epitomises the importance of timescales when dealing with Agulhas leakage trends. Nonetheless, Rouault et al. (2009) and van Sebille et al. (2009b), using different theoretical arguments, linked the reported multi-decadal trend to the dynamics of the Agulhas Current (section 1.4). The results presented here show that changes in the Agulhas Current alone do not translate to changes in leakage. It appears that the mechanism behind Agulhas leakage change is independent on changes in the incoming transport of the Agulhas Current. This will be examined in the following chapter.

For multi-centennial to millennial timescales, for instance, during the Last Glacial Maximum (approximately 20,000 years ago), Peeters et al. (2004) inferred reduced leakage from foraminifera assemblages. Yet, Franzese et al. (2009) reconstructed the pathway of the Agulhas Current using strontium isotopes, and reported no change in the retroflection position. This could possibly indicate that the process driving changes in leakage is not the same to that establishing the location of retroflection in the long term.

In light of the above discussion, it is evident that a correct representation in models of the retroflection position and energetics is paramount to the understanding of the controls of the exchange between the Indian and Atlantic Oceans. In Figure 3.6, differences in leakage change between the low (ORCA05 & AGIO) and high (INALT01 & ARC) resolution configurations were observed. Despite being statistically insignificant, ORCA05 and AGIO displayed some changes in Agulhas leakage. These can be attributed to the fact that the mesoscale energetics of retroflection are not represented within ORCA05 and over-represented within AGIO (Figure 2.5). This is in addition to the coarse representation of the topography which could impact the locking effect of

retroflection. At high resolution (INAT01 & ARC), these properties of the retroflection are adequately resolved. Hence, the model solutions converge to the conclusion that Agulhas leakage is decoupled from the Agulhas Current.

## 3.5. Summary

In this chapter, the possibility of a link between the Agulhas Current and Agulhas leakage was examined. In particular, the question of whether or not Agulhas leakage responds to changes in inertia of its associated western boundary current was explored. In order to induce changes in the Agulhas Current, the easterly trade winds of the Indian Ocean were altered within two global (ORCA05 & INALT01) and two regional (AGIO & ARC) model configurations. Agulhas leakage was monitored within all four configurations using the same approach, thus enabling inter-model comparison. Experiments were carried out whereby smooth anomalies were added to climatological wind stress in order to stimulate the Indian Ocean trade winds intensity by ±20 % and ±40 %. The anomalies were designed to induce changes to the wind stress only between the Equator and 32.5°S.

Many of the prominent features of the Indian Ocean respond linearly to the altered trade winds. These include the South Equatorial Current, the North and South East Madagascar Current and the Mozambique through-flow. The latter two constitute two important sources of Agulhas Current waters. While the Agulhas Current (at 32°S) responds to these modifications with significant changes in its transport, no significant change in Agulhas leakage is observed. Despite the fact that poleward of 32.5°S, no modifications were applied to the wind stress, upstream changes in the Agulhas Current is communicated downstream and the inertia at separation is altered. Moreover, the mean position of the retroflection loop remains stable in all cases. As a result, no changes in leakage occur. Instead, the retroflection mediates the upstream change through large mesoscale energy anomalies.

# 4. Agulhas leakage responds to the Southern Hemisphere westerlies

The content of this chapter appears in the following publication:

Durgadoo J.V., B.R. Loveday, C.J.C. Reason, P. Penven, A. Biastoch (2013) – Agulhas leakage predominantly responds to the Southern Hemisphere westerlies. *Journal of Physical Oceanography*, in press, doi:10.1175/JPO-D-13-047.1

The Agulhas system is sandwiched between two major wind belts, namely the southeast trades, between the Equator and about 30°S, and the westerlies, over roughly 30°S – 60°S. The trade winds are largely responsible for the inertia of the Agulhas Current. Chapter 3 demonstrated that large changes in the upstream transport of the Agulhas Current, induced by changes in trade winds, had almost no effect on the magnitude of Agulhas leakage. Despite large localised changes in both mean and eddy kinetic energy, the mean retroflection position remained stable, consistent with observed present-day (Dencausse et al. 2010b) and reconstructed past (Franzese et al. 2009) measurements. The locking effect of local topography on the retroflection position resulted in Agulhas leakage to be unaffected. The increase in kinetic energy possibly leads to a recently described turbulent retroflection regime (Le Bars et al. 2012), where leakage is no longer dependent on the incoming transport.

Given this decoupling between Agulhas leakage and Agulhas Current inertia, this chapter explores the possible dependency of leakage on the Southern Hemisphere westerlies. The position and magnitude of the westerly wind belt were systematically altered within three model configurations: ORCA05, AGIO and INALT01. The strategy employed is similar to that in chapter 3. The model configurations were all forced by the same atmospheric data (section 2.3), and consistent diagnostics (section 2.5) were derived. In so-doing, the aim is to disentangle the relationship between the magnitude of Agulhas leakage and the location and strength of the westerlies. It is found that Agulhas leakage responds predominantly to the westerlies. In addition, the response is transient and dependent on the large-scale adjustment.

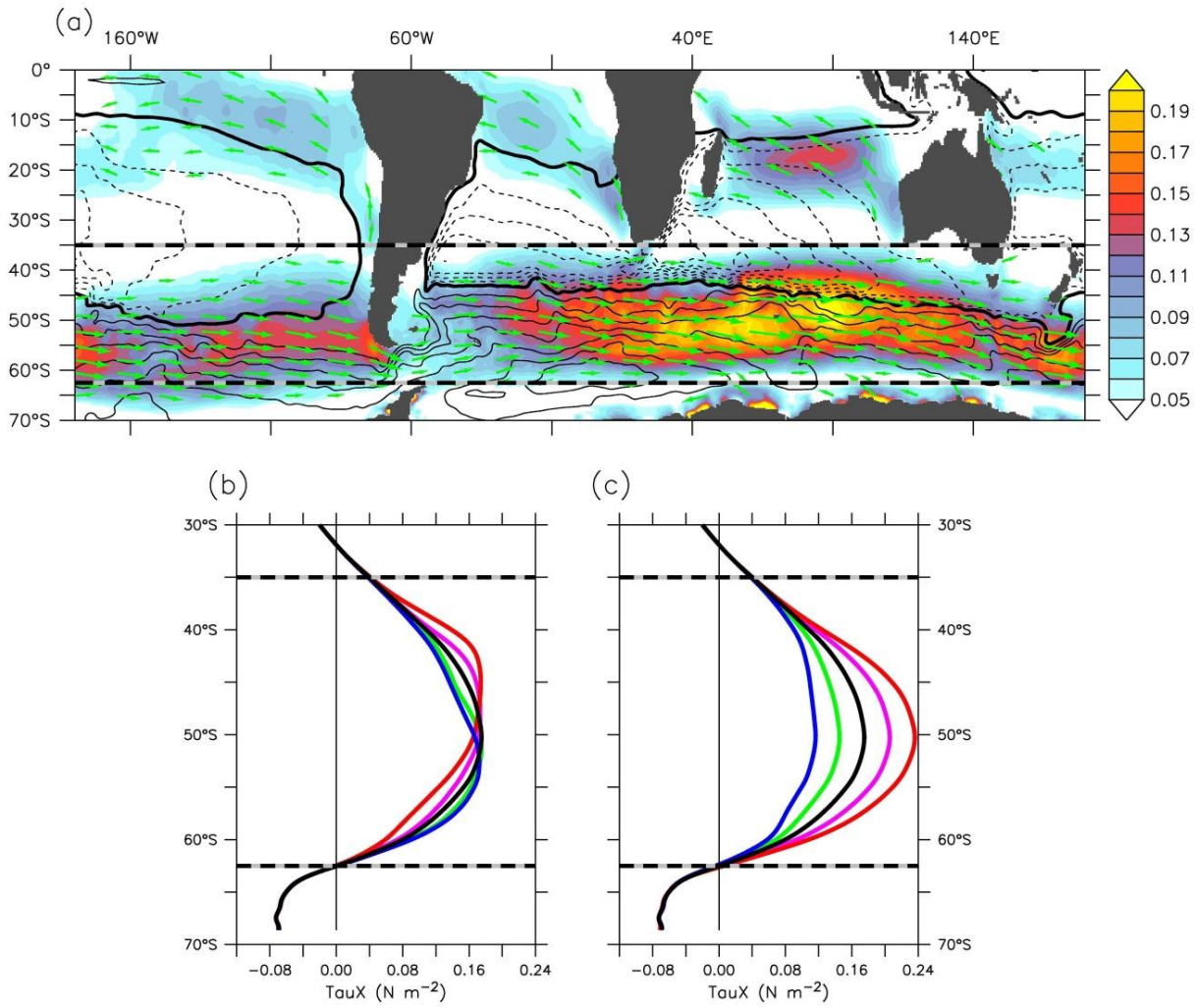


**FIGURE 4.1:** (a) Wind stress magnitude (shading, N $m^{-2}$) and direction (vector) with horizontal barotropic stream-function contours overlay (data extracted from ORCA05-REF experiment); contour interval at 10 and 25 Sv for negative (dashed line) and positive (full lines) values respectively, thick contour represent the zero-line. (b) and (c) Zonally averaged (20°E – 115°E) wind-stress (N $m^{-2}$) with thick black curve indicating the time- reference case. (b) Westerly position altered by -4° (blue), -2° (green), +2° (pink) and +4° (red) about the mean (black), without changing the total energy input. (c) Intensity change by -40 % (blue), -20 % (green), +20 % (pink), and +40 % (red) of the mean (black). Wind changes are applied within the region 35°S – 63°S. Taken from Durgadoo et al. (2013).

## 4.1. Experiment design

The experiments performed are to some extent similar to those presented by Oke and England (2004), Sijp and England (2008, 2009), and more recently Biastoch and Böning (2013), who performed their study within AG01 (forerunner of INALT01). Anomalies applied to the present-day wind patterns (Figure 4.1a) were designed to mimic different states in westerlies regime; equatorward and poleward shifts of ±2° and ±4° of latitude (Figure 4.1b), and intensity changes of ±20 % and ±40 % (Figure 4.1c). The values chosen roughly span the range of observed (Swart and

Fyfe 2012), 21st century projected (Fyfe and Saenko 2006; Fyfe et al. 2007), as well as past (Hodgson and Sime 2010; Sime et al. 2013) changes in westerly winds. These anomalies have a smooth shape to avoid any sharp changes or disruptions in the general wind stress curl pattern that would alter the general pattern of the circulation. Additional design considerations were: (*i*) Changes to the westerlies were limited to south of 35°S such that no changes were applied to the latitudes that would influence the inertia of the western boundary current; (*ii*) Shifts were constructed based on the latitudinal location of the maximum wind stress and the total energy input kept constant; (*iii*) The meridional wind stress component were unchanged. These considerations imposed limits on the extent to which the westerlies could be altered.

| | | | Model Configurations | | |
|---|---|---|---|---|---|
| **Experiment** | **Domain** | **Description** | **ORCA05** | **AGIO** | **INALT01** |
| IA | n/a | Inter-annual Reference | 1948 – 2007 | 1948 – 2007 | 1948 – 2007 |
| REF | n/a‡* | Climatological Reference | 1 – 110 | 1 – 60 | 1 – 60 |
| SHW+4 | FULL | 4° Equatorward shift | 31 – 60 | | 31 – 60 |
| SHW+2 | FULL | 2° Equatorward shift | 31 – 60 | | |
| SHW-2 | FULL | 2° Poleward shift | 31 – 60 | | 31 – 60 |
| SHW-4 | FULL | 4° Poleward shift | 31 – 60 | | |
| SHW-40% | FULL | 40 % Intensity decrease | 31 – 110 | 31 – 60 | 31 – 60 |
| | BASIN | | 31 – 60 | | |
| | LOCAL | | 31 – 60 | | |
| SHW-20% | FULL | 20 % Intensity decrease | 31 – 60 | 31 – 60 | |
| SHW+20% | FULL | 20 % Intensity increase | 31 – 60 | 31 – 60 | |
| SHW+40% | FULL‡* | 40 % Intensity increase | 31 – 110 | 31 – 60 | 31 – 60 |
| | BASIN | | 31 – 80 | | |
| | LOCAL | | 31 – 80 | | 31 – 60 |
| | ACC-P | | 31 – 60 | | |
| | ACC-B | | 31 – 60 | | |
| | ACC-L | | 31 – 60 | | |
| | ACC | AGIO boundary condition* | n/a | 31 – 60 | n/a |

‡These simulations, within ORCA05 only, were also performed with the Gent and McWilliam (1990) eddy parameterisation; *Further details in text.

**TABLE 4.1**: Sensitivity experiments and their integration periods (in years). IA: Inter-Annual; REF: Reference; SHW: Southern Hemisphere westerlies. Domain decompositions for the SHW±40% experiments (grey shading) are depicted in Figure 4.2. Taken from Durgadoo et al. (2013).

The resulting anomalies were reproduced onto the respective model-grids. Out of the 8 anomalies (Figure 4.1b,c), a total of 15 anomaly fields were produced (Table 4.1). For some anomalies, in particular the SHW+40% anomaly (westerlies intensity increase by 40 %), in addition to changing the intensity of the wind stress, the region over which these anomalies were applied was also altered

(Figure 4.2). These geographical decompositions attempt to determine the influence the Antarctic Circumpolar Current may have on the Agulhas system. For these cases, additional smoothing was applied along the boundaries in order to avoid spurious circulations (Figure 4.3). The 2-dimensional wind anomaly fields were added after calculation of the wind stress through bulk formula. Thus, the application influences the momentum and not the buoyancy input to the ocean/sea-ice.

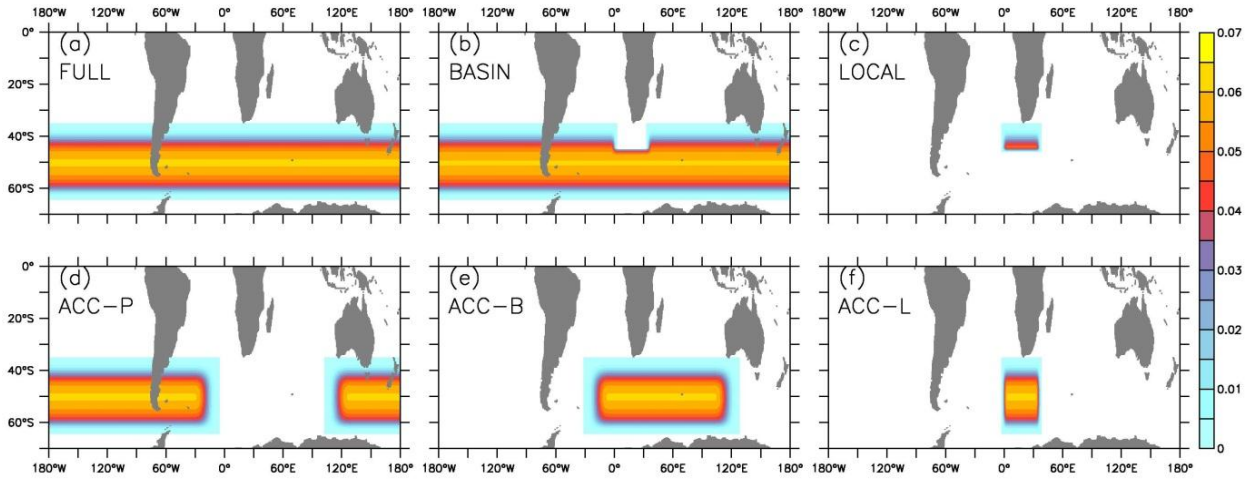


**FIGURE 4.2:** Application of the SHW+40% anomaly (40 % intensification of westerlies). The wind stress anomaly (N $m^{-2}$) is applied (a) circumpolarly (FULL); (b) circumpolarly except the region bounded by 0° – 35°E, north of 45°S (BASIN); (c) only over the region bounded by 0° – 35°E, north of 45°S (LOCAL); (d) over region west of 18°E and east of 115°E (ACC-P); (e) between region 18°W – 115°E (ACC-B); and (f) between region 0° – 35°E (ACC-L). Taken from Durgadoo et al. (2013).

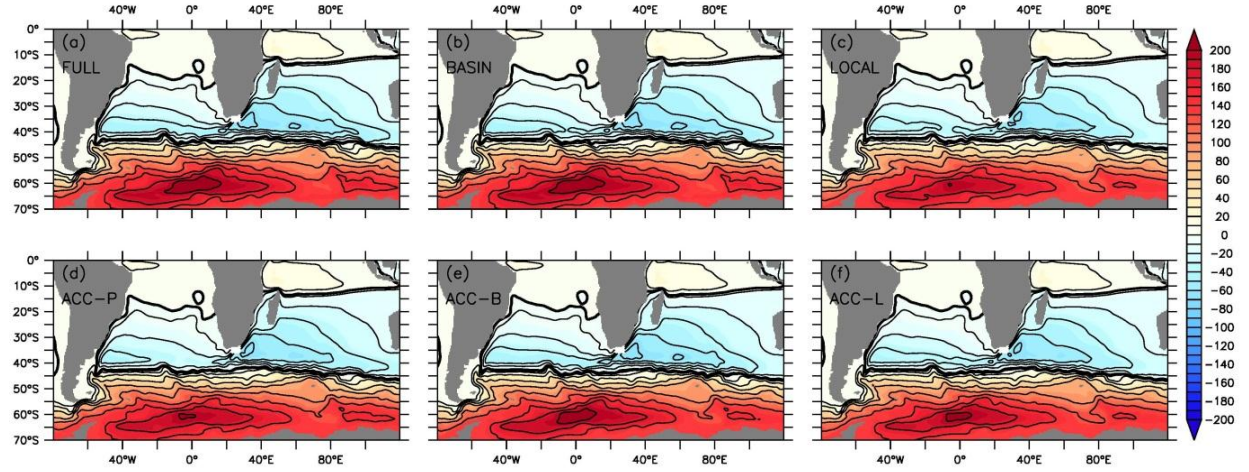


**FIGURE 4.3:** Barotropic stream-function (Sv) illustrating the horizontal circulation during the first decade (average over model years 31 – 40) after application of the geographically decomposed SHW+40% anomaly (shown in Figure 4.2) within the ORCA05 configuration. The general pattern of the horizontal circulation is not affected by the application of the anomalies.

All three model configurations, sharing the same 20-year spin-up history, were forced under background CORE climatological forcing. Figure 4.4 exemplifies the adjustment of the models. A

relatively fast adjustment in volume integrated kinetic energy to changes in resolution and forcing (application of anomaly) is noted. The reference experiments were integrated for 30 years before application of the anomalies. At first they were applied with a linear ramp-up over one year (model year 31) and subsequently in full. Reference and sensitivity simulations ran in parallel from model year 31. After two decades of parallel integration, analysis for all simulations was performed for a common period of 10 years (model years 51 – 60, blue shading Figure 4.4). The increasing kinetic energy after model year 45 in the global configurations for the SHW+40% examples shown in Figure 4.4 reflects the transient response of the Agulhas system to the enhanced winds. This is discussed in section 4.3. Some selected experiments were extended, as outlined in Table 4.1. The model configurations were additionally integrated under inter-annually varying surface forcing, providing 6 decades (1948 – 2007) of hind-cast simulations.

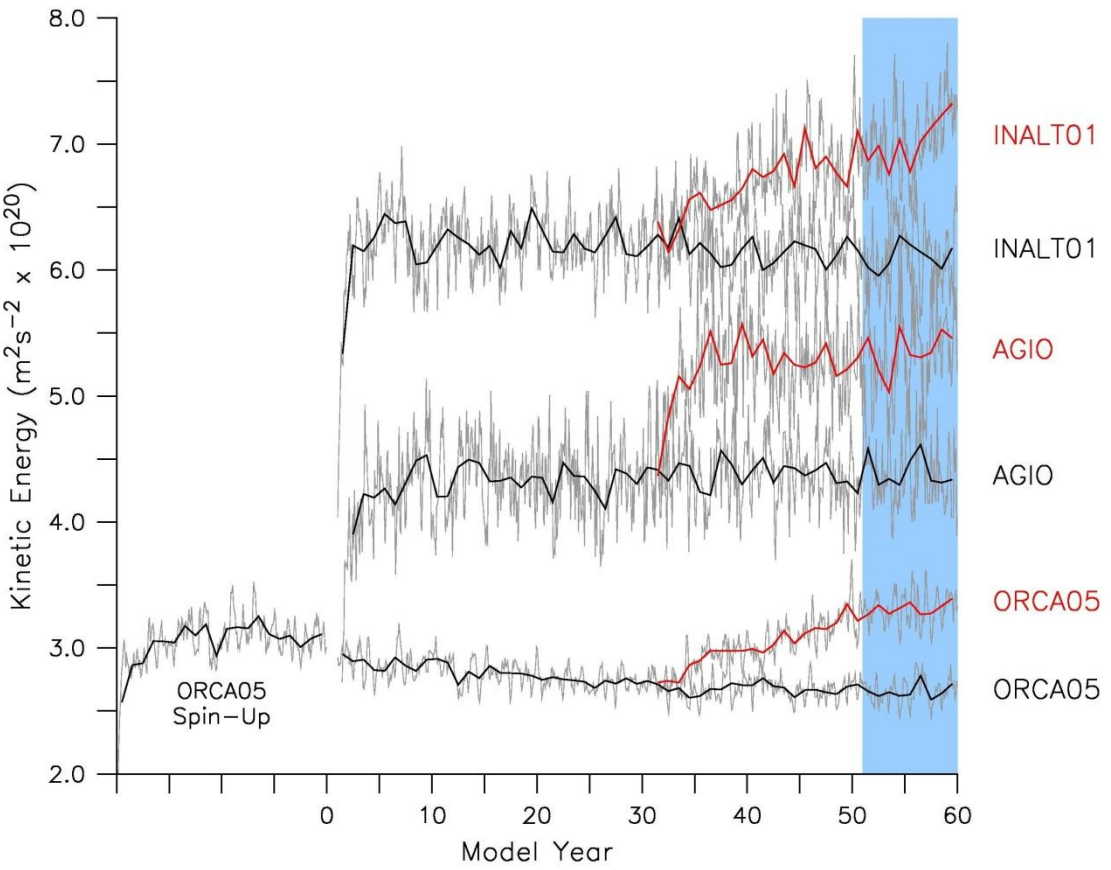


**FIGURE 4.4:** Volume integrated (10°W – 60°E; 10°S – 45°S) kinetic energy per unit mass ($m^2$ $s^{-2}$) with annual values (thick lines) overlaying monthly values (grey). Following a 20 year spin-up, reference (REF, black lines) experiments were performed for all three configurations. Wind anomalies were added from year 31; example of the SHW+40% (red lines) runs is shown. For the purpose of clarity, INALT01 values are offset by 1 x $10^{20}$ $m^2$ $s^{-2}$. Common analysis period (model years 51 – 60) for Figure 4.5 is indicated by the blue shading. Taken from Durgadoo et al. (2013).

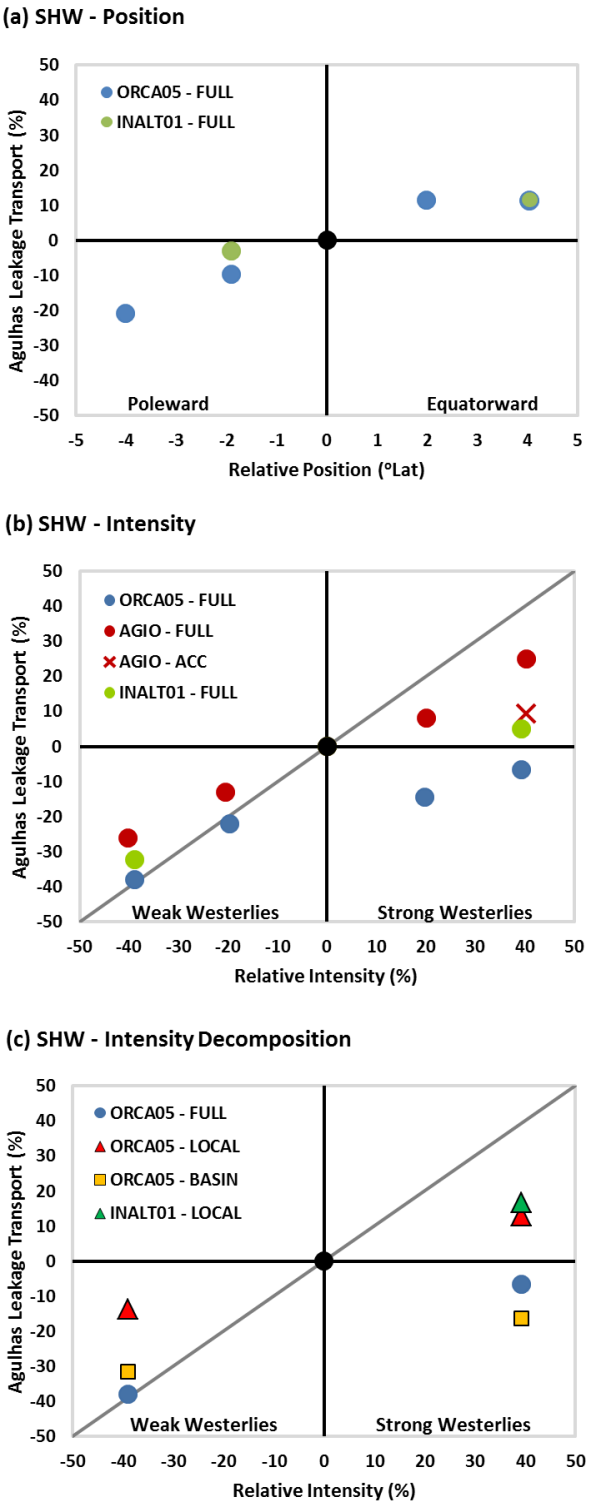


**FIGURE 4.5:** Change in Agulhas leakage (%) versus change in (a) position (°Lat) and (b & c) intensity (%) of the Southern Hemisphere westerlies (SHW). Reference values (black dot) are set at the origin for all three models and each dot represents a decade average (model years 51 – 60, blue shading in Figure 4.4). (c) The decompositions between FULL, BASIN and LOCAL are shown for the SHW-40% and SHW+40% cases. The grey lines in b & c represent the theoretical change in Sverdrup transport. Taken from Durgadoo et al. (2013).

## 4.2. Agulhas leakage equilibrium response

Using the method of determining Agulhas leakage described in section 2.5, values for model years 51 – 60 of the three REF experiments are 31.9 ± 1.5, 31.5 ± 1.4 and 16.6 ± 1.7 Sv for ORCA05, AGIO and INALT01 respectively. Owing to these different reference values of Agulhas leakage within the three configurations, the percentage change with respect to reference is adopted here as a measure of leakage response. This places all reference values at the origin. The 10-year-mean (model years 51 – 60) leakage response to changes in position (Figure 4.5a) and intensity (Figure 4.5b) of the westerlies display three clear patterns. Firstly, within the global configurations, an equatorward (poleward) shift in westerlies produces an increase (decrease) in leakage. Note that AGIO's southern boundary at 48°S makes shift experiments not sensible. Secondly, increasing westerlies intensity generally produces more leakage, but the relationship is not completely linear. Finally, leakage responds preferentially, and the magnitude of that response is more pronounced when changes are applied to the westerlies intensity than shifts. For this reason, the focus is set on the intensity cases. A discussion of the shift cases will be done in section 4.5. Interestingly, for strong wind stress in Figure 4.5b, both global configurations simulate very little leakage change and even reduction compared to the reference values. Conversely, a 20 % and 40 % reduction in wind stress produces approximately the same amount of leakage decrease. Consistent with Le Bars et al. (2012), there appears to be a threshold in leakage response to increased westerlies.

In order to investigate the reason for this threshold, additional experiments were carried out for the two extreme intensity cases, SHW±40%, within ORCA05. The Agulhas system, forming part of the subtropical gyres of the South Atlantic and South Indian Oceans (Ridgway and Dunn 2007) and bounded by the Antarctic Circumpolar Current (Figure 1.4), potentially could be influenced by numerous external factors. Therefore, in an attempt to distinguish between local and large-scale wind impact on leakage, a geographical decomposition of the SHW±40% experiments was performed (Figure 4.2a-c). The use of the coarse resolution ORCA05 configuration was favoured, since it is computationally less demanding. The response shown in Figure 4.5c reveals that the overall leakage change consists of the direct influence of the westerlies acting locally (over the Agulhas Retroflection and Cape Basin region) on the magnitude of the leakage and of the indirect influence of the winds via the adjacent currents. INALT01, the configuration that mimics the known complexity of the Agulhas system with the highest degree of semblance (section 2.4.2), reproduces the general behaviour in leakage. Leakage response within INALT01-SHW+40% with LOCAL decomposition shows that, despite the overestimation of absolute leakage values within the coarse resolution model, the change in

leakage is consistent. The decompositions further indicate that the threshold in leakage change originates from the large-scale circulation, within which the Agulhas system is embedded.

This hypothesis is tested by employing the regional configuration, AGIO, whose domain excludes much of the large-scale circulation (Figure 2.1b). The global ocean influences this regional configuration through lateral boundary conditions derived from climatology of the ORCA05-REF simulation. Here, leakage response is quasi-linear, monotonously increasing with strengthening westerlies (Figure 4.5b). This suggests that, with a constant climatological representation of large-scale circulation, in particular that of the Southern Ocean, the portion of the westerlies felt within AGIO's southern domain (35°S – 48°S) does not cause a threshold in leakage response. Altering the boundary conditions to that derived from the ORCA05-SHW+40% experiment, effectively allows for an assessment of the influence a different Southern Ocean state has on leakage. In this case, leakage behaviour is similar to that of the two global configurations (red cross in Figure 4.5b), supporting the hypothesis that the threshold observed in leakage originates from the large-scale circulation.

## 4.3. Agulhas leakage transient response to increased westerlies

For the purpose of exploring the time dependency of Agulhas leakage response to increased westerlies, the focus is set on the SHW+40% case. The ORCA05 simulations were expanded to beyond the 10 years of common analysis. Figure 4.6 shows the time evolution of leakage and other parameters associated with the greater Agulhas system. Presented, are the annual values beginning from model year 31, which is when the application of the anomaly fields started. Linear trends calculated from the reference experiment were removed from all runs. Under background climatological forcing, these minor trends (between 0.1 % and 2.5 % of the reference values per decade) represent the inherent numerical drift that can reasonably be assumed to be similar in all simulations. (This procedure was also applied for Figures 4.7 – 4.9 & 4.12). The BASIN and LOCAL decompositions are overlaid. Following a fast initial adjustment, three distinct stages in leakage behaviour in the ORCA05-SHW+40%-FULL case (red curve on Figure 4.6) can be noted; (*i*) A proportional increase (model year 34 – 47) followed by (*ii*) a rapid decline (model year 47 – 50) and finally (*iii*) return to and decadal modulation around reference values (beyond model year 50).

Stage-1: Lasting for about a decade, during Stage-1, the westerlies acting both locally and outside the Agulhas region contribute towards increasing the leakage. This produces an overall proportional response (40 % increase in winds resulting in ~40 % increase in leakage), with a 1:3 ratio between LOCAL and BASIN. During Stage-1, the mean value of leakage for the FULL experiment is significantly

different at the 99 % confidence level (Welch's t-test[1]) from the mean leakage value of the reference experiment. As anticipated, no changes are observed in the Agulhas Current, the Agulhas Return Current (ARC[2]) and Mozambique through-flow, since surface forcing is unchanged equatorward of 35°S. The Antarctic Circumpolar Current (ACC) and south-west Indian subgyre, during that period, adjust to the altered forcing, which thereafter determines the timescale of the leakage response. Note that the ACC is measured as the barotropic transport south of the African continent, the region that is most likely to impact the Agulhas system. Qualitatively, there is little difference from measuring at other choke points, at Drake Passage for example, where the reference value of ACC transport is about 120 Sv (Figure 2.3), falling within observed ranges (Meredith et al. 2011; Whitworth 1983).

Stage-2: Happening rapidly, within 4 model years (47 – 50), the decline in leakage appears to occur indirectly as a result of the large-scale circulation adjustment. Without the large-scale adjustment, a local increase in westerlies would maintain an increased leakage. The decline coincides with the peak in ACC, the increase in ARC transport and variability, and the increase in Mozambique through-flow. The Agulhas Current also begins to respond accordingly.

Stage-3: Approximately 2 decades after the initial anomaly application, leakage falls within the variability range of the reference experiment (with some decadal variations around it). For Stage-3, the mean leakage value of the FULL experiment is significantly not different at 99 % confidence level[1] from the reference value. In response to a 40 % increase in westerlies, the ACC stabilizes to ~20 % above reference (Figure 4.6). A strengthened subgyre is noted, in addition to an increase in Mozambique Channel flow (by ~25 %) and subsequent downstream increase of the Agulhas Current (by ~5 %). This Agulhas Current transport increase occurs as an indirect effect of the westerlies increase. No change in the East Madagascar Current transport is noted (not shown). The ARC speed remains at an increased level (~23 % above reference values), with a ~60 % increase in variance. Towards the end of the simulation (model year 90 onwards), due the increased wind stress curl acting only over the southern portion of the subtropical gyres, the stronger subgyre meridionally contracts and zonally widens. Slight reductions in Mozambique through-flow and Agulhas Current transports are also noted. The return of leakage to reference values occurs due to the large-scale circulation, as suggested by the BASIN experiment.

[1] Details of the significant test are in supplementary material S1.3.
[2] Throughout chapter 4, ARC refers to the Agulhas Return Current and not to the regional-nested configuration described in chapter 2; this configuration was not employed for the analysis presented in chapter 4.

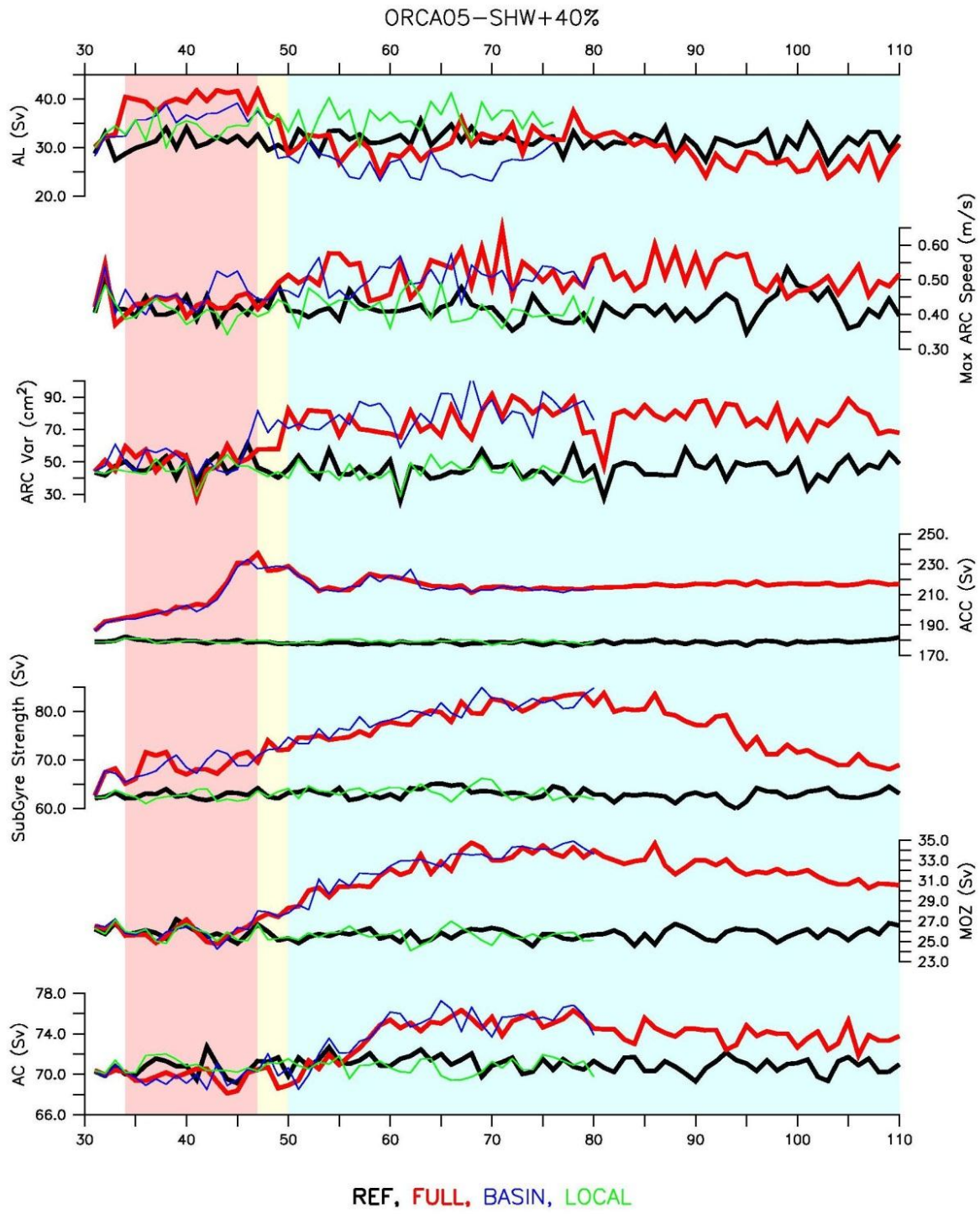


**FIGURE 4.6:** Time-series for the REF and SHW+40% cases within ORCA05. Aside from the Agulhas leakage (AL), all transports are measured from the barotropic stream-function: the Antarctic Circumpolar Current (ACC) as the maximum stream-function south of Africa between 20°E and 30°E; the subgyre strength as the minimum stream-function value between 30°E and 60°E; the Agulhas Current (AC) as the minimum stream-function along the section at 32°S; the Mozambique through-flow (Moz) across the narrows of the channel. For the Agulhas Return Current (ARC), speed is for the top 1000 m. The light red, yellow and blue shadings indicate Stage-1, Stage-2 and Stage-3 in ORCA05-SHW+40%-FULL leakage response respectively (details in text). Taken from Durgadoo et al. (2013).

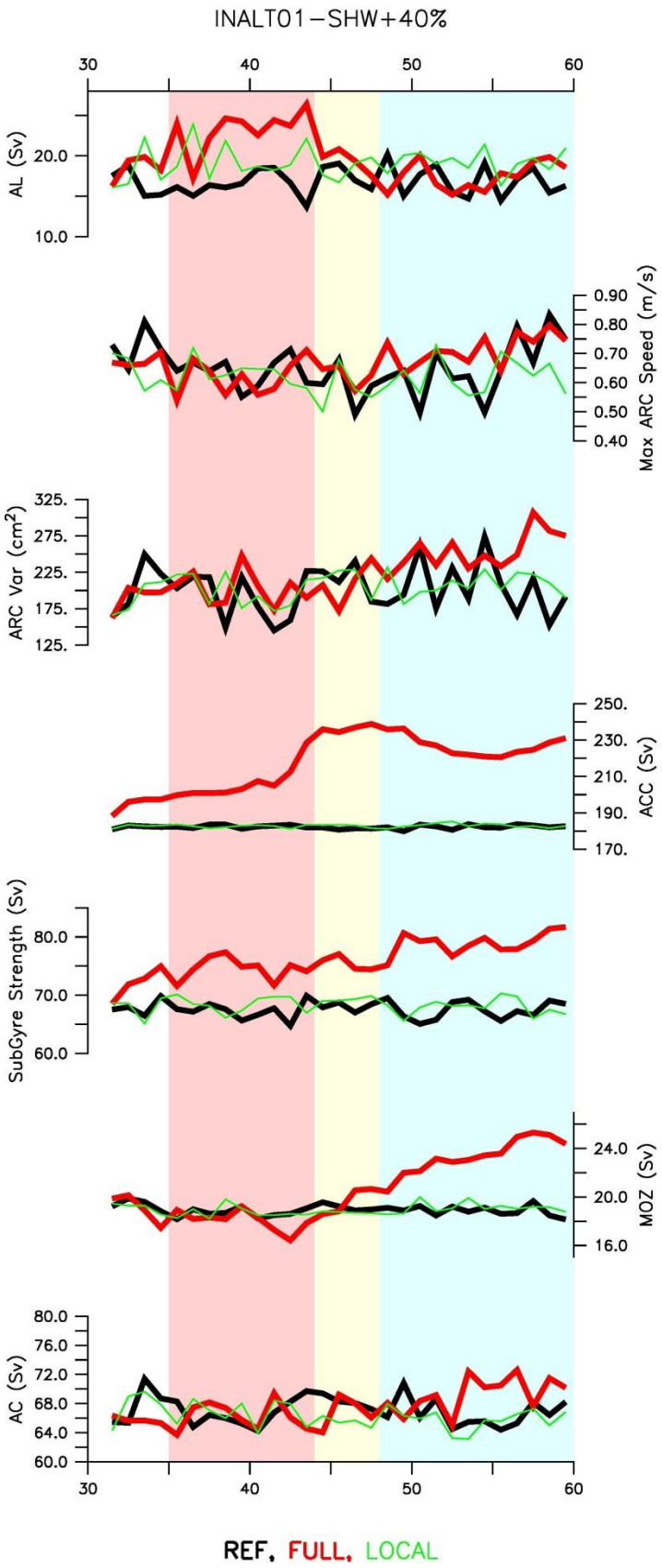


**FIGURE 4.7:** Same as Figure 4.6 for INALT01. Taken from Durgadoo et al. (2013).

Figure 4.7 shows the equivalent within INALT01. Comparing the two global configurations provides a way of diagnosing the impact mesoscale activities of the wider Agulhas region have on the leakage response. Perhaps surprisingly so, but as already seen in Figure 4.5, the general leakage response to westerly winds increase is not altered. The adjustment happens quicker, and Stage-3 is reached 2 – 3 years earlier. To test the impact of resolution on domain decomposition, the LOCAL experiment (only decomposition falling entirely within INALT01's nest boundaries) was repeated within INALT01. The response is similar, as anticipated (Figures 4.5b & 4.7). The fact that the models agree in leakage response points toward an underlying mechanism that is, to some extent, resolution independent (*i.e.* not dependent on the form of leakage).

The response seems to be linked to the development of the ACC. In the Atlantic sector of the Southern Ocean, an increase in westerlies promotes a spin-up of the Weddell gyre and, due to an increased pressure gradient, also its expansion (not shown). This in turn, leads to an overall increase in the width of the circumpolar current in the Atlantic. Within the two global configurations, the dynamic front between the supergyre and the ACC regime can be diagnosed from the zero barotropic stream-function line (Figure 4.1a). During Stage-3, immediately south of the leakage corridor, this boundary migrates by ~2° equatorward.

In the Southern Ocean, resolving eddies is known to be important (Böning et al. 2008; Hallberg and Gnanadesikan 2006; Spence et al. 2010). The ACC within INALT01 is represented at the same resolution as within ORCA05. Owing to the 2-way nesting scheme adopted for INALT01 and the requirement for consistent comparisons across models, the choice has been made not to parameterise eddies within ORCA05. However in order to assess the dependence of the 3-stage response on, firstly, Southern Ocean eddies, and secondly, on initial conditions, the ORCA05-REF and ORCA05-SHW+40%-FULL experiments were repeated, including the initial 20-year spin-up with parameterised eddies (Gent and McWilliams 1990). Thickness diffusivities used were capped at 1000 $m^2\ s^{-1}$, but vary spatially and temporally, increasing with stratification and isopycnal slope (Tréguier et al. 1997). These simulations indicate similar 3-stage behaviour in leakage response (Figure 4.8). The magnitude of the Stage-1 increase in this case is also proportional to the applied +40 % wind stress anomaly. A prolonged Stage-2 is noted, due to the parameterised saturating effect of eddies, retarding the ACC's evolution. Nevertheless, the decline in leakage during Stage-2 in Figure 4.8 also follows the adjustment of the ACC.

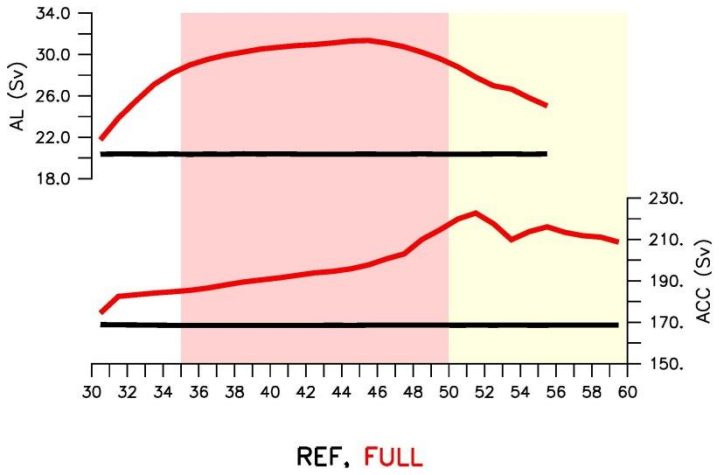


**FIGURE 4.8:** Time-series of Agulhas leakage (AL) and Antarctic Circumpolar Current (ACC) transport from the ORCA05-REF and ORCA05-SHW+40%-FULL simulations ran with the Gent and McWilliams (1990) eddy parameterisation. The light red and yellow shadings respectively indicate Stage-1 and Stage-2 in ORCA05-SHW+40%-FULL leakage response.

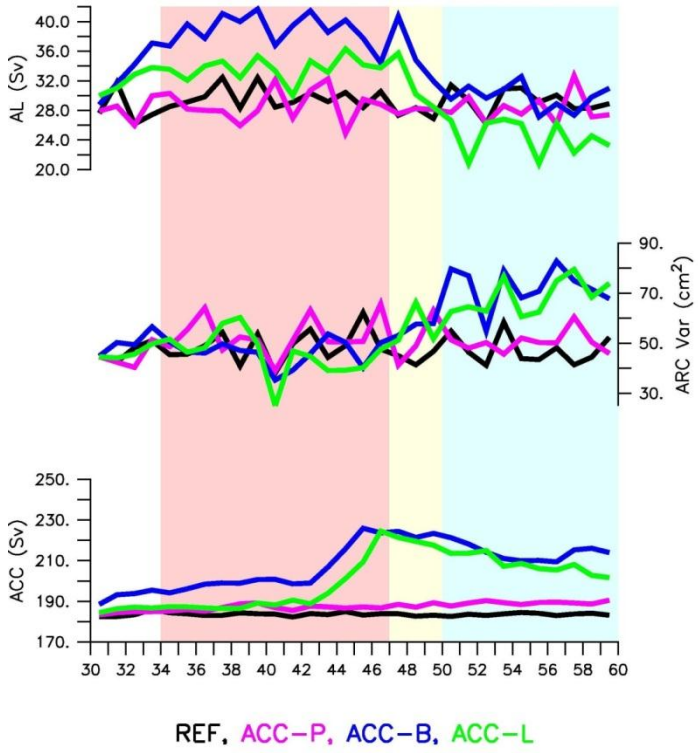


**FIGURE 4.9:** Time-series of Agulhas leakage (AL), Agulhas Return Current variance (ARC Var) and Antarctic Circumpolar Current (ACC) transport from the ACC-P (pink), ACC-B (blue) and ACC-L (green) decompositions of the SHW+40% anomaly within ORCA05. The light red, yellow and blue shadings indicate Stage-1, Stage-2 and Stage-3 in ORCA05-SHW+40%-FULL leakage response respectively (extracted from Figure 4.6). Taken from Durgadoo et al. (2013).

Seeking to confirm that the ACC influences Agulhas leakage, three additional experiments were undertaken. In these experiments, the SHW+40% anomaly field was further decomposed geographically and applied within ORCA05 (Figure 4.2d-f). Figure 4.9 shows that the general behaviour in ACC-B and ACC-L follow the same 3-stage pattern as for FULL (Figure 4.6). Within the given time frame, no response is seen when the ACC-P decomposition is applied, potentially indicating that the westerlies acting over the Pacific Ocean, Drake Passage and south of Australia, under this set-up, have no direct immediate impact on leakage. A possible reason for this would be that the westerlies, weaker in strength and lying about 5° poleward in the Pacific compared to the Indian-Atlantic sector (Figure 4.1), are not aligned to the core of the applied anomaly. The response in ACC-B, similar in magnitude to that of FULL, suggests that the winds in the region between 18°W and 115°E, corresponding to the region of maximum climatological westerlies (Figure 4.1), sets the leakage response. Further confirming the ACC's influence, ACC-L, a poleward extension of the LOCAL application, shows an initial increase of the same magnitude as LOCAL and a subsequent 3-stage leakage response.

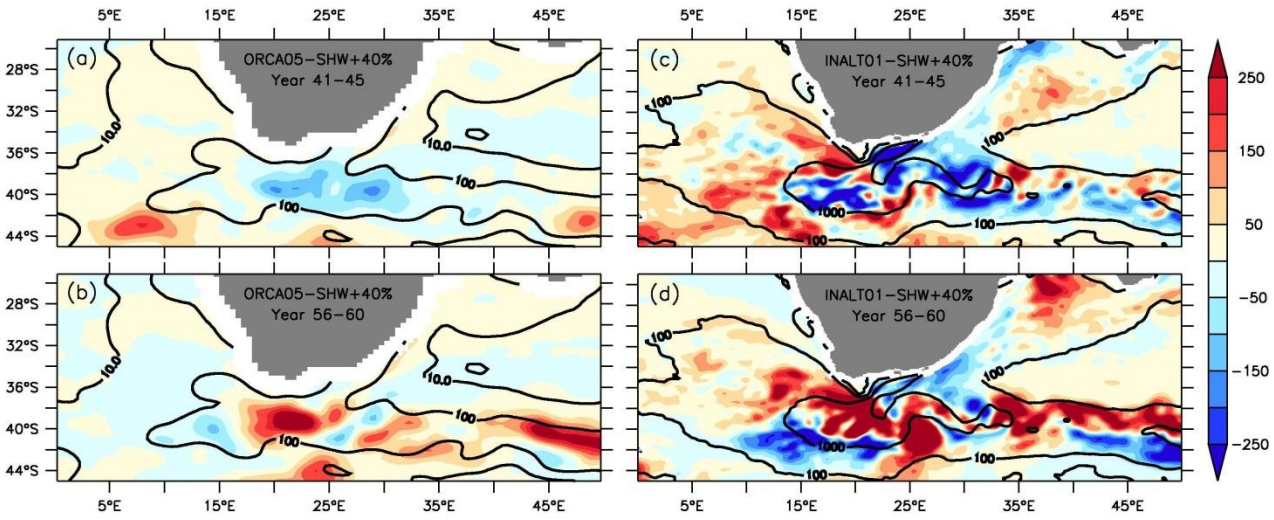


**FIGURE 4.10:** Eddy Kinetic Energy (EKE) per unit mass anomaly at 100 m ($cm^2\ s^{-2}$) within ORCA05 (left) and INALT01 (right) averaged over model years 41 – 45 (a & c) and 56 – 60 (b & d). Contours indicate the respective averaged reference EKE values for model years 41 - 60. Taken from Durgadoo et al. (2013).

The time scale is set by the ACC. Following the ACC peak, both the leakage and the ARC (transport and variance) react with a decline and an increase respectively (Figures 4.6 – 4.9). Averaging over two 5-year periods reveals that in Stage-1, the leakage increase is coincidental with an increased eddy kinetic energy in the Cape Basin, but with a decrease in the retroflection region (Figure 4.10a,c). Flowing adjoined and unidirectional to each other, the interaction between the ACC and the ARC become important in Stage-3, where both the retroflection and the ARC become more energetic and

variable (Figure. 4.6, 4.7, 4.9 & 4.10b,d). This is characteristic of a turbulent retroflection regime (Le Bars et al. 2012). This regime, which occurs at strong winds, leads to the increased volume transport (seen in Stage-1 as increased leakage) to be lost through an enhanced interaction between the ARC and the ACC.

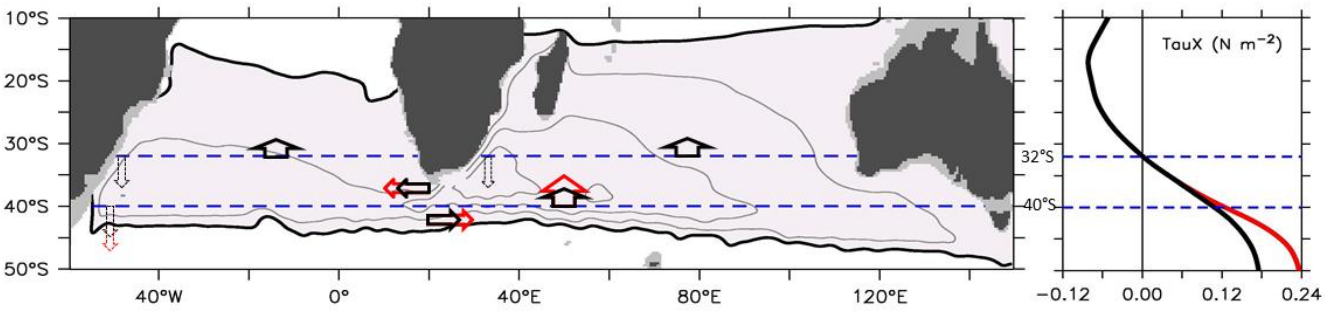


**FIGURE 4.11:** Schematic of the proposed mechanism of leakage response to the westerlies. Contours of barotropic stream function portray the anticyclonic supergyre (shaded area) connecting the South Indian and South Atlantic oceans, with thick black contour demarcating its boundaries (data extracted from ORCA05-REF experiment). Thick arrows indicate the meridional Sverdrup interior flow and the corresponding zonal transport that results from the wind stress application (REF in black and SHW+40% case in red; wind stress shown on the right panel). The circulation is closed by the return flow of the western boundary currents (dotted arrows). Taken from Durgadoo et al. (2013).

## 4.4. Mechanism of Agulhas leakage response to the westerlies

The region of positive wind stress curl in the South Indian and South Atlantic Oceans roughly lies between 15°S (maximum trades) and 50°S (maximum westerlies). The wind stress curl yields negative Ekman vertical velocities (*i.e.* pumping) over this region, which promotes an equatorward Sverdrup transport of the interior (Marshall and Plumb 2007). Figure 4.11 schematically portrays the proposed mechanism of leakage response to changes in the westerlies. Increasing the westerlies in the manner presented in this study leads to an increased wind stress curl between the latitudes 35°S and 50°S. The equatorward interior flow across the southern portion of the supergyre is therefore enhanced. In Figure 4.11, this is depicted along 40°S, which roughly is the latitude of separation between the westward flowing Agulhas leakage and the eastward flowing Agulhas Return Current. By construction no change is applied to the winds at the latitudes of the Agulhas Current, north of 35°S. Through continuity, the increased meridional transport must result in a westward mass transport towards the South American coast. Closing the circulation, the western boundary current subsequently increases.

Figures 4.5b & 4.5c (grey lines) also show the change in theoretical meridional interior flow (Sverdrup transport) along 40°S resulting from the added intensity anomalies. As anticipated, the change in

Sverdrup transport is a linear function of the change in wind stress curl. The results show that leakage change within the global configurations follows the proportional Sverdrup transport change over the entire time-series for the reduced westerlies cases (Figure 4.5b) and during Stage-1 of the intensified westerlies simulations (Figures 4.6 – 4.8).

Agulhas leakage response is transient (Figures 4.6 – 4.9). The time dependency is a question of wave propagation, in particular internal planetary waves, similar to the process that communicates the dynamical imprint of leakage across the South Atlantic (Biastoch et al. 2008b; van Sebille and van Leeuwen 2007). Rossby waves set the adjustment time of the ocean to large-scale forcing. The initial rapid oceanic adjustment to the applied high-frequency wind forcing prior to Stage-1 (model years 31 – 33) is a result of the fast propagation of barotropic Rossby waves, which establishes the Sverdrup balance. Meanwhile, the westerly winds influence induces a baroclinic adjustment of the eastward flowing ACC on decadal timescale. Additional controls, such as its width, its variability, and buoyant convection within and outside of the current further influence the adjustment timescale of the ACC (Allison et al. 2011). The timing in Figures 4.6 – 4.9 suggests that the interaction between the ACC and the Agulhas system become important after 1 – 2 decades. The decrease in leakage in Stage-3 is preceded by an increasing variability of the ARC, which occurs when the ACC reaches its peak. Since both currents are unidirectional and adjacent, meridional exchanges in lateral momentum and tracers between them may be a likely explanation.

## 4.5. Agulhas leakage response to shifts in the westerlies

Thus far, the focus was set on the impact of westerlies intensity on the Agulhas system. As noted in section 4.2, idealised equatorward shifts of the westerly wind belt induces an increase in leakage (Figure 4.5a). Using the mechanism described in the previous section, it can be deduced that this occurs as a result of the redistribution of momentum. The application of a northward shift of the westerlies strengthens the wind stress curl between 35°S and 45°S, while reducing it over the core of ACC (45°S – 60°S). The overall effect is similar to an increase in westerlies over the southern portion of the Indian Ocean subtropical gyre which leads to an increase in leakage. In this case, leakage remains at a constant increased level (persistent Stage-1), and a weaker ACC does not result in leakage to be hampered (Figure 4.12). The opposite for poleward shifts also holds; reduced northward Sverdrup transport across the southern boundary of the supergyre boundary leads to reduced leakage. Towards the end of the SHW-4 simulation (model year 56 onwards), there is an indication that the leakage may further decrease, exacerbated by an increased ACC (Stage-2), which

stimulates an enhanced interaction with the retroflection and ARC (Figure 4.12). Once again, this is dynamically consistent as described in the previous section.

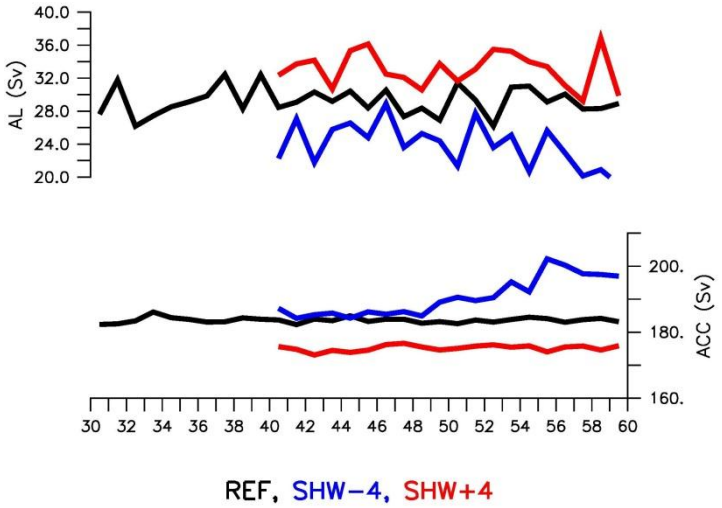


**FIGURE 4.12:** Time-series of Agulhas leakage (AL) and Antarctic Circumpolar Current (ACC) transport from the REF and SHW±4-FULL cases within ORCA05.

There is the common belief that a displacement of the zero wind stress curl line equatorward (poleward) would narrow (widen) the gateway south of Africa allowing less (more) leakage (Zahn et al. 2010). The results presented here show the converse. Paleoceanographic interpretations propose that, on centennial-millennial timescales, a displacement of the subtropical front at the northern boundary of the ACC south of Africa, concomitant with shifts and intensity changes in the westerlies, could be a major drive in modulating the amount of leakage (Bard and Rickaby 2009; Caley et al. 2012; Peeters et al. 2004). The series of experiments performed here reveal no significant change in the latitudinal position of the hydrographically-defined subtropical front (maximum temperature gradient) south of Africa in response to changes in position of the zero wind stress curl line (not shown). However, it cannot be concluded that the front does not respond to westerly changes, since no corresponding thermohaline forcing was applied. The ocean/sea-ice only simulations here addressed the transient response of the Agulhas system. Processes such as deep and bottom water formation, which indirectly respond to changing wind patterns, would in the long term affect the hydrography of the Southern Ocean leading to possible shifts of its fronts (Downes et al. 2011; Graham et al. 2012; Spence et al. 2010).

## 4.6. Implications

In the portrayal shown in Figure 4.11 and described in section 4.4, leakage corresponds to the westward flow south of the African continent and is, de facto, a passive component of the supergyre circulation. This, together with the results presented in chapter 3, has three major implications.

- Firstly, it suggests that the process determining leakage would be independent of retroflection energetics. In support for this, it is shown that eddy kinetic energy of the retroflection in Figure 4.10 matches in sign with neither the initial increase in leakage of Stage-1 nor the return to reference values in Stage-3. Eddy kinetic energy of the retroflection is increased in Stage-3 compared to reference levels, while leakage is unchanged. Furthermore, in chapter 3, it was observed that changes in inertia of the Agulhas Current are communicated to the retroflection region thereby modulating its mesoscale variability. Yet, no leakage change was noted (section 3.3, Figures 3.6 – 3.9). Therefore, there seems to be no link between the energetics of the retroflection and the process behind leakage.
- Secondly, the mechanism put forward complements the main conclusion of the previous chapter that leakage change is decoupled from changes in the Agulhas Current. Here, during Stage-1, large response in leakage occurs without any change in Agulhas Current. Figures 3.5 – 3.7 showed that changes in the easterly trades result in changes in the transport of the Agulhas Current, without any attendant changes in leakage. Moreover, in Stage-3, here, the increase in Agulhas Current results in no change in leakage. It is important to note here that the Stage-3 response in Agulhas Current occurs as an indirect consequence of the westerlies increase. Thus, leakage appears to respond solely to the westerly winds, while the western boundary current reacts to changes of the positive wind stress curl region (between the maximum easterlies and maximum westerlies). Yet, Rouault et al. (2009) and van Sebille et al. (2009b) both related the strength of the Agulhas Current with the magnitude of leakage and found a linear relationship between the two variables. However, within the present-day range of transport values, the authors did disagree on the sign of that relationship. Since, the results presented here suggest that changes in leakage do not necessitate variations in upstream transport, it can be concluded that their disagreement was most likely an outcome of the different wind field products (each with inherent trends) used in forcing their respective models. In general, within an integral large-scale atmospheric system, statistical relationships between the Agulhas Current and leakage do not necessarily imply cause and impact, but instead are manifestations of individual external forcing.
- Thirdly, as noted in Figures 4.5 – 4.7, the general pattern of leakage response to the westerlies change is reflected at all resolutions; in other words, irrespective of the form of leakage. It is important to mention here that the claim is not that leakage follows Sverdrup dynamics since non-

linearity plays a crucial role in determining the amount of water entering the South Atlantic. Instead, given a change in the westerlies, leakage responds in the same way the interior adjustment (described by the Sverdrup balanced) does.

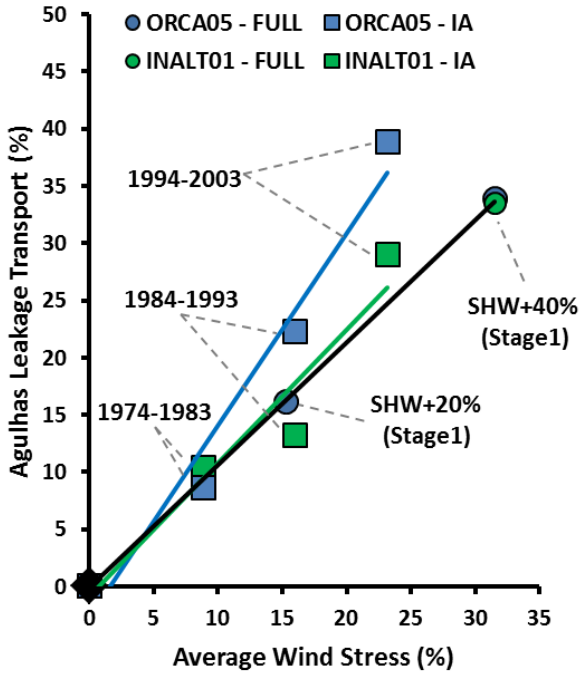


**FIGURE 4.13:** Change in Agulhas leakage (%) versus change in wind stress (%) averaged over the region 20°W – 140°E, 35°S - 65°S. Squares represent decadal averages from hind-cast inter-annual (IA) simulations of ORCA05-IA (light blue) and INALT01-IA (light green), with the period 1964-1973 taken as reference (set at origin); Circles represent Stage-1 averages (model years 41-45) from the FULL application of the SHW+20% and SHW+40% anomalies as well as the corresponding REF (set at origin) within ORCA05 (blue) and INALT01 (green). Taken from Durgadoo et al. (2013).

Resolution is an important aspect of Agulhas system modelling. The necessity to resolve the Agulhas system adequately has been amply emphasised in the literature (*e.g.* Biastoch and Krauss 1999; Biastoch et al. 2008c). Beal et al. (2011) even recommend that at least a tenth-degree horizontal resolution (*e.g.* INALT01) is required, and such resolution has not yet been reached by most coupled climate models used for future predictions (Taylor et al. 2012; Weijer et al. 2012). Here, while the series of experiments demonstrate that leakage response to a constant change in westerly winds is represented at all resolutions, it is important to consider the magnitude of the response. For example, a 40 % increase in westerlies during Stage-1 results in approximately the same percentage increase in leakage, which at low-resolution (ORCA05) is ~10 Sv and at high-resolution (INALT01) is ~6 Sv. Coarse resolution models clearly overestimate the actual volumetric transport and corresponding amount of heat and salt exported into the Atlantic, which ultimately is of critical importance because of the implications for the Atlantic meridional overturning circulation and global

climate. Notwithstanding, within the 0.5° – 0.1° range, the mechanism behind the response of leakage to changes in the westerlies is consistent.

During the Last Glacial Maximum (~20 kyears ago), leakage reduction (Franzese et al. 2006; Peeters et al. 2004), and possible ACC increase (Franzese et al. 2006; Otto-Bliesner et al. 2006) with no change in retroflection position (Franzese et al. 2009) have been suggested. There is, however, large uncertainty regarding the state of the Southern Hemisphere winds during glacial times (Kohfeld et al. 2013). To name but a few examples of recent studies, Anderson et al. (2002), Wyrwoll et al. (2000), and Sime et al. (2013) reported an intensifying poleward displacement of the westerly jet; Rojas et al. (2008) concluded a decrease with no significant latitudinal shift, while Toggweiler et al. (2006) deduced an equatorward shift. It is therefore not possible, given the present limited knowledge of the wind patterns of the Last Glacial Maximum, to confirm whether or not the dependency of Agulhas leakage on the westerlies was dominant. Nonetheless, a leakage reduction accompanied by a more vigorous ACC would be in line with the results presented here.

Of current relevance, models simulate an increase in contemporary Agulhas leakage (Biastoch et al. 2009b; Rouault et al. 2009). Biastoch et al. (2009b) proposed that a poleward shift in contemporary westerlies is responsible for this increase. Swart and Fyfe (2012) questioned the robustness of such a latitudinal shift in present-day westerlies in an analysis of various coupled climate model products as well as observational reanalyses, and found that instead significant strengthening of the westerlies rather than shift has occurred. In the last 40 years, the westerlies have increased by about 25 % (Figure 4.13). It was showed that leakage initially responds proportionally to increased westerlies (Stage-1 in Figures 4.5 & 4.6). In Figure 4.13, this is reflected by the linear relationship for the SHW+20% and SHW+40% cases. Note that Figure 4.13 shows the area-averaged (20°W – 140°E, 35°S – 65°S) change in westerlies and not the change in maximum zonal-averaged westerlies. Also shown are decadal averages in leakage change derived from the hind-cast experiments of ORCA05 and INALT01. Given the strong linear relationship ($r = 0.98$ and 0.96 for ORCA05 and INALT01 respectively), similar to that of the sensitivity experiments, it can be concluded that the upward trend in leakage reported by Biastoch et al. (2009b) and Rouault et al. (2009) may reflect an unadjusted oceanic response to the continuously increasing momentum input by the westerlies akin to Stage-1. One could further speculate that, should the on-going wind change lessen or halt (Watson et al. 2012) in response to decadal variability of the Southern Annual Mode (Visbeck 2009), future decadal trend in leakage could weaken. This would naturally also depend on the timing and magnitude of the ACC response. It is unclear whether or not the ACC is already eddy saturated (Böning et al. 2008; Hallberg and Gnanadesikan 2006; Spence et al. 2010). It has been shown that the

circumpolar current plays a relatively critical role in the transient 3-stage leakage response. Therefore, should the ACC be weakly responsive (or unresponsive) to the present-day increasing westerlies, a delay in the onset of a Stage-2-type leakage response can be expected.

This study describes leakage response in the context of changes in the zonal component of westerlies that are constant in time. In reality, the wind system changes progressively and leakage is expected to respond non-linearly to the compounding effects of migrations, and magnitudes (deviation from linearity seen in Figure 4.13). The meridional component of the wind stress, albeit relatively small on average, may additionally play a role which was not considered here. Furthermore, changes in the transition zone between the easterlies and westerlies (between 25°S and 35°S) as well as the impact of altered wind forcing on the thermohaline field may also be important.

## 4.7. Summary

The manner by which the Southern Hemisphere westerlies affect Agulhas leakage was systematically deconstructed, and the conclusion was reached that the intensity of the wind belt is predominantly responsible in controlling the Indian-Atlantic transport. Agulhas leakage responds rapidly (within 2 – 3 years) and proportionally to changes in the westerly wind stress. Change in leakage is comparable to the change in Sverdrup transport across the southern portion of the supergyre. Shifts and modifications to the intensity of the wind belt result in changes in wind energy input that, following Sverdrup dynamics, cause an adjustment of the interior flow. South of Africa, that change is in turn reflected as a change of leakage.

Simulations where the intensity of the westerlies was increased show a transient response in leakage. Initially, leakage responds proportionally to the wind increase. Subsequently, after 1 – 2 decades, leakage subsides to normal reference levels. The transient response occurs due to the adjustment of the large-scale circulation. In particular, energetic interactions between the Antarctic Circumpolar Current and the Agulhas system cause the subsidence in leakage.

It was also shown that the impact of a displacement of the westerly wind belt on leakage can be regarded as a redistribution of momentum. Shifts of the westerlies equatorward increase the energy input over the southern portion of the supergyre, and reduce it over the Southern Ocean. This results in enhanced leakage. Conversely, poleward shifts reduce leakage, and the reduction would be accentuated following the adjustment (strengthening) of the circumpolar current. This result is at odds with previous claims.

The investigation further suggested that the process behind the leakage response to changes in the westerlies is independent of model resolution, upstream transport of the Agulhas Current, and possibly retroflection energetics. However, this does not discredit the importance of non-linearity in the region. The volumetric change in leakage within models is highly dependent on the correct representation of the numerous non-linear interactions in the Agulhas system. More importantly, the corresponding changes in the amount of heat and salt being exported have the potential of impacting the circulation in the Atlantic.

# 5. Agulhas leakage impacts the South Atlantic circulation

The content of this chapter is partly based on the following publication:

Rühs S., J.V. Durgadoo, E. Behrens, A. Biastoch (2013) – Advective timescales and pathways of Agulhas leakage. *Geophysical Research Letters*, 40, 3997–4000, doi: 10.1002/grl.50782

The Agulhas system is found in a region of confluence (Figure 1.4): atmospherically, in a transition zone between the easterly trades and westerlies; and in the ocean, between the South Atlantic subtropical gyre, the South Indian subtropical gyre and the Antarctic Circumpolar Current. Therefore, the controls and impact of Agulhas leakage are not trivial. The previous two chapters examined the manner in which the wind system of the Southern Hemisphere influences the exchange of waters south of Africa. It has been shown that, while the trade winds have no impact on leakage (chapter 3), changes in the westerlies induce large responses in Agulhas leakage (chapter 4). The intensity of the westerly wind belt was found to be the main cause of the contemporary leakage increase reported by hind-cast model studies. Furthermore, the adjustment of the large-scale circulation to changes in westerlies has important consequences in terms of the timescale it imposes on the leakage response. It is difficult to diagnose and distinguish the direct and indirect impacts of the westerlies on the Atlantic circulation since both the Southern Ocean and the Agulhas system are susceptible to changes in winds. The upper limb of the Atlantic overturning circulation responds to changes in both the cold- and warm-water routes (Figure 1.1). Biastoch and Böning (2013) recently made an attempt to determine the role of Agulhas leakage on the Atlantic overturning circulation in a simulation where the global wind pattern was altered to reflect that of future predictions. They noted the difficulty in separating the contribution of Agulhas leakage from the other components on the South Atlantic overturning circulation (*e.g*. Ekman dynamics and the spin-up of the Deacon Cell).

Benefiting from the knowledge that an increase in leakage can be simulated in isolation by increasing the westerlies only over the Agulhas region (LOCAL experiment in chapter 4), this chapter examines the impact of an increased Indo-Atlantic transport on the South Atlantic circulation. For this purpose, only the global-nested configuration, INALT01, was used. It is found that the dynamic and advective

impacts of Agulhas leakage are felt across the Equator within a decade. Advection of leakage waters follows the mean horizontal circulation of the South Atlantic.

## 5.1. Experiment design

The Southern Hemisphere westerlies impact directly the circulation of the Southern Ocean (Allison et al. 2010) and indirectly the global ocean (Allison et al. 2011; Gnanadesikan and Hallberg 2000). Chapter 4 has shown that Agulhas leakage is also sensitive to changes in the westerlies. In particular, a localised increase in the westerly winds was found to be sufficient to stimulate leakage. Here, 'localised' refers to the portion of the westerlies acting over the region bounded by the Agulhas system (0° – 45°E and 35°S – 45°S). For the SHW+40%-LOCAL simulations presented in chapter 4 (Figures 4.2c & 4.3c), leakage change with respect to the reference experiment was 13 % (4.0 Sv) and 17 % (2.8 Sv) within ORCA05 and INALT01 respectively (Figure 4.5c). While the percentage changes in leakage are similar for both configurations, ORCA05 overestimates the mean value of leakage (section 2.5, Figure 2.9). Therefore, the additional amount of Indian Ocean water (including heat and salt) penetrating the South Atlantic is also overestimated within ORCA05. For this reason, the analysis presented in this chapter considers the response of the South Atlantic to an increase in leakage only within INALT01. The high-resolution nested region of INALT01 encompasses the entire South Atlantic basin (50°S – 8°N). Two experiments are analysed: INALT01-REF and INALT01-SHW+40%-LOCAL (increase of the westerlies by 40 % between 0° – 45°E and 35°S – 45°S; Table 4.1). Both simulations were forced using climatological fields. Model years 31 – 60 were considered.

The advantage of the LOCAL decomposition of the westerlies (Figures 4.2c) is that a realistic increase in leakage is produced without changes applied to the large-scale circulation. In contrast to the studies of Oke and England (2004), Sijp and England (2009) and Biastoch and Böning (2013), the Ekman transport of the South Atlantic and the Deacon cell (Speer et al. 2000) are not (directly) altered by the sensitivity experiment. Consequently, changes to the South Atlantic circulation can be attributed to an increase in leakage. The overall pattern of the horizontal circulation is not affected by the localised application of the +40 % westerlies anomaly (section 4.1; Figure 4.3). The only other study of this kind was undertaken by Weijer et al. (2002), who linearly parameterised the impact of leakage within a coarse resolution global model by extracting heat and salt from the Indian Ocean and injecting them into the South Atlantic.

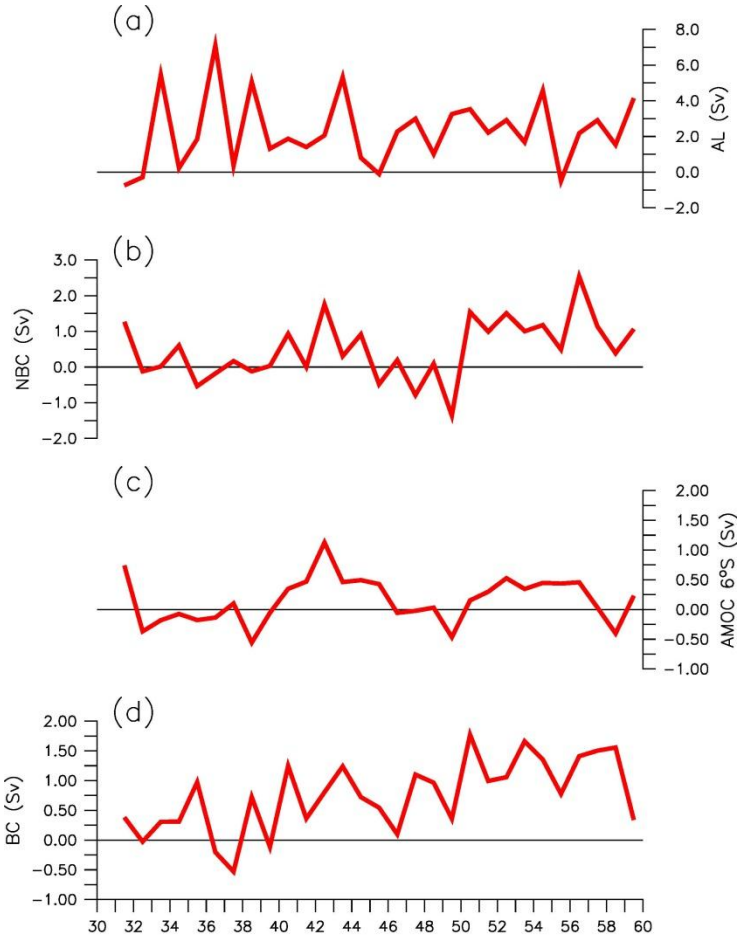


**FIGURE 5.1:** Time-series of transport anomalies (Sv) of the INALT01-SHW±4-LOCAL (red lines) experiment with respect to INALT01-REF. Agulhas leakage (AL), North Brazil Current transport (NBC, at 6°S, integrated over the region 32.75°W – 35.25°W, 100 – 1300 m), Atlantic meridional overturning circulation (AMOC at 6°S) and the Brazil Current transport (BC, minimum barotropic stream-function at 33°S).

## 5.2. Dynamic imprint of Agulhas leakage in the South Atlantic

Agulhas leakage (measured using the method described in section 2.5) rapidly and linearly responds to the change in westerlies intensity. In line with the mechanism proposed in chapter 4 (section 4.4), an increase of the winds east of 20°E yields an enhanced leakage of about 17 % or ~2.8 Sv (averaged over model years 51 – 60, Figure 5.1a). This amount is about half of the hind-cast increase of ~5 Sv since the late 1960s (Figure 2.9b; Biastoch et al. 2009b). Despite the inter-annual variability in leakage, the mean leakage value in the LOCAL experiment (19.36 ± 1.41 Sv) is significantly different from the mean value of the REF experiment (16.59 ± 1.63 Sv) at the 99 % confidence level[1] (model years 51 – 60). Additional to the heightened leakage, an increase of the wind stress curl over the eastern portion of the South Atlantic subtropical gyre (0° – 20°E) gives rise to an enhanced

[1] Details of the significant test are in supplementary material S1.4.

equatorward interior flow. Consequently, the horizontal circulation of the South Atlantic intensifies by about 4 – 6 Sv (Figure 5.2). The Brazil Current exhibits a significant[1] increase of about 1 Sv (model years 51 – 60).

The cross-equatorial flow is concentrated along the South American coast, and is achieved by the North Brazil Current (Bourlès et al. 1999; Johns et al. 1998; Schott et al. 1998). At 6°S, changes in the North Brazil Current transport are observed about a decade after leakage has increased (Figure 5.1b). The response timescale based only on the propagation of planetary and coastal waves ought to be of the order of 4 – 6 years (Biastoch et al. 2008b; van Sebille and van Leeuwen 2007; Weijer et al. 2002). However, the advective response cannot be disentangled from the dynamic response. For the period 41 – 50, while the mean North Brazil Current of the sensitivity experiment is unchanged with respect to reference values, inter-annual modulations are observed in the time-series (Figure 5.1b). For model years 51 – 60, the current exhibits a significant[1] increase of ~1.2 Sv with respect to the reference value of 19.90 ± 0.62 Sv.

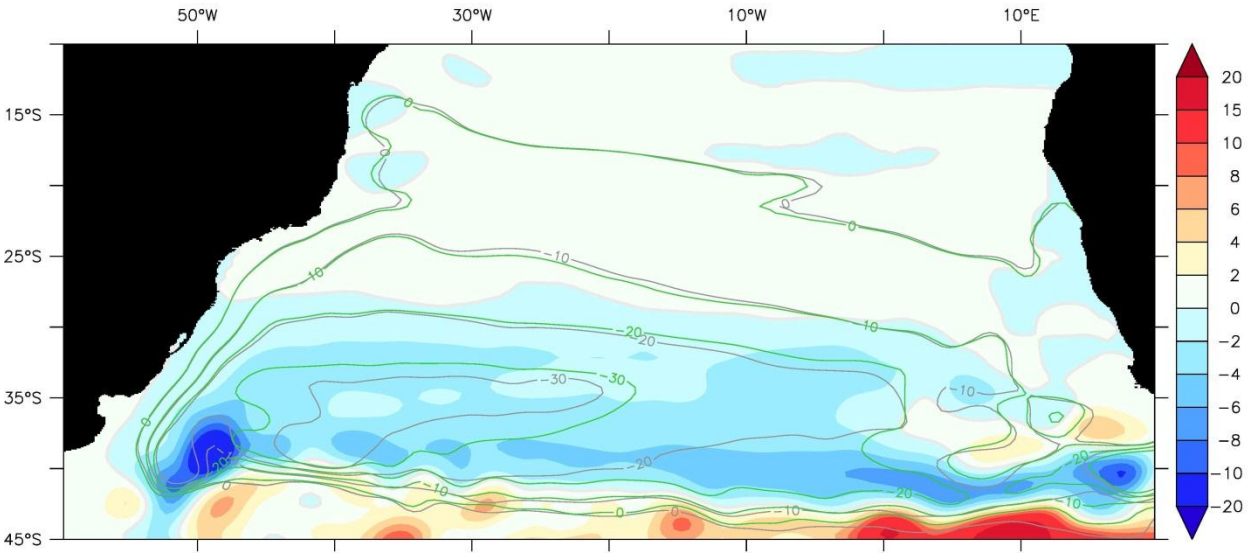


**FIGURE 5.2:** Changes in horizontal circulation (barotropic stream-function, shading, Sv), INALT01-SHW+40%-LOCAL minus INALT01-REF, model years 51 – 60. Barotropic stream-function contours (Sv) from the INALT01-REF (dark grey) and INALT01-SHW+40%-LOCAL (green) experiments are overlaid.

Changes in the upper limb of the South Atlantic meridional overturning circulation (MOC) at 6°S are also related to fluctuations of the North Brazil Current (Hazeleger and Drijfhout 2006; Zhang et al. 2011). Concomitant with a ~1.2 Sv of the current, the MOC at 6S increases by ~0.3 Sv (Figure 5.1c;

[1] Details of the significant test are in supplementary material S1.4.

averaged over model years 51 – 61; significant at the 95 % confidence level[1]). The inter-annual variability of leakage within the REF experiment is not congruent with that within the LOCAL experiment (Figure 4.6) due to different atmospheric state of the respective simulations and non-linearity of the Agulhas system. Therefore, further diagnosing the isolated impact of the increase in leakage on the South Atlantic MOC from the Eulerian fields is not possible. However, employing the Lagrangian method described in section 2.5, it is possible to tag and follow the advection of Agulhas waters.

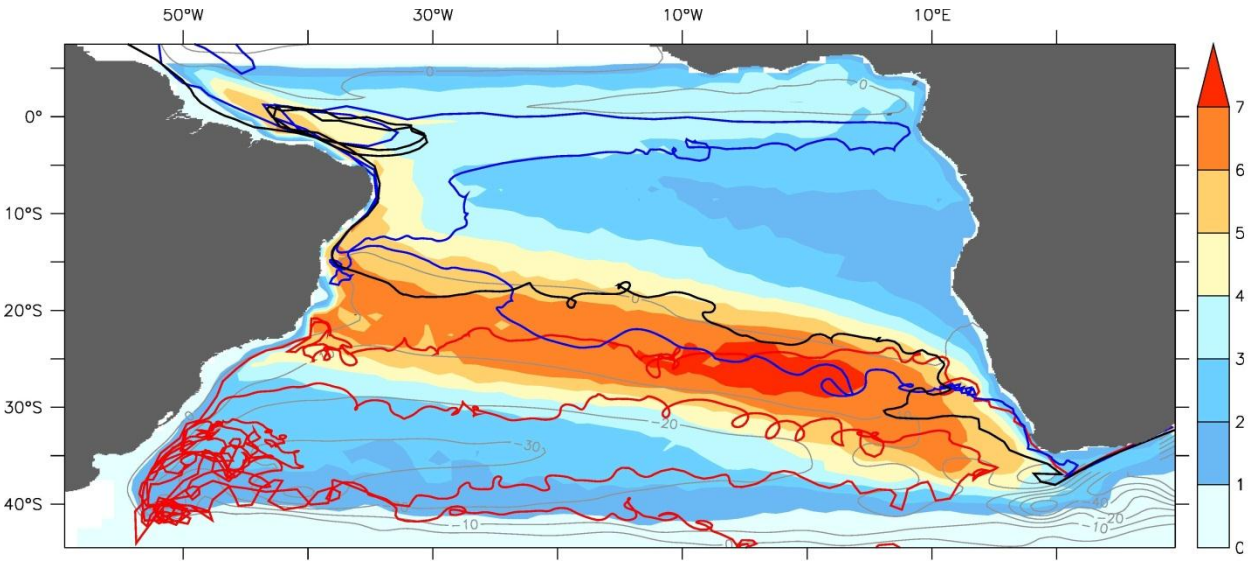


**FIGURE 5.3:** Probability density of Agulhas leakage waters reaching 6°N (shading x $10^{-4}$, normalised by the number of occurrences per 0.5° x 0.5° grid box). Using the Lagrangian method, described in section 2.5, water particles, originating from the Agulhas Current at 32°S, were tagged as they crossed the Good-Hope section (Agulhas leakage) and followed until they reached 6°N. These particles were released over a period of 10 years, and were subsequently followed forward for a period of 90 years. The probability density was calculated based on their trajectories. Barotropic stream-function contours (Sv) from the INALT01-REF (grey) show the mean horizontal circulation. Three trajectories that illustrate the pathways of Agulhas leakage are overlaid.

## 5.3. Advection of Agulhas leakage into the South Atlantic

The thermohaline properties of Agulhas leakage is communicated equatorward through advection. In order to investigate the pathways associated with the advection of leakage across the Equator, waters originating from the Agulhas Current, and crossing the Good-Hope line were tracked forward in time and their fate was studied (Rühs et al. 2013). By definition, waters crossing the Good-Hope line constitute leakage (section 2.5; Figure 2.9). The analysis shows that a dominant and direct pathway exists across the South Atlantic: from the Cape Basin to the North Brazil Current via the

[1] Details of the significant test are in supplementary material S1.4.

Benguela and South Equatorial Currents (Figure 5.3). Through this direct pathway (illustrated by the black and blue trajectories in Figure 5.3), leakage waters feed into the North Brazil Current at 6°S within a modal period of 5 – 7 years (Rühs et al. 2013). A bifurcation of trajectories occurs around 20°S along the South American coast. A portion of leakage waters are typically trapped within the doubled-cell South Atlantic subtropical gyre (Vianna and Menezes 2011; red trajectory in Figure 5.3). Eventually, these waters either join the main pathway towards to the Equator or get carried by the South Atlantic Current into the Indian Ocean. Leakage waters captured by the North Brazil Current take approximately another 2 years to cross the Equator and enter the North Atlantic (at 6°N) in about a decade (Rühs et al. 2013). Deviations through the equatorial regime are likely to occur (Brandt et al. 2006), and multiple recirculations delay the cross-equatorial advection of leakage.

In Figure 5.3, the bifurcation of leakage pathway appears to be at ~20°S, 40°W. To quantitatively assess the proportion of leakage feeding the narrow route towards the Equator through the North Brazil Current and the re-circulatory route through the Brazil Current, six Lagrangian experiments were performed within the INALT01-REF and INALT01-SHW+40%-LOCAL simulations. In these experiments, water parcels, each carrying maximum transport of 0.1 Sv, were released across the Agulhas Current at 32°S for a period of 10 years, and tracked forward for a total period of 20 (experiment sets A & B) or 30 (experiment set C) years (Table 5.1). The method follows that described in section 2.5, with the domain enlarged to capture water exiting through the North Brazil Current and the Brazil Current (sections shown in Figure 5.4). The partitioning of leakage between the North Brazil and Brazil Currents remain similar within the INALT01-REF and INALT01-SHW+40%-LOCAL individual simulations (Table 5.1). Within 2 decades, ~40 % of leakage feeds the direct route through the North Brazil Current and ~30 % feeds the re-circulatory route. The ratio is maintained for both 10-year periods tested irrespective of the inter-annual variability in leakage (experiment set A & B). In line with Rühs et al. (2013), the majority of leakage waters find their fate within the first decades. The 30-year integration Lagrangian experiments (set C) show an additional 5 % of leakage waters passing through each of the routes. Less than 5 % of leakage crosses 6°S outside of the North Brazil Current.

How do the increase in leakage and the enhanced South Atlantic subtropical gyre within INALT01-SHW+40%-LOCAL affect this pattern? For experiment set A (first decade release), out of a 2.5 Sv increase in leakage, 0.5 Sv and 1.2 Sv end up within North Brazil Current and Brazil Current respectively. For the second decade (experiment set B), out of a 1.8 Sv leakage increase, 0.7 Sv and 1.1 Sv are captured within the North Brazil Current and Brazil current respectively. Here, the proportion of the additional leakage that veers poleward feeding the re-circulatory route appears

larger, about 50 – 60 %. This is achieved by the strengthened South Atlantic subtropical gyre, and is further illustrated in Figure 5.4. While the two prominent paths of advection still stand out, the probability density anomalies show Agulhas waters spreading the entire South Atlantic subtropical gyre.

| | Lagrangian Setup | | AL | | | NBC | | | BC | | |
|---|---|---|---|---|---|---|---|---|---|---|---|
| | Release | Integrate | REF | LOCAL | diff. | REF | LOCAL | diff. | REF | LOCAL | diff. |
| **A** | 31 – 40 | 31 – 50 | 16.5 | 19.0 | 2.5 | 6.6 | 7.1 | 0.5 | 4.8 | 6.0 | 1.2 |
| **B** | 41 – 50 | 41 – 60 | 17.2 | 19.1 | 1.8 | 7.0 | 7.7 | 0.7 | 5.2 | 6.2 | 1.1 |
| **C** | 31 – 40 | 31 – 60 | 16.5 | 19.0 | 2.5 | 7.4 | 8.0 | 0.6 | 5.5 | 6.9 | 1.4 |

**TABLE 5.1:** Amount of Agulhas waters (Sv) within the Agulhas leakage (AL), the North Brazil Current (NBC) and the Brazil Current (BC). Sections along which the NBC and BC were measured are shown in Figure 5.4. Three sets of Lagrangian experiments were performed (A, B and C) within INALT01-REF and INALT01-SHW+40%-LOCAL. For each experiment, water parcels were released for a 10 year period and integrated for a total of 20 (A & B) and 30 (C) years.

The thermohaline anomalies of the North Brazil Current in the Eulerian fields are inspected in Figures 5.5 & 5.6 for the upper 1500 m. Rühs et al (2013) showed that leakage water within the current is concentrated in the upper 500 m. In the second decade of integration, the upper core of the North Brazil Current between 100 and 200 m shows a cooling of about ~0.1°C and a freshening of ~0.05. In contrast, between 200 and 500 m, the water column is warmer and slightly saltier. This dipolar pattern is observed across the entire South Atlantic basin (not shown). Within the thin layer (100 – 200 m), the density contribution from temperature dominates; hence the layer experiences a densification. During that period, large fluctuations in the North Brazil Current transport are seen in Figure 5.1, ranging from -1.5 to +2 Sv around the mean. In the third decade, the current shows a sustained increase in transport. The water column of the offshore edge of the North Brazil Current between 100 and 900 m is warmer by about 0.2°C and saltier by 0.05 compared to the reference experiment. The strongest signal remains at depth between 100 and 300 m. During this period (model years 51 – 60), temperature contributes negatively to the density anomaly, while salinity contributes positively (Figure 5.7). The temperature anomaly dominates and a density decrease of ~0.03 kg $m^{-3}$ is observed offshore of the North Brazil current. The inner core of the current, centred at 150 m between 35°W and 34.6°W is, in contrast, slightly denser.

It is believed that most of the heat associated with Agulhas Rings is rapidly lost to the atmosphere in the Cape Basin (Schmid et al. 2003; Schonten et al. 2000; van Aken et al. 2003), and that the relevant quantity is the additional salt they bring into the South Atlantic. While this is true for the surface mixed-layer, it is shown here that heat resulting from Agulhas leakage is advected equatorward at

6°S at depths of 100 – 900m, corresponding to the upper limb of the Atlantic MOC. Weijer et al. (2002) and van Sebille et al. (2011) reported that the advective timescale further north, into regions of convection, is of the order of 3 – 4 decades. Whether the density signal is maintained or attenuated through circulatory delays is uncertain.

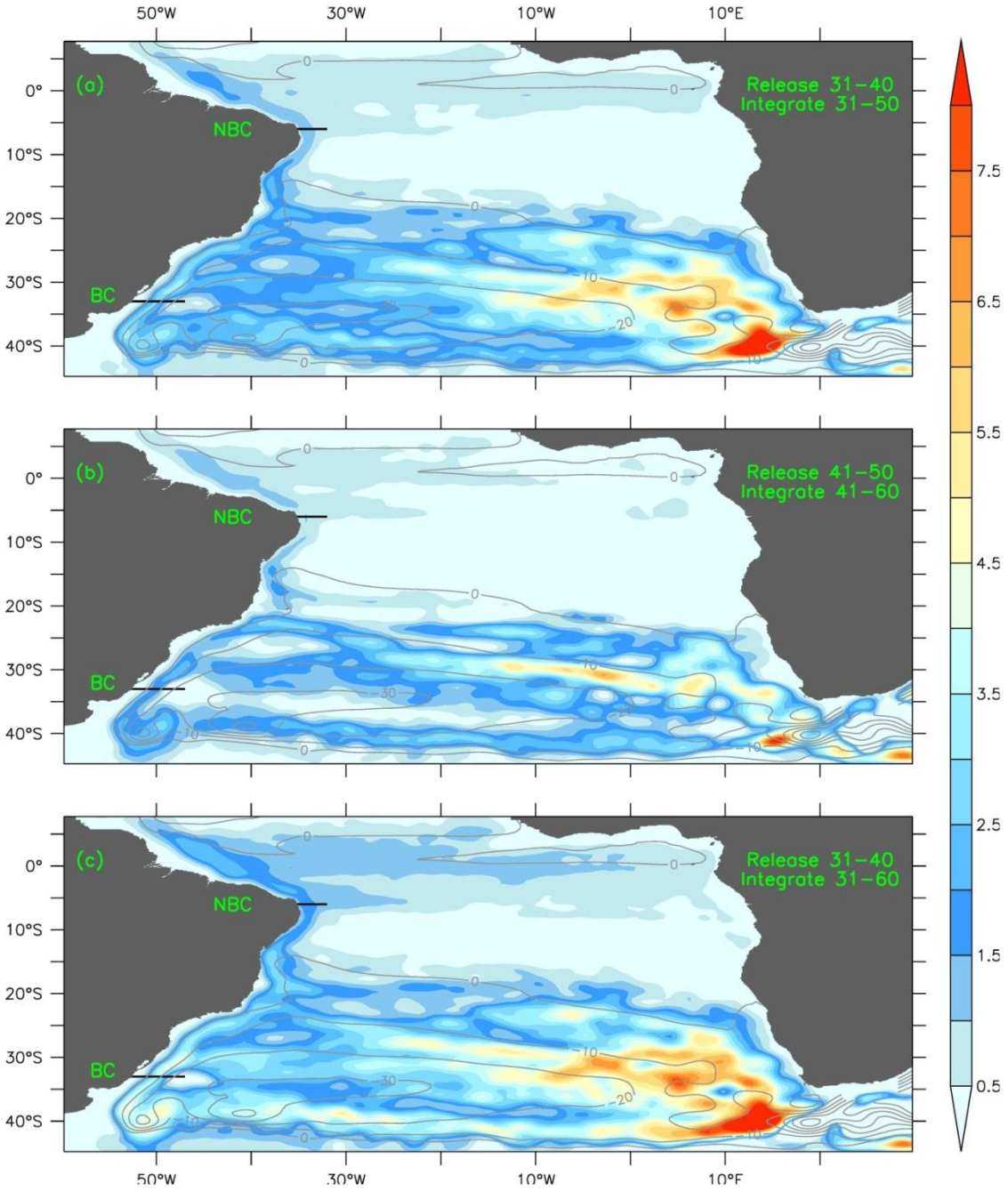


**FIGURE 5.4:** Probability density difference of Agulhas waters spread in the South Atlantic (shading x $10^{-3}$, normalised by the number of occurrences per 0.5° x 0.5° grid box). INALT01-SHW±4-LOCAL minus INALT01-REF for Lagrangian experiments A, B and C described in Table 5.1. Sections along which the North Brazil Current (NBC) and Brazil Current (BC) were measured are shown. Barotropic stream-function contours (Sv) from the INALT01-REF (grey) show the mean horizontal circulation.

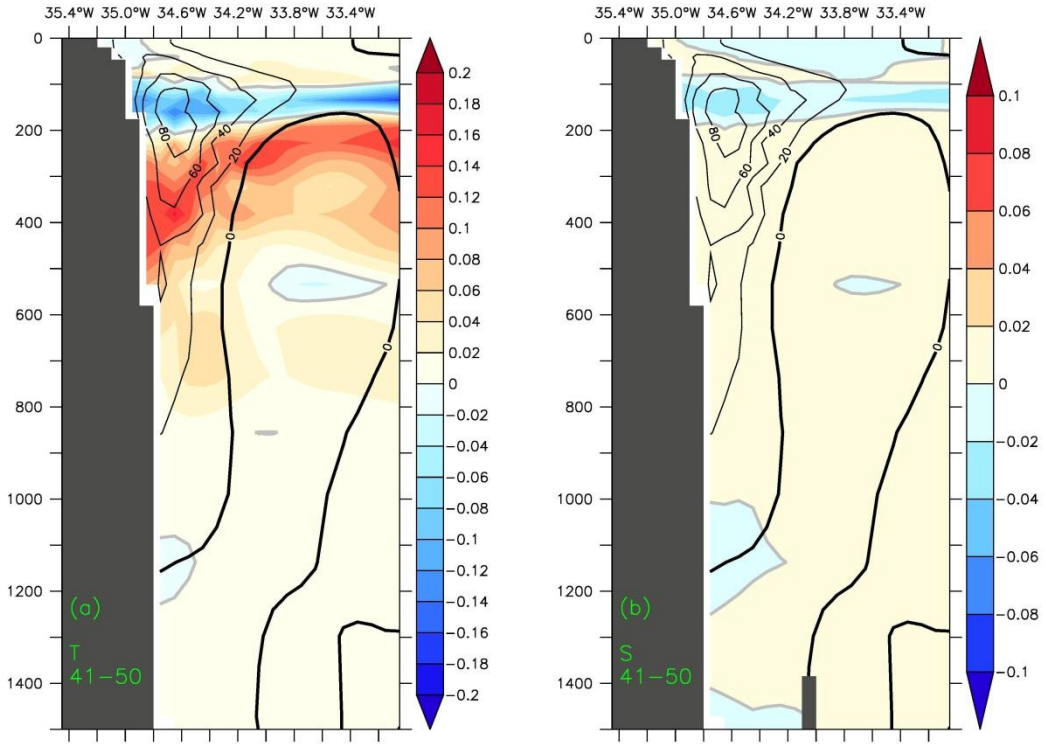


**FIGURE 5.5:** Changes in temperature (T, °C) and salinity (S) of the North Brazil Current at 6°S, INALT01-SHW+40%-LOCAL minus INALT01-REF, averaged over model years 41 – 50. Black contours of average meridional velocity (cm $s^{-1}$) from the INALT01-REF experiment illustrate the structure of the North Brazil Current at that latitude.

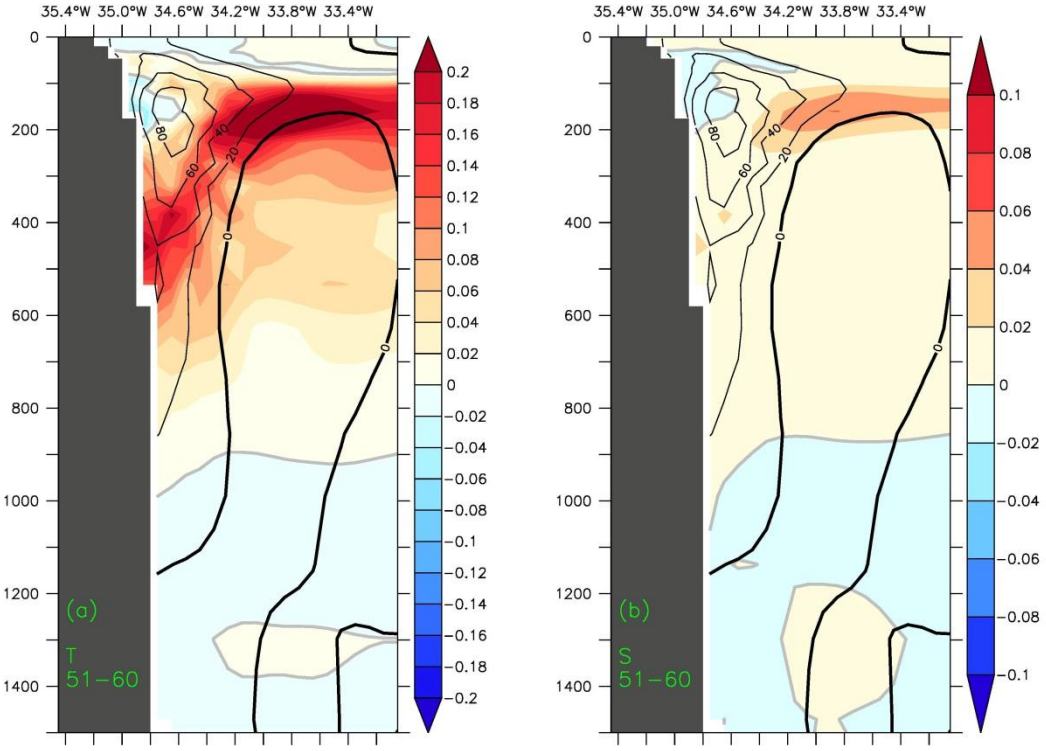


**FIGURE 5.6:** Same as Figure 5.5 for model years 51 – 60.

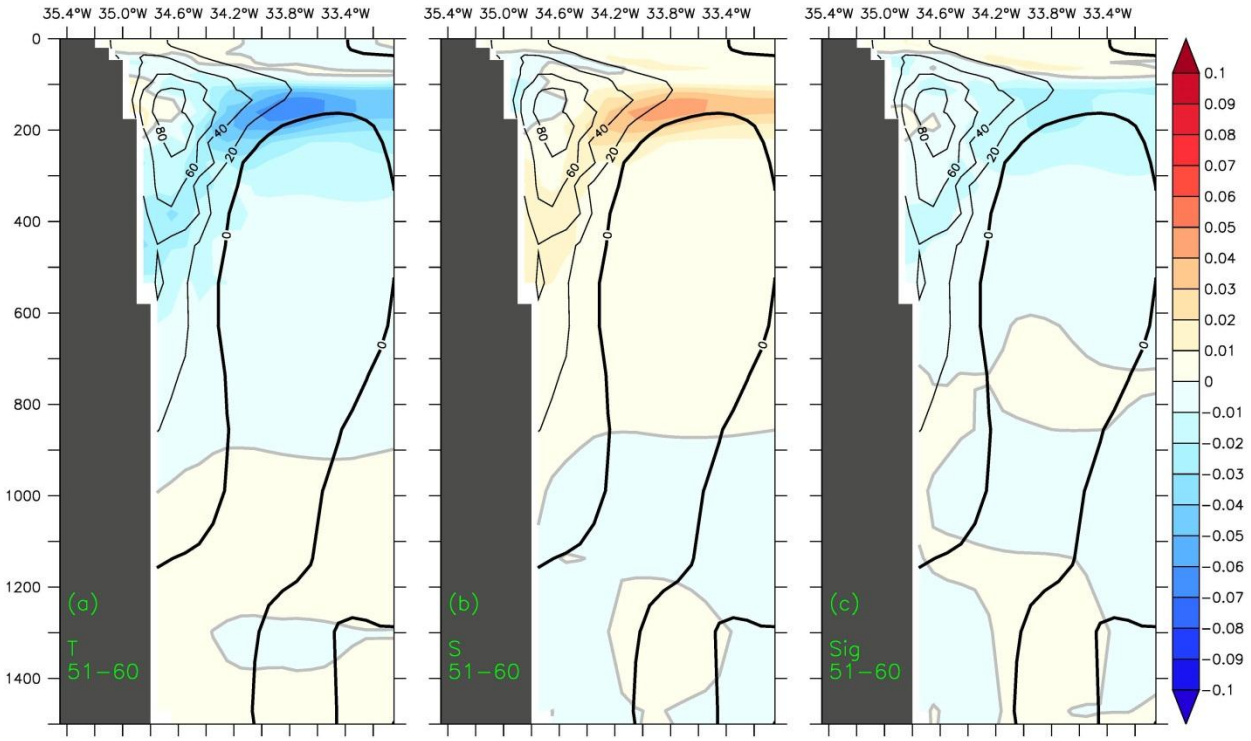


**FIGURE 5.7:** Changes in density ($\sigma_0$, kg $m^{-3}$) across the North Brazil Current at 6°S (c), as well as the density contribution from (a) temperature and (b) salinity anomalies shown in Figure 5.6. INALT01-SHW+40%-LOCAL minus INALT01-REF, averaged over model years 51 – 60. Black contours of average meridional velocity (cm $s^{-1}$) from the INALT01-REF experiment illustrate the structure of the North Brazil Current at that latitude.

## 5.4. Implications

The experiment performed was an attempt to examine in isolation the contribution of Agulhas leakage to the upper branch of the Atlantic Meridional Overturning Circulation. The first results have been presented in this chapter. An increase in leakage conveys both a dynamic and a buoyant signal across the South Atlantic basin. The dynamic signal is transported by means of Rossby and Kelvin waves, and the timescale associated with the response is of the order of 4 – 6 years (Biastoch et al. 2008b; van Sebille and van Leeuwen 2007; Weijer et al. 2002). In the South Atlantic, it has been shown here that the advective timescale of density anomalies is of the same order as the radiative timescale. The most probable timescale associated with advection of leakage waters across the equatorial Atlantic occurs in less than a decade. The localised increase in westerly wind south of Africa induces both a leakage increase and an enhanced South Atlantic subtropical gyre. The Lagrangian analysis (Table 5.1, Figure 5.4) shows that a large part of the additional leakage into the Atlantic is trapped within the subtropical gyre in the first 2 – 3 decades. This may explain the relatively weak salt advection by the North Brazil Current in the Eulerian fields (Figure 5.7).

In chapter 4, the mechanism proposed for leakage response to the westerlies implied a passive role of leakage within the supergyre. Here, it is shown that the main pathway of leakage across the South Atlantic follows the mean horizontal circulation (Figures 5.3 & 5.4). These observations lend some support to the view that leakage may behave passively within the supergyre of the Southern Hemisphere. It remains to be investigated whether the impact of leakage, be it dynamic or advective, on the Atlantic MOC can be regarded as active or passive (Kuhlbrodt et al. 2007; Sijp and England 2009; Weijer et al. 1999).

With regards to the claims that the Agulhas gateway was a critical drive of past climate changes, most studies have focused on the invasion of warm waters of Indian Ocean origin (leakage) into the Cape Basin (*e.g.* Caley et al. 2012; Peeters et al. 2004). While undulations of the pycnocline necessary to influence the velocity field of the Atlantic basins have their source in the Cape Basin, the advection of salt anomalies requires leakage waters (through Agulhas Rings) to cross the Walvis Ridge (Figure 1.3) and be incorporated into the South Atlantic horizontal circulation. Recent evidence has been presented, where variability of the pycnocline over the Walvis Ridge, associated with the passing of Agulhas Rings, has been reconstructed (Scussolini et al. 2013). This suggests that an enhanced Indo-Atlantic exchange during glacial terminations, presumably stimulated by changes in the Southern Hemisphere winds, resulted in density modifications of the South Atlantic.

## 5.5. Summary

In a changing climate, it is not trivial to isolate the impact of Agulhas leakage (increase) on the Atlantic circulation. The fact that the Agulhas system is embedded within the subtropical gyres of the South Atlantic and South Indian Oceans and bounded south by the Antarctic Circumpolar Current makes the assessment particularly difficult. Here, an attempt has been made to induce an increase in leakage without directly changing the large-scale circulation. The impact of that increase in leakage on the South Atlantic was assessed and first results were presented.

Changes to the Agulhas leakage was induced by applying a wind anomaly locally (0° – 45°E and 35°S – 45°S, LOCAL experiment presented in chapter 4). No changes were applied to the turbulent flux over the South Atlantic and Southern Oceans. An average increase in leakage of ~2.8 Sv results in changes in both the velocity and the buoyancy fields of the South Atlantic. The horizontal gyre of the South Atlantic is enhanced by about 4 – 6 Sv. Agulhas leakage advected across the South Atlantic follow a preferred pathway following the Benguela Current and the South Equatorial Current. At ~20°S along the South American coast, a bifurcation occurs and approximately 40 % and 30 % of

leakage waters feed into North Brazil Current and Brazil Current respectively within 2 decades. However, owing to the enhanced South Atlantic subtropical gyre, more than half of the simulated ~2.8 Sv increase in leakage follows the re-circulatory route. The thermohaline characteristics of the North Brazil current show a densification in the upper 100 m, but a lightening between 100 m and 900 m.

# 6. Conclusions

Agulhas leakage refers to the water exported from the Indian Ocean to the Atlantic Ocean by the Agulhas Current system, and forms a central cog of the global meridional overturning circulation. In this thesis, the controls and impact of Agulhas leakage were investigated. The general question was:

**How does the wind pattern of the Southern Hemisphere control the magnitude of Agulhas leakage?**

This question was addressed using a suite of state-of-the-art numerical model configurations. Two global configurations were constructed especially for this thesis (chapter 2). Furthermore, two complementary regional configurations were employed. The use of models enabled a series of dedicated sensitivity simulations that were purposefully designed to investigate the controls of Agulhas leakage (chapters 3 and 4). In chapter 5, the impact of an isolated increase in Agulhas leakage on the Atlantic circulation was explored.

The global configurations, ORCA05 and INALT01, are outcomes of this thesis. ORCA05 is a stand-alone global configuration with a half-degree horizontal resolution and 46 z-levels. INALT01 is a 2-way nested configuration: its base is identical to ORCA05 and its nest refines the horizontal grid to a tenth-degree in the region between 70°W – 70°E and 50°S – 8°N. These configurations adequately represent the large-scale circulation, and INALT01 is capable to represent verisimilarly the complexities of the Agulhas system. Two regional configurations, AGIO and ARC, were additionally used, and were developed through joint collaboration at the University of Cape Town. AGIO is a stand-alone regional configuration (29°W – 115°E, 48°S – 7°N) with a quarter-degree horizontal resolution and 32 σ-levels. ARC is a 2-way nested regional configuration with base that is identical to AGIO and a nest that refines the horizontal grid to a twelfth-degree between 0° – 40°E and 45°S – 30°S. Both regional configurations obtained lateral boundary conditions from the ORCA05 simulations, and all four configurations were forced at the surface using the same dataset. Furthermore, within all configurations, Agulhas leakage was defined and assessed identically using a Lagrangian method. These measures ensured a reasonable degree of consistency and made inter-model comparisons possible. The results presented in this thesis are therefore robust.

In order to investigate the central question of this thesis of how the winds of the Southern Hemisphere influence Agulhas leakage, a series of sensitivity experiments were performed. Each of these experiments altered only one aspect of the wind stress pattern: either the position or the

intensity of either the Indian Ocean easterly trades (between 0° and 32.5°S) or the westerlies (between 35°S and 63°S). The changes to the wind stress were carried out through the application of anomalies onto the momentum flux used to force the models. The degree of changes imposed by these anomalies was representative of the reconstructed past, the present-day and predicted future scenarios: Intensity change of the trades and westerlies by ±20 % and ±40 %; Latitudinal shifts of the maximum westerlies by ±2° and ±4°. A total of 47 model simulations were undertaken, of which 8 reference runs (4 climatologically forced and 4 inter-annually forced).

## 6.1. Summary of the main results

Three questions were addressed in this thesis (chapters 3 – 5) and the following provides a summary of the results.

### Chapter 3: How is Agulhas leakage influenced by upstream dynamics?

- The trade winds linearly affect several features of the Indian Ocean current, namely, the South Equatorial Current, the North and South East Madagascar Currents, and the flow through the Mozambique Channel. The Agulhas Current transport significantly responds to changes in easterly trades. Agulhas leakage is unaffected by changes in easterly trades.
- The mean kinetic energy of the Agulhas Current is altered, and the changes in transport are communicated downstream (Indian Ocean trade winds were not modified south of 32.5°S), such that the inertia of the current at separation also changes. Mesoscale variability of the retroflection and of the Agulhas Return Current is altered. The retroflection loop is stably maintained by topography. Consequently, leakage is unaffected.
- This implies that the control of Agulhas leakage is decoupled from upstream dynamics.

### Chapter 4: How is Agulhas leakage influenced by the Southern Hemisphere westerlies?

- Agulhas leakage responds predominantly to the westerlies. Leakage responds rapidly (within 2 – 3 years) and proportionally to changes in westerlies.
- An equatorward shift of the westerlies results in more leakage, due to the increased momentum input over the southern portion of the supergyre. Conversely, a poleward shift of the westerlies yields less leakage, due to the decreased momentum input over the southern portion of the supergyre.

- An increase in westerlies intensity results in a transient leakage response: Initial proportional increase in leakage and subsequent subsidence to normal levels. The timescale is dependent on the adjustment of the large-scale circulation. Interactions between the Antarctic Circumpolar Current and the Agulhas system become important after 1 – 2 decades.
- Change in leakage is comparable to the change in Sverdrup transport across the southern portion of the supergyre. Leakage itself does not follow Sverdrup dynamics. The mechanism behind leakage response to changes in westerlies is consistent for both shifts and intensity changes of the westerly wind belt.
- These results were reached by using both global configurations, implying that resolution does not influence the process behind leakage response to changes in the westerlies. Moreover, eddy kinetic energy of the retroflection and in the Cape Basin is dissociated from leakage response.

### Chapter 5: How does an increase in Agulhas leakage impact the South Atlantic circulation?

- The first radiative and advective imprints of an increased leakage are seen across the Equator after about a decade.
- Leakage waters have a preferred pathway across the South Atlantic following the mean circulation through the Benguela Current and the South Equatorial Current. Upon reaching the South American coast, at ~20°S, leakage waters bifurcates, feeding into the North Brazil Current (40 % of leakage within 2 decades) and into the Brazil Current (30 % of leakage within 2 decades). Waters captured within the Brazil Current forms a re-circulatory route around the South Atlantic subtropical gyre.
- Increase in the westerlies causes the South Atlantic subtropical gyre to intensify. This results in an enhanced re-circulatory route. More than 50 % of the simulated increase in leakage recirculates.
- The thermohaline characteristics of the North Brazil Current show a densification in the upper 100 m, but a lightening between 100 m and 900 m.

## 6.2. Implications for present-day climate

In the introductory chapter, the results of Biastoch et al. (2009b), Rouault et al. (2009) and van Sebille et al. (2009b) were mentioned (section 1.4). In particular, the latter two studies deduced a link between Agulhas Current and Agulhas leakage from simulations of modern-day climate. However, they disagreed on the sign of the relationship between the two variables: Rouault et al.

(2009) saw a direct relationship, while van Sebille et al. (2009b) noticed an inverse relationship. Furthermore, they reported trends in the current and leakage that matched the relationships. It was hypothesised in sections 1.4 and 3.1 that the different forcing fields employed by the authors may have been the cause of the conflicting results. The simulations for this thesis were performed under the same forcing conditions. AGIO and INALT01 are analogous to the configurations employed by Rouault et al. (2009) and van Sebille et al. (2009b) respectively (chapter 2). Figure 6.1 shows the time-series of Agulhas Current and Agulhas leakage within the hind-cast simulations of AGIO and INALT01. Despite the differences in the magnitude of the transports reproduced by the two model solutions (possible causes discussed in section 2.5 and chapter 3), it is evident that both configurations exhibit trends of the same sign for each of the variables when forced by the same atmospheric fields. For the period 1968 – 2003, a negative (positive) trend in Agulhas Current (leakage) is noted. AGIO's steeper trends (twice that of INALT01) could be due to the stronger recirculations found in that configuration, which results in larger inter-annual variability of the Agulhas Current system. Therefore, this indicates dependence of the results on the forcing fields. To reinforce and ascertain this conclusion, it may be instructive in the future to test another set of coherent and globally balanced forcing fields. Moreover, in light of results presented in chapters 3 and 4, it can be concluded that statistical relationships between Agulhas Current and leakage do not imply cause and impact. Instead, such relationships, particularly within the contemporary climate, express the compounding effects of individual trends present in the modern-day wind field of the Southern Hemisphere. It has been shown that the Agulhas Current responds to changes (trends) in both trades and westerlies, while Agulhas leakage responds to the westerlies.

Arguably, the most important result of chapter 4 is that Agulhas leakage increase (due to strengthened westerlies) has an associated timescale. This is particularly relevant for the present-day climate since the westerlies have been increasing (Swart and Fyfe 2012). Chapter 4 (Figure 4.13 in particular) demonstrated that the strengthening westerly winds are predominantly responsible for the positive trend in leakage over the last 3 – 4 decades (Figure 6.1). The results further suggest that response in leakage in the future may subside, contingent on, firstly, future trends in westerlies strength and migration, and secondly, on the response of the large-scale circulation (the Southern Ocean, in particular).

The mechanism of leakage response to changes in westerly winds suggests that leakage possibly behaves as a passive component of the supergyre circulation. This paradigm is supported further by results in chapter 5, where the preferred pathway of leakage water advection across the Equator is observed to follow the mean horizontal circulation of the South Atlantic.

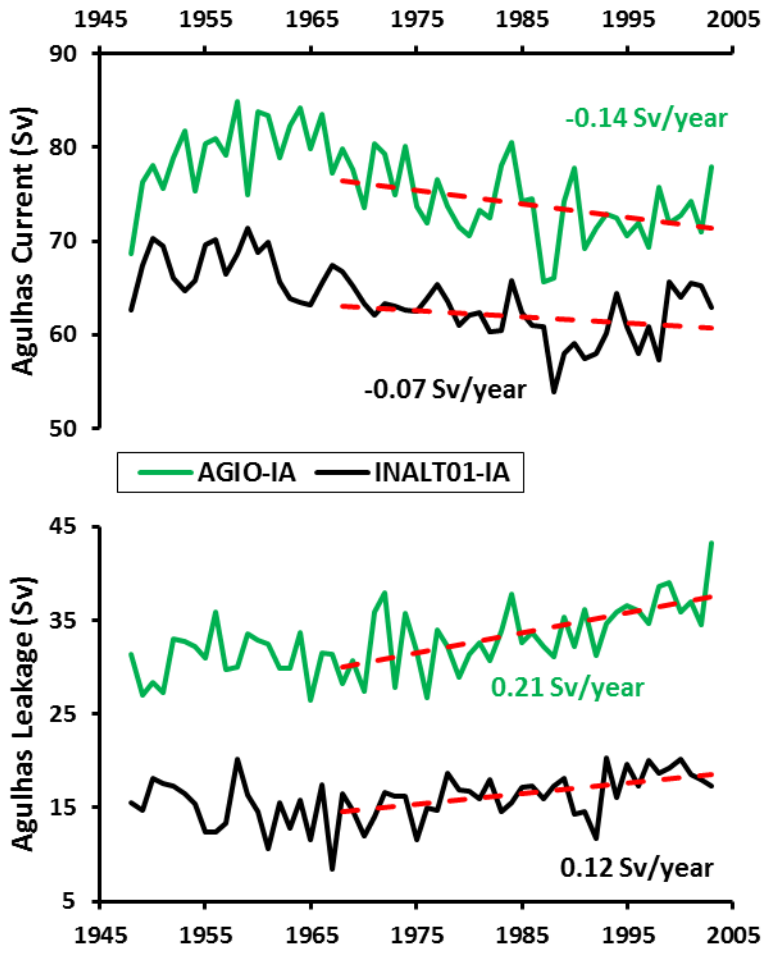


**FIGURE 6.1:** Time-series of Agulhas Current and Agulhas leakage within the inter-annually (IA) forced realisations of the AGIO and INALT01 configurations. Linear trends (dashed red) were computed for the period 1968 – 2003.

## 6.3. Prospect for further research

Results presented in this dissertation pave the way for further investigations. The importance of interactions between the Southern Ocean and the Agulhas system has been shown in chapter 4. In particular, the adjustment of the circumpolar current to an increase in the westerlies sets a timescale in Agulhas leakage response. A detailed investigation of the non-linear exchange between these two systems would shed light on precise mechanism of the interaction. Furthermore, the Southern Ocean is represented at relatively coarse horizontal resolution within the global configurations used here (section 4.3 and 4.5). As such, the mesoscale is not adequately reproduced. An attempt at parameterising the impact of eddies indicated that the adjustment timescale is prolonged. Therefore, in order to ascertain the timescale, it would be desirable to assess Agulhas leakage response within a model configuration that has an eddying Southern Ocean. Such a configuration would additionally

enable the investigation of the impact of a change in westerly wind intensity and/or position on both the cold- and warm-water routes.

The investigation of the controls of Agulhas leakage presented in this thesis focused on the dynamical response of the ocean circulation to altered surface momentum flux. The effect of changing winds on surface buoyancy fluxes was not considered. Additional insights could be obtained by implementing the effect of the application of wind stress anomalies on the thermohaline forcing, or by performing simulations within coupled models. This would be particularly relevant since paleoceanographic records relate displacements of the subtropical front to leakage modulation on centennial-millennial timescales (Bard and Rickaby 2009; Peeters et al. 2004). While, the discussion presented in this thesis did not focus on such long timescales, the results do provide a framework for the interpretation of paleo-proxy records. On paleo-timescale, atmospheric feedbacks on the thermohaline fields are important. It is not straight-forward that movements of the Southern Ocean wind belts would result to the movement of the subtropical front. In fact, the very definition of the subtropical front is of current contention (de Boer et al. 2013b; Graham and de Boer 2013). More research effort is necessary in order to clarify the precise role of the subtropical front in relation to Agulhas leakage.

Agulhas leakage is one component of the exchange that occurs south of Africa; it refers to the Indian-Atlantic transfer in the upper 1500 m that is mediated by the Agulhas Current system (red and light blue arrows in Figure 1.1). At depth, between about 1500 and 4000 m, water from the Atlantic Ocean is exported to the Indian Ocean (dark blue arrow in Figure 1.1). This flow is referred to as the Atlantic-Indian exchange, and comprises mainly of North Atlantic Deep Water (Arhan et al. 2003). Little is known about Atlantic-Indian deep transfer, and the pathway taken by this exchange is unclear. Part of the North Atlantic Deep Water feeds the Agulhas Under-Current (Beal and Bryden 1997; Beal 2009; Biastoch et al. 2009a). Topographic obstacles, such as the Mozambique Ridge, seem to hinder the furtherance of this under-current into the Indian Ocean. However, the existence of under-currents in the Mozambique Channel (de Ruijter 2002; Ridderinkhof et al. 2010) and east of Madagascar (Nauw et al. 2008), which likewise carry North Atlantic Deep Water (van Aken et al. 2004), suggests that the Atlantic-Indian exchange may have other pathways. An investigation of the Atlantic-Indian exchange could potentially be undertaken within INALT01. The southward export of North Atlantic Deep Water is realistically reproduced by INALT01, and its pathway across the South Atlantic is linked to the Agulhas Ring corridor (van Sebille et al. 2012), which is likewise successfully simulated. Furthermore, employing the sensitivity experiments presented in chapter 4, the direct

and indirect influence of the Southern Hemisphere westerlies on the Atlantic-Indian exchange can be explored.

Results presented in chapter 5 show that diagnosing the impact of Agulhas leakage in the South Atlantic is not trivial. Even more elusive is the contribution of leakage in the meridional overturning circulation. In the course of climate change, the strengthening Southern Hemisphere winds would cause the South Atlantic subtropical gyre to intensify and shift (Biastoch et al. 2009b; Biastoch and Böning 2013). Since leakage waters follow the mean circulation, this would imply more leakage waters would be trapped within a re-circulatory path rather than being advected across the Equator by the North Brazil Current. The implications on the hypothesised thermohaline contribution of leakage in the North Atlantic are profound, and remain to be investigated.

The utility of the INALT01 configuration is by no means limited to the understanding of the large-scale circulation. The Agulhas Current has substantial regional impact, and INALT01 could be employed to investigate a number of questions pertaining to the interaction of the Agulhas Current with the coastal circulation. For example, how do the kinematic upwelling events occurring along the east coast of South Africa (Lutjeharms and Stockton 1987; Lutjeharms et al. 2000) vary with time? Jackson et al. (2012) recently observed that during the passing of a single Natal Pulse, the leading edge of the Agulhas Current penetrated far inshore, and swept away immotile larvae from the shelf to the open ocean – Does this occur for each passing of a Natal Pulse? The implications for larvae could be simulated through Lagrangian experiments.

## 6.4. Final remark

Within a modelling framework, this thesis disentangled the manner in which the winds of the Southern Hemisphere control Agulhas leakage. The sensitivity of the leakage on the westerlies has been shown, and the relevance for current climate discussed. While satellite wind products have been available for over a decade, observing leakage in the real ocean remains a challenge. Therefore, the present-day state of leakage with respect to the strength and position of the westerlies is yet to be confirmed. In the quest to determine simple methods of estimating Agulhas leakage from observed datasets, INALT01 is currently being employed as a test bed to develop a method of deducing leakage from sea surface height (Le Bars et al. in prep). This endeavour promises to provide two decades of observed Agulhas leakage from satellite altimetry.

# Supplementary material

## S1. Results of significance tests

This addendum provides the details of the statistical significance tests performed in chapters 3 – 5. These were carried out using the Welch's two-tailed *t*-test (Welch 1947) for samples of unequal variances. In all cases, the null-hypothesis was $\overline{X_1} = \overline{X_2}$. The *t*-statistic and effective degrees of freedom were calculated as follows,

$$t - statistic \quad = \quad \frac{\overline{X_1} - \overline{X_2}}{\sqrt{\frac{s_1^2}{N_1} + \frac{s_2^2}{N_2}}}$$

$$Effective\ degrees\ of\ freedom, \quad d.f \quad = \quad \frac{\left(\frac{s_1^2}{N_1} + \frac{s_2^2}{N_2}\right)^2}{\frac{s_1^4}{N_1^2(N_1 - 1)} + \frac{s_2^4}{N_2^2(N_2 - 1)}}$$

, where $\bar{X}, s\ and\ N$ were the sample mean (units in Sv throughout), standard-deviation (units in Sv throughout) and size respectively. For the *t-statistic*, the absolute value is taken.

### S1.1. Chapter 3, Section 3.2, Figure 3.5.

INALT01-AC

REF $\overline{X_1}$ = 68.57; $s_1$ = 2.07; $N_1$ = 20.

STW-40% $\overline{X_2}$ = 65.83; $s_2$ = 2.21; $N_2$ = 20.

*t* = 4.05; *t*(*d.f* = 37, *p* = 0.01) = 2.715; reject null hypothesis.

STW+40% $\overline{X_2}$ = 71.49; $s_2$ = 3.04; $N_2$ = 20.

*t* = 3.56; *t*(*d.f* = 33, *p* = 0.01) = 2.733; reject null hypothesis.

INALT01-MOZ

REF $\overline{X_1}$ = 18.78; $s_1$ = 0.52; $N_1$ = 20.

STW-40% $\overline{X_2}$ = 17.01; $s_2$ = 0.59; $N_2$ = 20.

*t* = 10.05; *t*(*d.f* = 37, *p* = 0.01) = 2.715; reject null hypothesis.

STW+40% $\overline{X_2}$ = 20.80; $s_2$ = 0.70; $N_2$ = 20.

*t* = 10.37; *t*(*d.f* = 35, *p* = 0.01) = 2.723; reject null hypothesis.

INALT01-SEMC

REF $\overline{X_1}$ = 18.70; $s_1$ = 2.76; $N_1$ = 20.

STW-40% $\overline{X_2}$ = 11.21; $s_2$ = 1.95; $N_2$ = 20.

$t$ = 9.91; $t$(*d.f* = 34, $p$ = 0.01) = 2.728; reject null hypothesis.

STW+40% $\overline{X_2}$ = 23.64; $s_2$ = 3.11; $N_2$ = 20.

$t$ = 5.31; $t$(*d.f* = 37, $p$ = 0.01) = 2.715; reject null hypothesis.

ARC-AC

REF $\overline{X_1}$ = 69.70; $s_1$ = 4.30; $N_1$ = 20.

STW-40% $\overline{X_2}$ = 61.70; $s_2$ = 2.20; $N_2$ = 20.

$t$ = 7.55; $t$(*d.f* = 28, $p$ = 0.01) = 2.763; reject null hypothesis.

STW+40% $\overline{X_2}$ = 79.00; $s_2$ = 3.80; $N_2$ = 20.

$t$ = 7.34; $t$(*d.f* = 37, $p$ = 0.01) = 2.715; reject null hypothesis.

ARC-MOZ

REF $\overline{X_1}$ = 25.20; $s_1$ = 0.90; $N_1$ = 20.

STW-40% $\overline{X_2}$ = 22.70; $s_2$ = 0.80; $N_2$ = 20.

$t$ = 9.28; $t$(*d.f* = 37, $p$ = 0.01) = 2.715; reject null hypothesis.

STW+40% $\overline{X_2}$ = 27.4; $s_2$ = 1.30; $N_2$ = 20.

$t$ = 6.22; $t$(*d.f* = 33, $p$ = 0.01) = 2.733; reject null hypothesis.

ARC-SEMC

REF $\overline{X_1}$ = 24.7; $s_1$ = 1.90; $N_1$ = 20.

STW-40% $\overline{X_2}$ = 18.20; $s_2$ = 2.40; $N_2$ = 20.

$t$ = 9.50; $t$(*d.f* = 36, $p$ = 0.01) = 2.719; reject null hypothesis.

STW+40% $\overline{X_2}$ = 30.10; $s_2$ = 1.80; $N_2$ = 20.

$t$ = 9.23; $t$(*d.f* = 37, $p$ = 0.01) = 2.715; reject null hypothesis.

## S1.2. Chapter 3, Section 3.3, Figure 3.6.

| Agulhas Current | | $\overline{X}$ | *s* | *t* | *d.f* | *t*-table *p*=0.01 | null-hypothesis |
|---|---|---|---|---|---|---|---|
| ORCA05 | REF | 69.77 | 0.96 | | | | |
| | STW-20% | 68.20 | 0.60 | 5.50 | 25 | 2.787 | reject |
| | STW-40% | 66.73 | 0.73 | 10.06 | 28 | 2.763 | reject |
| | STW+20% | 70.99 | 0.61 | 4.29 | 25 | 2.787 | reject |
| | STW+40% | 72.90 | 1.13 | 8.43 | 29 | 2.756 | reject |
| AGIO | REF | 73.11 | 2.39 | | | | |
| | STW-20% | 68.67 | 2.34 | 5.31 | 30 | 2.750 | reject |
| | STW-40% | 66.01 | 2.25 | 8.65 | 30 | 2.750 | reject |
| | STW+20% | 76.67 | 2.15 | 4.43 | 30 | 2.750 | reject |
| | STW+40% | 80.98 | 4.48 | 6.20 | 23 | 2.807 | reject |
| INALT01 | REF | 65.45 | 1.74 | | | | |
| | STW-40% | 61.72 | 1.73 | 6.09 | 30 | 2.750 | reject |
| | STW+40% | 67.89 | 2.72 | 3.02 | 26 | 2.779 | reject |
| ARC | REF | 66.36 | 2.96 | | | | |
| | STW-40% | 59.64 | 2.64 | 6.77 | 30 | 2.750 | reject |
| | STW+40% | 75.94 | 2.73 | 9.51 | 30 | 2.750 | reject |

**TABLE S1.1:** Significance tests for changes in the Agulhas Current due changes in the trade winds. For each configuration, ($\overline{X_1}$, $s_1$) is the REF value and ($\overline{X_2}$, $s_2$) is the sensitivity experiment; $N_1 = N_2 = 16$.

| Agulhas leakage | | $\overline{X}$ | *s* | *t* | *d.f* | *t*-table *p*=0.01 | null-hypothesis |
|---|---|---|---|---|---|---|---|
| ORCA05 | REF | 29.59 | 1.54 | | | | |
| | STW-20% | 30.36 | 2.19 | 1.15 | 27 | 3.690 | accept |
| | STW-40% | 30.26 | 1.52 | 1.23 | 30 | 3.646 | accept |
| | STW+20% | 28.45 | 1.70 | 1.99 | 30 | 3.646 | accept |
| | STW+40% | 28.63 | 1.23 | 1.95 | 29 | 3.659 | accept |
| AGIO | REF | 31.87 | 1.42 | | | | |
| | STW-20% | 30.48 | 2.17 | 2.12 | 27 | 3.690 | accept |
| | STW-40% | 29.28 | 2.06 | 4.09 | 28 | 3.674 | reject † |
| | STW+20% | 32.02 | 2.67 | 0.20 | 24 | 3.745 | accept |
| | STW+40% | 32.96 | 2.20 | 1.63 | 27 | 3.690 | accept |
| INALT01 | REF | 17.27 | 1.94 | | | | |
| | STW-40% | 17.18 | 1.43 | 0.16 | 21 | 3.819 | accept |
| | STW+40% | 17.47 | 2.11 | 0.29 | 24 | 3.745 | accept |
| ARC | REF | 19.85 | 1.62 | | | | |
| | STW-40% | 18.03 | 2.06 | 2.80 | 27 | 3.690 | accept |
| | STW+40% | 19.35 | 1.91 | 0.80 | 28 | 3.674 | accept |

**TABLE S1.2:** Same as Table S1.1 for Agulhas leakage. In contrast to the Agulhas Current, changes in Indian Ocean trade winds do not significantly induce changes in Agulhas leakage (except for †).

## S1.3. Chapter 4, Section 4.3, Figure 4.6.

ORCA05, model years 35 – 44

REF $\overline{X_1}$ = 31.40; $s_1$ = 1.47; $N_1$ = 10.

SHW+40%-FULL $\overline{X_2}$ = 39.94; $s_2$ = 1.28; $N_2$ = 10.

$t$ = 13.83; $t(d.f = 17, p = 0.01)$ = 2.898; reject null hypothesis.

ORCA05, model years 51 – 110

REF $\overline{X_1}$ = 31.70; $s_1$ = 1.66; $N_1$ = 60.

SHW+40%-FULL $\overline{X_2}$ = 30.99; $s_2$ = 2.52; $N_2$ = 60.

$t$ = 1.82; $t(d.f = 101, p = 0.01)$ = 2.625; accept null hypothesis.

## S1.4. Chapter 5, Section 5.2, Figure 5.1.

INALT01, Agulhas Leakage (AL), model years 51 – 60

REF $\overline{X_1}$ = 16.59; $s_1$ = 1.63; $N_1$ = 10.

SHW+40%-LOCAL $\overline{X_2}$ = 19.36; $s_2$ = 1.41; $N_2$ = 10.

$t$ = 4.07; $t(d.f = 17, p = 0.01)$ = 2.898; reject null hypothesis.

INALT01, North Brazil Current (NBC), model years 51 – 60

REF $\overline{X_1}$ = 19.90; $s_1$ = 0.62; $N_1$ = 10.

SHW+40%-LOCAL $\overline{X_2}$ = 21.04; $s_2$ = 0.60; $N_2$ = 10.

$t$ = 4.18; $t(d.f = 17, p = 0.01)$ = 2.898; reject null hypothesis.

INALT01, Atlantic Meridional Overturning Circulation (AMOC) at 6°S, model years 51 – 60

REF $\overline{X_1}$ = 15.55; $s_1$ = 0.21; $N_1$ = 10.

SHW+40%-LOCAL $\overline{X_2}$ = 15.83; $s_2$ = 0.27; $N_2$ = 10.

$t$ = 2.58; $t(d.f = 16, p = 0.05)$ = 2.120; reject null hypothesis.

INALT01, Brazil Current, model years 51 – 60

REF $\overline{X_1}$ = 15.13; $s_1$ = 0.74; $N_1$ = 10.

SHW+40%-LOCAL $\overline{X_2}$ = 16.09; $s_2$ = 0.39; $N_2$ = 10.

$t$ = 3.62; $t(d.f = 13, p = 0.01)$ = 3.012; reject null hypothesis.

# Bibliography


Allison, L. C., H. L. Johnson, D. P. Marshall, and D. R. Munday, 2010: Where do winds drive the Antarctic Circumpolar Current? *Geophysical Research Letters*, **37**, 1–5, doi:10.1029/2010GL043355.

Allison, L. C., H. L. Johnson, and D. P. Marshall, 2011: Spin-up and adjustment of the Antarctic Circumpolar Current and global pycnocline. *Journal of Marine Research*, **69**, 167–189, doi:10.1357/002224011798765330.

Anderson, R. F., Z. Chase, M. Q. Fleisher, and J. Sachs, 2002: The Southern Ocean's biological pump during the Last Glacial Maximum. *Deep-Sea Research*, **49**, 1909–1938, doi:10.1016/S0967-0645(02)00018-8.

Ansorge, I., S. Speich, J. R. E. Lutjeharms, G. J. Goni, C. J. de W. Rautenbach, P. Froneman, M. Rouault, and S. L. Garzoli, 2005: Monitoring the oceanic flow between Africa and Antarctica: Report of the first GoodHope cruise. *South African Journal of Science*, **101**, 29–35.

Arakawa, A., and Y.-J. G. Hsu, 1990: Energy conserving and potential-entrophy dissipating schemes for the shallow water equations. *Monthly Weather Review*, **118**, 1960–1969.

Arhan, M., H. Mercier, and Y.-H. Park, 2003: On the deep water circulation of the eastern South Atlantic Ocean. *Deep Sea Research*, **50**, 889–916, doi:10.1016/S0967-0637(03)00072-4.

Backeberg, B. C., and C. J. C. Reason, 2010: A connection between the South Equatorial Current north of Madagascar and Mozambique Channel Eddies. *Geophysical Research Letters*, **37**, L04604, doi:10.1029/2009GL041950.

Backeberg, B. C., P. Penven, and M. Rouault, 2012: Impact of intensified Indian Ocean winds on mesoscale variability in the Agulhas system. *Nature Climate Change*, **2**, 608–612, doi:10.1038/nclimate1587.

Bamber, J., M. van den Broeke, J. Ettema, J. Lenaerts, and E. Rignot, 2012: Recent large increases in freshwater fluxes from Greenland into the North Atlantic. *Geophysical Research Letters*, **39**, L19501, doi:10.1029/2012GL052552.

Bard, E., and R. E. M. Rickaby, 2009: Migration of the subtropical front as a modulator of glacial climate. *Nature*, **460**, 380–383, doi:10.1038/nature08189.

Barnier, B. and Coauthors, 2006: Impact of partial steps and momentum advection schemes in a global ocean circulation model at eddy-permitting resolution. *Ocean Dynamics*, **56**, 543–567, doi:10.1007/s10236-006-0082-1.

Beal, L. M., 2009: A Time Series of Agulhas Undercurrent Transport. *Journal of Physical Oceanography*, **39**, 2436–2450, doi:10.1175/2009JPO4195.1.

Beal, L. M., and H. L. Bryden, 1997: Observations of an Agulhas Undercurrent. *Deep Sea Research*, **44**, 1715–1724, doi:10.1016/S0967-0637(97)00033-2.

Beal, L. M., and H. L. Bryden, 1999: The velocity and vorticity structure of the Agulhas Current at 32°S. *Journal of Geophysical Research*, **104**, 5151–5176, doi:10.1029/1998JC900056.

Beal, L. M., W. P. M. de Ruijter, A. Biastoch, R. Zahn, and SCOR/WCRP/IAPSO-Working-Group-136, 2011: On the role of the Agulhas system in ocean circulation and climate. *Nature*, **472**, 429–436, doi:10.1038/nature09983.

Behrens, E., A. Biastoch, and C. W. Böning, 2013: Spurious AMOC trends in global ocean sea-ice models related to subarctic freshwater forcing. *Ocean Modelling*, **69**, 39–49, doi:10.1016/j.ocemod.2013.05.004.

Biastoch, A., and W. Krauss, 1999: The Role of Mesoscale Eddies in the Source Regions of the Agulhas Current. *Journal of Physical Oceanography*, **29**, 2303–2317.

Biastoch, A., and C. W. Böning, 2013: Anthropogenic impact on Agulhas leakage. *Geophysical Research Letters*, **40**, 1138–1143, doi:10.1002/grl.50243.

Biastoch, A., C. J. C. Reason, J. R. E. Lutjeharms, and O. Boebel, 1999: The importance of flow in the Mozambique Channel to seasonality in the Greater Agulhas Current System. *Geophysical Research Letters*, **26**, 3321–3324, doi:10.1029/1999GL002349.

Biastoch, A., C. W. Böning, J. Getzlaff, J.-M. Molines, and G. Madec, 2008a: Causes of Interannual–Decadal Variability in the Meridional Overturning Circulation of the Midlatitude North Atlantic Ocean. *Journal of Climate*, **21**, 6599–6615, doi:10.1175/2008JCLI2404.1.

Biastoch, A., C. W. Böning, and J. R. E. Lutjeharms, 2008b: Agulhas leakage dynamics affects decadal variability in Atlantic overturning circulation. *Nature*, **456**, 489–492, doi:10.1038/nature07426.

Biastoch, A., J. R. E. Lutjeharms, C. W. Böning, and M. Scheinert, 2008c: Mesoscale perturbations control inter-ocean exchange south of Africa. *Geophysical Research Letters*, **35**, L20602, doi:10.1029/2008GL035132.

Biastoch, A., L. M. Beal, J. R. E. Lutjeharms, and T. G. D. Casal, 2009a: Variability and Coherence of the Agulhas Undercurrent in a High-Resolution Ocean General Circulation Model. *Journal of Physical Oceanography*, **39**, 2417–2435, doi:10.1175/2009JPO4184.1.

Biastoch, A., C. W. Böning, F. U. Schwarzkopf, and J. R. E. Lutjeharms, 2009b: Increase in Agulhas leakage due to poleward shift of Southern Hemisphere westerlies. *Nature*, **462**, 495–498, doi:10.1038/nature08519.

Blanke, B., and P. Delecluse, 1993: Variability of the tropical Atlantic Ocean simulated by a general circulation model with two different mixed-layer physics. *Journal of Physical Oceanography*, **23**, 1363–1388.

Boebel, O., J. Lutjeharms, C. Schmid, W. Zenk, T. Rossby, and C. Barron, 2003a: The Cape Cauldron: a regime of turbulent inter-ocean exchange. *Deep-Sea Research*, **50**, 57–86.

Boebel, O., T. Rossby, J. Lutjeharms, W. Zenk, and C. Barron, 2003b: Path and variability of the Agulhas Return Current. *Deep Sea Research*, **50**, 35–56, doi:10.1016/S0967-0645(02)00377-6.

Böning, C. W., A. Dispert, M. Visbeck, S. R. Rintoul, and F. U. Schwarzkopf, 2008: The response of the Antarctic Circumpolar Current to recent climate change. *Nature Geoscience*, **1**, 864–869, doi:10.1038/ngeo362.

Boudra, D. B., and W. P. M. De Ruijter, 1986: The wind-driven circulation of the South Atlantic-Indian ocean — II. Experiments using a multi-layer numerical model. *Deep Sea Research*, **33**, 447–482, doi:10.1016/0198-0149(86)90126-3.

Boudra, D. B., and E. P. Chassignet, 1988: Dynamics of Agulhas Retroflection and Ring Formation in a Numerical Model. Part I: The Vorticity Balance. *Journal of Physical Oceanography*, **18**, 280–303, doi:10.1175/1520-0485(1988)018<0280:DOARAR>2.0.CO;2.

Bourlès, B., Y. Gouriou, and R. Chuchla, 1999: On the circulation in the upper layer of the western equatorial Atlantic. *Journal of Geophysical Research*, **104**, 21151, doi:10.1029/1999JC900058.

Brandt, P., F. A. Schott, C. Provost, A. Kartavtseff, V. Hormann, B. Bourlès, and J. Fischer, 2006: Circulation in the central equatorial Atlantic: Mean and intraseasonal to seasonal variability. *Geophysical Research Letters*, **33**, L07609, doi:10.1029/2005GL025498.

Bryden, H. L., L. M. Beal, and L. M. Duncan, 2005: Structure and Transport of the Agulhas Current and Its Temporal Variability. *Journal of Oceanography*, **61**, 479–492, doi:10.1007/s10872-005-0057-8.

Byrne, D. A., A. L. Gordon, and W. F. Haxby, 1995: Agulhas Eddies: A Synoptic View Using Geosat ERM Data. *Journal of Physical Oceanography*, **25**, 902–917, doi:10.1175/1520-0485(1995)025<0902:AEASVU>2.0.CO;2.

Cai, W., 2006: Antarctic ozone depletion causes an intensification of the Southern Ocean super-gyre circulation. *Geophysical Research Letters*, **33**, L03712, doi:10.1029/2005GL024911.

Caley, T., J. Giraudeau, B. Malaizé, L. Rossignol, and C. Pierre, 2012: Agulhas leakage as a key process in the modes of Quaternary climate changes. *Proceedings of the National Academy of Sciences of the United States of America*, **109**, 6835–6839, doi:10.1073/pnas.1115545109.

Carton, J. A., G. Chepurin, X. Cao, and B. Giese, 2000: A Simple Ocean Data Assimilation Analysis of the Global Upper Ocean 1950–95. Part I: Methodology. *Journal of Physical Oceanography*, **30**, 294–309, doi:10.1175/1520-0485(2000)030<0294:ASODAA>2.0.CO;2.

Chassignet, E. P., and D. P. Marshall, 2008: Gulf Stream separation in Numerical Ocean Model, in *Ocean Modeling in an Eddying Regime*. M.W. Hecht and H. Hasumi, Eds. American Geophysical Union, doi:10.1029/177GM05.

Chassignet, E. P., H. E. Hurlburt, O. M. Smedstad, G. R. Halliwell, P. J. Hogan, A. J. Wallcraft, R. Baraille, and R. Bleck, 2007: The HYCOM (HYbrid Coordinate Ocean Model) data assimilative system. *Journal of Marine Systems*, **65**, 60–83, doi:10.1016/j.jmarsys.2005.09.016.

Chelton, D. B., R. A. DeSzoeke, M. G. Schlax, E. N. Karim, and S. Nicolas, 1998: Geographical variability of the first baroclinic Rossby radius of deformation. *Journal of Physical Oceanography*, **28**, 433 – 460.

Chiessi, C. M., S. Mulitza, A. Paul, J. Pätzold, J. Groeneveld, and G. Wefer, 2008: South Atlantic interocean exchange as the trigger for the Bølling warm event. *Geology*, **36**, 919, doi:10.1130/G24979A.1.

Cronin, M. F., T. Tozuka, A. Biastoch, J. V. Durgadoo, and L. M. Beal, 2013: Prevalence of strong bottom currents in the greater Agulhas system. *Geophysical Research Letters*, **40**, 1772–1776, doi:10.1002/grl.50400.

Cunningham, S. A., and R. Marsh, 2010: Observing and modeling changes in the Atlantic MOC. *Wiley Interdisciplinary Reviews: Climate Change*, **1**, 180–191, doi:10.1002/wcc.22.

de Boer, A. M., A. B. Collier, and R. Caballero, 2013a: Processes driving thunderstorms over the Agulhas Current. *Journal of Geophysical Research*, **118**, 2220–2228, doi:10.1002/jgrd.50238.

de Boer, A. M., R. M. Graham, M. D. Thomas, and K. E. Kohfeld, 2013b: The control of the Southern Hemisphere Westerlies on the position of the Subtropical Front. *Journal of Geophysical Research*, under revision.

de Ruijter, W. P. M., 1982: Asymptotic Analysis of the Agulhas and Brazil Current Systems. *Journal of Physical Oceanography*, **12**, 361–373, doi:10.1175/1520-0485(1982)012<0361:AAOTAA>2.0.CO;2.

de Ruijter, W. P. M., 2002: Observations of the flow in the Mozambique Channel. *Geophysical Research Letters*, **29**, 1502, doi:10.1029/2001GL013714.

de Ruijter, W. P. M., and D. B. Boudra, 1985: The wind-driven circulation in the South Atlantic-Indian Ocean—I. Numerical experiments in a one-layer model. *Deep Sea Research*, **32**, 557–574, doi:10.1016/0198-0149(85)90044-5.

de Ruijter, W. P. M., A. Biastoch, S. S. Drijfhout, J. R. E. Lutjeharms, R. P. Matano, T. Pichevin, P. J. van Leeuwen, and W. Weijer, 1999: Indian-Atlantic interocean Dynamics , estimation and impact ring shedding. *Journal of Geophysical Research*, **104**, 20885 – 20910.

de Ruijter, W. P. M., H. M. va. Aken, E. J. Beier, J. R. E. Lutjeharms, R. P. Matano, and M. W. Schouten, 2004: Eddies and dipoles around South Madagascar: formation, pathways and large-scale impact. *Deep Sea Research*, **51**, 383–400, doi:10.1016/j.dsr.2003.10.011.

Debreu, L., and E. Blayo, 2008: Two-way embedding algorithms: a review. *Ocean Dynamics*, **58**, 415–428, doi:10.1007/s10236-008-0150-9.

Dencausse, G., M. Arhan, and S. Speich, 2010a: Routes of Agulhas rings in the southeastern Cape Basin. *Deep-Sea Research*, **57**, 1406–1421, doi:10.1016/j.dsr.2010.07.008.

Dencausse, G., M. Arhan, and S. Speich, 2010b: Spatio-temporal characteristics of the Agulhas Current retroflection. *Deep-Sea Research*, **57**, 1392–1405, doi:10.1016/j.dsr.2010.07.004.

Dencausse, G., M. Arhan, and S. Speich, 2011: Is there a continuous Subtropical Front south of Africa? *Journal of Geophysical Research*, **116**, C02027, doi:10.1029/2010JC006587.

Deshayes, J. and Coauthors, 2013: Oceanic hindcast simulations at high resolution suggest that the Atlantic MOC is bistable. *Geophysical Research Letters*, **40**, 3069–3073, doi:10.1002/grl.50534.

Dijkstra, H. A., and W. P. M. de Ruijter, 2001: On the Physics of the Agulhas Current: Steady Retroflection Regimes. *Journal of Physical Oceanography*, **31**, 2971–2985.

Doglioli, a. M., M. Veneziani, B. Blanke, S. Speich, and A. Griffa, 2006: A Lagrangian analysis of the Indian-Atlantic interocean exchange in a regional model. *Geophysical Research Letters*, **33**, L14611, doi:10.1029/2006GL026498.

Donners, J., and S. Drijfhout, 2004: The Lagrangian view of South Atlantic interocean exchange in a global ocean model compared with inverse model results. *Journal of physical oceanography*, **34**, 1019–1035.

Donners, J., S. S. Drijfhout, and A. C. Coward, 2004: Impact of cooling on the water mass exchange of Agulhas rings in a high resolution ocean model. *Geophysical Research Letters*, **31**, L16312, doi:10.1029/2004GL020644.

Downes, S. M., a. S. Budnick, J. L. Sarmiento, and R. Farneti, 2011: Impacts of wind stress on the Antarctic Circumpolar Current fronts and associated subduction. *Geophysical Research Letters*, **38**, 3–8, doi:10.1029/2011GL047668.

Duhaut, T. H. A., and D. N. Straub, 2006: Wind Stress Dependence on Ocean Surface Velocity: Implications for Mechanical Energy Input to Ocean Circulation. *Journal of Physical Oceanography*, **36**, 202–211, doi:10.1175/JPO2842.1.

Duncombe Rae, C. M., 1991: Agulhas retroflection rings in the South Atlantic Ocean: an overview. *South African Journal of Marine Science*, **11**, 327–344, doi:10.2989/025776191784287574.

Duncombe Rae, C. M., S. L. Garzoli, and A. L. Gordon, 1996: The eddy field of the southeast Atlantic Ocean: A statistical census from the Benguela Sources and Transports Project. *Journal of Geophysical Research*, **101**, 11949, doi:10.1029/95JC03360.

Durgadoo, J. V., and A. Biastoch, 2013: The Agulhas System as a Key Region of the Global Oceanic Circulation. *High Performance Computing in Science and Engineering '12*, W.E. Nagel, D.H. Kröner, and M.M. Resch, Eds., Springer Berlin Heidelberg, Berlin, Heidelberg, 407–414.

Durgadoo, J. V., B. R. Loveday, C. J. C. Reason, P. Penven, and A. Biastoch, 2013: Agulhas Leakage Predominantly Responds to the Southern Hemisphere Westerlies. *Journal of Physical Oceanography*, in press, doi:10.1175/JPO-D-13-047.1.

Fairall, C. W., E. F. Bradley, D. P. Rogers, J. B. Edson, and G. S. Young, 1996: Bulk parameterization of air-sea fluxes for Tropical Ocean-Global Atmosphere Coupled-Ocean Atmosphere Response Experiment. *Journal of Geophysical Research*, **101**, 3747, doi:10.1029/95JC03205.

Feron, R. C. V., W. P. M. De Ruijter, and D. Oskam, 1992: Ring shedding in the Agulhas Current System. *Journal of Geophysical Research*, **97**, 9467, doi:10.1029/92JC00736.

Franzese, A. M., S. R. Hemming, S. L. Goldstein, and R. F. Anderson, 2006: Reduced Agulhas Leakage during the Last Glacial Maximum inferred from an integrated provenance and flux study. *Earth and Planetary Science Letters*, **250**, 72–88, doi:10.1016/j.epsl.2006.07.002.

Franzese, A. M., S. R. Hemming, and S. L. Goldstein, 2009: Use of strontium isotopes in detrital sediments to constrain the glacial position of the Agulhas Retroflection. *Paleoceanography*, **24**, PA2217, doi:10.1029/2008PA001706.

Friocourt, Y., S. Drijfhout, B. Blanke, and S. Speich, 2005: Water Mass Export from Drake Passage to the Atlantic, Indian, and Pacific Oceans: A Lagrangian Model Analysis. *Journal of Physical Oceanography*, **35**, 1206–1222, doi:10.1175/JPO2748.1.

Fyfe, J. C., and O. A. Saenko, 2006: Simulated changes in the extratropical Southern Hemisphere winds and currents. *Geophysical Research Letters*, **33**, L06701, doi:10.1029/2005GL025332.

Fyfe, J. C., O. A. Saenko, K. Zickfeld, M. Eby, and A. J. Weaver, 2007: The Role of Poleward-Intensifying Winds on Southern Ocean Warming. *Journal of Climate*, **20**, 5391–5400, doi:10.1175/2007JCLI1764.1.

Garzoli, S. L., and R. Matano, 2011: The South Atlantic and the Atlantic Meridional Overturning Circulation. *Deep Sea Research*, **58**, 1837–1847, doi:10.1016/j.dsr2.2010.10.063.

Garzoli, S. L., P. L. Richardson, C. M. Duncombe Rae, D. M. Fratantoni, G. J. Goñi, and A. J. Roubicek, 1999: Three Agulhas rings observed during the Benguela Current Experiment. *Journal of Geophysical Research*, **104**, 20971, doi:10.1029/1999JC900060.

Gent, P. R., and J. C. McWilliams, 1990: Isopycnal Mixing in Ocean Circulation Models. *Journal of Physical Oceanography*, **20**, 150–155.

Giulivi, C. F., and A. L. Gordon, 2006: Isopycnal displacements within the Cape Basin thermocline as revealed by the Hydrographic Data Archive. *Deep Sea Research*, **53**, 1285–1300, doi:10.1016/j.dsr.2006.05.011.

Gnanadesikan, A., and R. W. Hallberg, 2000: On the Relationship of the Circumpolar Current to Southern Hemisphere Winds in Coarse-Resolution Ocean Models. *Journal of Physical Oceanography*, **30**, 2013–2034, doi:10.1175/1520-0485(2000)030<2013:OTROTC>2.0.CO;2.

Goni, G. J., S. L. Garzoli, A. J. Roubicek, D. B. Olson, and O. B. Brown, 1997: Agulhas ring dynamics from TOPEX/POSEIDON satellite altimeter data. *Journal of Marine Research*, **55**, 861–883, doi:10.1357/0022240973224175.

Gordon, A. L., 1986: Interocean exchange of thermocline water. *Journal of Geophysical Research*, **91**, 5037, doi:10.1029/JC091iC04p05037.

Gordon, A. L., and W. F. Haxby, 1990: Agulhas eddies invade the south Atlantic: Evidence From Geosat altimeter and shipboard conductivity-temperature-depth survey. *Journal of Geophysical Research*, **95**, 3117–3125, doi:10.1029/JC095iC03p03117.

Gordon, A. L., R. F. Weiss, W. M. Smethie, and M. J. Warner, 1992: Thermocline and intermediate water communication between the south Atlantic and Indian oceans. *Journal of Geophysical Research*, **97**, 7223, doi:10.1029/92JC00485.

Graham, R. M., and A. M. de Boer, 2013: The Dynamical Subtropical Front. *Journal of Geophysical Research*, under revision.

Graham, R. M., A. M. de Boer, K. J. Heywood, M. R. Chapman, and D. P. Stevens, 2012: Southern Ocean fronts: Controlled by wind or topography? *Journal of Geophysical Research*, **117**, 1–14, doi:10.1029/2012JC007887.

Griffies, S. M. and Coauthors, 2009: Coordinated Ocean-ice Reference Experiments (COREs). *Ocean Modelling*, **26**, 1–46, doi:10.1016/j.ocemod.2008.08.007.

Gründlingh, M. L., 1983: On the Course of the Agulhas Current. *South African Geographical Journal*, **65**, 49–57, doi:10.1080/03736245.1983.10559671.

Haidvogel, D. B., and A. Beckmann, 1999: Numerical Ocean Circulation Modeling. *Series on Environmental Science and Management: Volume 2*, 344pp.

Hall, C., and J. R. E. Lutjeharms, 2011: Cyclonic eddies identified in the Cape Basin of the South Atlantic Ocean. *Journal of Marine Systems*, **85**, 1–10, doi:10.1016/j.jmarsys.2010.10.003.

Hallberg, R., and A. Gnanadesikan, 2006: The Role of Eddies in Determining the Structure and Response of the Wind-Driven Southern Hemisphere Overturning: Results from the Modeling Eddies in the Southern Ocean (MESO) Project. *Journal of Physical Oceanography*, **36**, 2232–2252, doi:10.1175/JPO2980.1.

Han, W. and Coauthors, 2010: Patterns of Indian Ocean sea-level change in a warming climate. *Nature Geoscience*, **3**, 546–550, doi:10.1038/ngeo901.

Harlander, U., H. Ridderinkhof, M. W. Schouten, and W. P. M. de Ruijter, 2009: Long-term observations of transport, eddies, and Rossby waves in the Mozambique Channel. *Journal of Geophysical Research*, **114**, C02003, doi:10.1029/2008JC004846.

Hazeleger, W., and S. Drijfhout, 2006: Subtropical cells and meridional overturning circulation pathways in the tropical Atlantic. *Journal of Geophysical Research*, **111**, C03013, doi:10.1029/2005JC002942.

Heywood, K. J., E. Barton, and G. I. Allen, 1994: South equatorial current of the indian-ocean - a 50-day oscillation. *Oceanologica Acta*, **17**, 255–261.

Hodgson, D. a., and L. C. Sime, 2010: Palaeoclimate: Southern westerlies and CO2. *Nature Geoscience*, **3**, 666–667, doi:10.1038/ngeo970.

Hughes, C. W., and C. Wilson, 2008: Wind work on the geostrophic ocean circulation: An observational study of the effect of small scales in the wind stress. *Journal of Geophysical Research*, **113**, C02016, doi:10.1029/2007JC004371.

Jackson, J. M., L. Rainville, M. J. Roberts, C. D. McQuaid, and J. R. E. Lutjeharms, 2012: Mesoscale bio-physical interactions between the Agulhas Current and the Agulhas Bank, South Africa. *Continental Shelf Research*, **49**, 10–24, doi:10.1016/j.csr.2012.09.005.

Johns, W. E., T. N. Lee, R. C. Beardsley, J. Candela, R. Limeburner, and B. Castro, 1998: Annual Cycle and Variability of the North Brazil Current. *Journal of Physical Oceanography*, **28**, 103–128, doi:10.1175/1520-0485(1998)028<0103:ACAVOT>2.0.CO;2.

Knorr, G., and G. Lohmann, 2003: Southern Ocean origin for the resumption of Atlantic thermohaline circulation during deglaciation. *Nature*, **424**, 532–536, doi:10.1038/nature01855.
Kohfeld, K. E., R. M. Graham, A. M. de Boer, L. C. Sime, E. W. Wolff, C. Le Quéré, and L. Bopp, 2013: Southern Hemisphere westerly wind changes during the Last Glacial Maximum: paleo-data synthesis. *Quaternary Science Reviews*, **68**, 76–95, doi:10.1016/j.quascirev.2013.01.017.
Krug, M., and J. Tournadre, 2012: Satellite observations of an annual cycle in the Agulhas Current. *Geophysical Research Letters*, **39**, L15607, doi:10.1029/2012GL052335.
Kuhlbrodt, T., A. Griesel, M. Montoya, A. Levermann, M. Hofmann, and S. Rahmstorf, 2007: On the driving processes of the Atlantic meridional overturning circulation. *Reviews of Geophysics*, **45**, RG2001, doi:10.1029/2004RG000166.
Large, W. G., and S. G. Yeager, 2004: Diurnal to decadal global forcing for ocean and sea-ice models: The data sets and flux climatologies. *NCAR Technical Note NCAR/TN-460+STR*, doi:10.5065/D6KK98Q6.
Large, W. G., and S. G. Yeager, 2009: The global climatology of an interannually varying air–sea flux data set. *Climate Dynamics*, **33**, 341–364, doi:10.1007/s00382-008-0441-3.
Large, W. G., J. C. Mcwilliams, and S. C. Doney, 1994: Oceanic vertical mixing: A review and a model with a nonlocal boundary layer parameterization. *Reviews of Geophysics*, **32**, 363–403.
Le Bars, D., J. V. Durgadoo, W. P. M. de Ruijter, H. A. Dijkstra, and A. Biastoch, Agulhas leakage estimated from sea surface height. in prep.
Le Bars, D., W. P. M. de Ruijter, and H. A. Dijkstra, 2012: A New Regime of the Agulhas Current Retroflection: Turbulent Choking of Indian–Atlantic leakage. *Journal of Physical Oceanography*, **42**, 1158–1172, doi:10.1175/JPO-D-11-0119.1.
Liu, W. T., X. Xie, and P. P. Niiler, 2007: Ocean–Atmosphere Interaction over Agulhas Extension Meanders. *Journal of Climate*, **20**, 5784–5797, doi:10.1175/2007JCLI1732.1.
Lohmann, K., H. Drange, and M. Bentsen, 2008: Response of the North Atlantic subpolar gyre to persistent North Atlantic oscillation like forcing. *Climate Dynamics*, **32**, 273–285, doi:10.1007/s00382-008-0467-6.
Loveday, B. R., J. V. Durgadoo, C. J. C. Reason, A. Biastoch, and P. Penven, 2013: Decoupling the Agulhas leakage and Agulhas Current. *Journal of Physical Oceanography*, under review.
Lutjeharms, J.R.E., J.V. Durgadoo, and I. Ansorge, 2007: Surface drift at the western edge of the Agulhas Bank. *South African Journal of Science*, **103**, 63–67.
Lutjeharms, J. R.E., and R. C. van Ballegooyen, 1988: Anomalous upstream retroflection in the agulhas current. *Science (New York, N.Y.)*, **240**, 1770, doi:10.1126/science.240.4860.1770.
Lutjeharms, J. R. E., J. Cooper, and M. Roberts, 2000: Upwelling at the inshore edge of the Agulhas Current. *Continental Shelf Research*, **20**, 737–761, doi:10.1016/S0278-4343(99)00092-8.
Lutjeharms, J. R. E., 2006: *The Agulhas Current*. Springer-Verlag, Berlin Heidelberg. 329pp.
Lutjeharms, J. R. E., and A. L. Gordon, 1987: Shedding of an Agulhas ring observed at sea. *Nature*, **325**, 138–140, doi:10.1038/325138a0.
Lutjeharms, J. R. E., and P. L. Stockton, 1987: Kinematics of the upwelling front off southern Africa. *South African Journal of Marine Science*, **5**, 35–49, doi:10.2989/025776187784522612.
Lutjeharms, J. R. E., and H. R. Roberts, 1988: The Natal pulse: An extreme transient on the Agulhas Current. *Journal of Geophysical Research*, **93**, 631, doi:10.1029/JC093iC01p00631.
Lutjeharms, J. R. E., and J. Cooper, 1996: Interbasin leakage through Agulhas current filaments. *Deep Sea Research*, **43**, 213–238, doi:10.1016/0967-0637(96)00002-7.
Lutjeharms, J. R. E., and I. J. Ansorge, 2001: The Agulhas Return Current. *Journal of Marine Systems*, **30**, 115–138, doi:10.1016/S0924-7963(01)00041-0.
Lutjeharms, J. R. E., N. D. Bang, and C. P. Duncan, 1981: Characteristics of the currents east and south of Madagascar. *Deep Sea Research*, **28**, 879–899, doi:10.1016/0198-0149(81)90008-X.
Lutjeharms, J. R. E., A. Biastoch, P. M. Van der Werf, H. Ridderinkhof, and W. P. M. de Ruijter, 2012: On the discontinuous nature of the Mozambique Current. *South African Journal of Science*, **108**, doi:10.4102/sajs.v108i1/2.428.

Madec, G., 2008: NEMO ocean engine. *Note du Pole de modeisation de l'Institut Pierre-Simon Laplace No 27*, ISSN No 12, 215.

Madec, G., and M. Imbard, 1996: A global ocean mesh to overcome the North Pole singularity. *Climate Dynamics*, **12**, 381–388, doi:10.1007/BF00211684.

Marchesiello, P., J. C. McWilliams, and A. Shchepetkin, 2001: Open boundary conditions for long-term integration of regional oceanic models. *Ocean Modelling*, **3**, 1–20, doi:10.1016/S1463-5003(00)00013-5.

Marchesiello, P., L. Debreu, and X. Couvelard, 2009: Spurious diapycnal mixing in terrain-following coordinate models: The problem and a solution. *Ocean Modelling*, **26**, 156–169, doi:10.1016/j.ocemod.2008.09.004.

Marshall, J., and F. Schott, 1999: Open-ocean convection: Observations, theory, and models. *Reviews of Geophysics*, **37**, 1–64, doi:10.1029/98RG02739.

Marshall, J., and R. A. Plumb, 2007: *Atmosphere, Ocean and Climate Dynamics: An Introductory Text (International Geophysics)*. Academic Press, 344pp.

Masumoto, Y., H. Sasaki, T. Kagimoto, N. Komori, A. Ishida, Y. Sasai, and E. Al., 2004: A Fifty-Year Eddy-Resolving Simulation of the World Ocean - Preliminary Outcomes of OFES (OGCM for the Earth Simulator). *Journal of the Earth Simulator*, **1**, 35–56.

Matano, R. ., and E. . Beier, 2003: A kinematic analysis of the Indian/Atlantic interocean exchange. *Deep Sea Research*, **50**, 229–249, doi:10.1016/S0967-0645(02)00395-8.

Matano, R. P., 1996: A Numerical Study of the Agulhas Retroflection: The Role of Bottom Topography. *Journal of Physical Oceanography*, **26**, 2267–2279, doi:10.1175/1520-0485(1996)026<2267:ANSOTA>2.0.CO;2.

Matano, R. P., E. J. Beier, P. T. Strub, and R. Tokmakian, 2002: Large-Scale Forcing of the Agulhas Variability: The Seasonal Cycle. *Journal of Physical Oceanography*, **32**, 1228–1241, doi:10.1175/1520-0485(2002)032<1228:LSFOTA>2.0.CO;2.

McCartney, M. S., and M. E. Woodgate-Jones, 1991: A deep-reaching anticyclonic eddy in the subtropical gyre of the eastern South Atlantic. *Deep Sea Research*, **38**, S411–S443, doi:10.1016/S0198-0149(12)80019-7.

Meredith, M. P. and Coauthors, 2011: Sustained Monitoring of the Southern Ocean At Drake Passage: Past Achievements and Future Priorities. *Reviews of Geophysics*, **49**, RG4005, doi:10.1029/2010RG000348.

Nakamura, M., 2012: Impacts of SST Anomalies in the Agulhas Current System on the Regional Climate Variability. *Journal of Climate*, **25**, 1213–1229, doi:10.1175/JCLI-D-11-00088.1.

Nauw, J. J., H. M. van Aken, A. Webb, J. R. E. Lutjeharms, and W. P. M. de Ruijter, 2008: Observations of the southern East Madagascar Current and undercurrent and countercurrent system. *Journal of Geophysical Research*, **113**, C08006, doi:10.1029/2007JC004639.

Nof, D., V. Zharkov, J. Ortiz, N. Paldor, W. Arruda, and E. Chassignet, 2011: The arrested Agulhas retroflection. *Journal of Marine Research*, **69**, 659–691, doi:10.1357/002224011799849453.

Oke, P. R., and M. H. England, 2004: Oceanic Response to Changes in the Latitude of the Southern Hemisphere Subpolar Westerly Winds. *Journal of Climate*, **17**, 1040–1054, doi:10.1175/1520-0442(2004)017<1040:ORTCIT>2.0.CO;2.

Olson, D. B., and R. H. Evans, 1986: Rings of the Agulhas current. *Deep Sea Research*, **33**, 27–42, doi:10.1016/0198-0149(86)90106-8.

Otto-Bliesner, B. L., E. C. Brady, G. Clauzet, R. Tomas, S. Levis, and Z. Kothavala, 2006: Last Glacial Maximum and Holocene Climate in CCSM3. *Journal of Climate*, **19**, 2526–2544, doi:10.1175/JCLI3748.1.

Ou, H., and W. de Ruijter, 1986: Separation of an inertial boundary current from a curved coastline. *Journal of Physical Oceanography*, **16**, 280–289.

Peeters, F. J. C., R. Acheson, G.-J. a Brummer, W. P. M. De Ruijter, R. R. Schneider, G. M. Ganssen, E. Ufkes, and D. Kroon, 2004: Vigorous exchange between the Indian and Atlantic oceans at the end of the past five glacial periods. *Nature*, **430**, 661–665, doi:10.1038/nature02785.

Penven, P., J. R. E. Lutjeharms, and P. Florenchie, 2006: Madagascar: A pacemaker for the Agulhas Current system? *Geophysical Research Letters*, **33**, L17609, doi:10.1029/2006GL026854.
Penven, P., P. Marchesiello, L. Debreu, and J. Lefèvre, 2008: Software tools for pre- and post-processing of oceanic regional simulations. *Environmental Modelling & Software*, **23**, 660–662, doi:10.1016/j.envsoft.2007.07.004.
Quartly, G. D., and M. a. Srokosz, 2004: Eddies in the southern Mozambique Channel. *Deep Sea Research*, **51**, 69–83, doi:10.1016/j.dsr2.2003.03.001.
Quartly, G. D., J. J. H. Buck, M. a. Srokosz, and A. C. Coward, 2006: Eddies around Madagascar — The retroflection re-considered. *Journal of Marine Systems*, **63**, 115–129, doi:10.1016/j.jmarsys.2006.06.001.
Quartly, G. D., B. a. de Cuevas, and A. C. Coward, 2013: Mozambique Channel eddies in GCMs: A question of resolution and slippage. *Ocean Modelling*, doi:10.1016/j.ocemod.2012.12.011.
Richardson, P. L., 2007: Agulhas leakage into the Atlantic estimated with subsurface floats and surface drifters. *Deep-Sea Research I*, **54**, 1361–1389, doi:10.1016/j.dsr.2007.04.010.
Ridderinkhof, H., P. M. van der Werf, J. E. Ullgren, H. M. van Aken, P. J. van Leeuwen, and W. P. M. de Ruijter, 2010: Seasonal and interannual variability in the Mozambique Channel from moored current observations. *Journal of Geophysical Research*, **115**, C06010, doi:10.1029/2009JC005619.
Ridderinkhof, W., D. Le Bars, a. S. von der Heydt, and W. P. M. de Ruijter, 2013: Dipoles of the South East Madagascar Current. *Geophysical Research Letters*, **40**, 558–562, doi:10.1002/grl.50157.
Ridgway, K. R., and J. R. Dunn, 2007: Observational evidence for a Southern Hemisphere oceanic supergyre. *Geophysical Research Letters*, **34**, L13612, doi:10.1029/2007GL030392.
Rimaud, J., S. Speich, B. Blanke, and N. Grima, 2012: The exchange of Intermediate Water in the southeast Atlantic: Water mass transformations diagnosed from the Lagrangian analysis of a regional ocean model. *Journal of Geophysical Research*, **117**, C08034, doi:10.1029/2012JC008059.
Rojas, M. and Coauthors, 2008: The Southern Westerlies during the last glacial maximum in PMIP2 simulations. *Climate Dynamics*, **32**, 525–548, doi:10.1007/s00382-008-0421-7.
Roman, R. ., and J. R. E. Lutjeharms, 2010: Antarctic intermediate water at the Agulhas Current retroflection region. *Journal of Marine Systems*, **81**, 273–285, doi:10.1016/j.jmarsys.2010.01.003.
Roman, R. E., and J. R. E. Lutjeharms, 2007: Red Sea Intermediate Water at the Agulhas Current termination. *Deep Sea Research*, **54**, 1329–1340, doi:10.1016/j.dsr.2007.04.009.
Rouault, M., S. A. White, C. J. C. Reason, J. R. E. Lutjeharms, and I. Jobard, 2002: Ocean–Atmosphere Interaction in the Agulhas Current Region and a South African Extreme Weather Event. *Weather and Forecasting*, **17**, 655–669, doi:10.1175/1520-0434(2002)017<0655:OAIITA>2.0.CO;2.
Rouault, M., P. Penven, and B. Pohl, 2009: Warming in the Agulhas Current system since the 1980's. *Geophysical Research Letters*, **36**, L12602, doi:10.1029/2009GL037987.
Rouault, M. J., and P. Penven, 2011: New perspectives on Natal Pulses from satellite observations. *Journal of Geophysical Research*, **116**, C07013, doi:10.1029/2010JC006866.
Rouault, M. J., A. Mouche, F. Collard, J. a. Johannessen, and B. Chapron, 2010: Mapping the Agulhas Current from space: An assessment of ASAR surface current velocities. *Journal of Geophysical Research*, **115**, C10026, doi:10.1029/2009JC006050.
Rühs, S., J. V. Durgadoo, E. Behrens, and A. Biastoch, 2013: Advective timescales and pathways of agulhas leakage. *Geophysical Research Letters*, **40**, 3997–4000, doi:10.1002/grl.50782.
Rusciano, E., S. Speich, and M. Ollitrault, 2012: Interocean exchanges and the spreading of Antarctic Intermediate Water south of Africa. *Journal of Geophysical Research*, **117**, 1–21, doi:10.1029/2012JC008266.
Schmid, C., O. Boebel, W. Zenk, J. R. . Lutjeharms, S. . Garzoli, P. . Richardson, and C. Barron, 2003: Early evolution of an Agulhas Ring. *Deep Sea Research*, **50**, 141–166, doi:10.1016/S0967-0645(02)00382-X.

Schott, F. A., J. Fischer, and L. Stramma, 1998: Transports and Pathways of the Upper-Layer Circulation in the Western Tropical Atlantic. *Journal of Physical Oceanography*, **28**, 1904–1928, doi:10.1175/1520-0485(1998)028<1904:TAPOTU>2.0.CO;2.

Schouten, M. W., W. P. M. de Ruijter, P. J. van Leeuwen, and J. R. E. Lutjeharms, 2000: Translation, decay and splitting of Agulhas rings in the southeastern Atlantic Ocean. *Journal of Geophysical Research*, **105**, 21913, doi:10.1029/1999JC000046.

Schouten, M., 2002: Upstream control of Agulhas Ring shedding. *Journal of Geophysical Research*, **107**, 3109.

Schouten, M. W., W. P. M. de Ruijter, P. J. van Leeuwen, and H. Ridderinkhof, 2003: Eddies and variability in the Mozambique Channel. *Deep Sea Research*, **50**, 1987–2003, doi:10.1016/S0967-0645(03)00042-0.

Scussolini, P., E. van Sebille, and J. V. Durgadoo, 2013: Paleo Agulhas rings enter the subtropical gyre during the penultimate deglaciation. *Climate of the Past*, under review.

Shchepetkin, A. F., and J. C. McWilliams, 1998: Quasi-monotone advection schemes based on explicit locally adaptive dissipation. *Monthly Weather Review*, **126**, 1542–1580.

Shchepetkin, A. F., and J. C. McWilliams, 2005: The regional oceanic modeling system (ROMS): a split-explicit, free-surface, topography-following-coordinate oceanic model. *Ocean Modelling*, **9**, 347–404, doi:10.1016/j.ocemod.2004.08.002.

Siedler, G., M. Rouault, and J. R. E. Lutjeharms, 2006: Structure and origin of the subtropical South Indian Ocean Countercurrent. *Geophysical Research Letters*, **33**, L24609, doi:10.1029/2006GL027399.

Siedler, G., M. Rouault, A. Biastoch, B. Backeberg, C. J. C. Reason, and J. R. E. Lutjeharms, 2009: Modes of the southern extension of the East Madagascar Current. *Journal of Geophysical Research*, **114**, C01005, doi:10.1029/2008JC004921.

Sijp, W. P., and M. H. England, 2008: The effect of a northward shift in the southern hemisphere westerlies on the global ocean. *Progress in Oceanography*, **79**, 1–19, doi:10.1016/j.pocean.2008.07.002.

Sijp, W. P., and M. H. England, 2009: Southern Hemisphere Westerly Wind Control over the Ocean's Thermohaline Circulation. *Journal of Climate*, **22**, 1277–1286, doi:10.1175/2008JCLI2310.1.

Sime, L. C., K. E. Kohfeld, C. Le Quéré, E. W. Wolff, A. M. de Boer, R. M. Graham, and L. Bopp, 2013: Southern Hemisphere westerly wind changes during the Last Glacial Maximum: model-data comparison. *Quaternary Science Reviews*, **64**, 104–120, doi:10.1016/j.quascirev.2012.12.008.

Smagorinsky, J., 1963: General Circulation Experiments with the primitive equations. I. The basic experiment. *Monthly Weather Review*, **27**, 99–164.

Smith, S. R., D. M. Legler, and K. V. Verzone, 2001: Quantifying Uncertainties in NCEP Reanalyses Using High-Quality Research Vessel Observations. *Journal of Climate*, **14**, 4062–4072, doi:10.1175/1520-0442(2001)014<4062:QUINRU>2.0.CO;2.

Son, S.-W. and Coauthors, 2010: Impact of stratospheric ozone on Southern Hemisphere circulation change: A multimodel assessment. *Journal of Geophysical Research*, **115**, D00M07, doi:10.1029/2010JD014271.

Souza, J. M. a. C., C. de Boyer Montégut, C. Cabanes, and P. Klein, 2011: Estimation of the Agulhas ring impacts on meridional heat fluxes and transport using ARGO floats and satellite data. *Geophysical Research Letters*, **38**, 1–5, doi:10.1029/2011GL049359.

Speer, K., S. Rintoul, and B. Sloyan, 2000: The Diabatic Deacon Cell. *Journal of Physical Oceanography*, **30**, 3212–3222.

Speich, S., B. Blanke, and G. Madec, 2001: Warm and cold water routes of an OGCM thermohaline conveyor belt. *Geophysical research letters*, **28**, 311–314.

Speich, S., B. Blanke, P. de Vries, S. S. Drijfhout, K. Döös, A. Ganachaud, and R. Marsh, 2002: Tasman leakage: A new route in the global ocean conveyor belt. *Geophysical Research Letters*, **29**, 1416, doi:10.1029/2001GL014586.

Speich, S., J. R. E. Lutjeharms, P. Penven, and B. Blanke, 2006: Role of bathymetry in Agulhas Current configuration and behaviour. *Geophysical Research Letters*, **33**, L23611, doi:10.1029/2006GL027157.

Speich, S., B. Blanke, and W. Cai, 2007: Atlantic meridional overturning circulation and the Southern Hemisphere supergyre. *Geophysical Research Letters*, **34**, L23614, doi:10.1029/2007GL031583.

Spence, P., J. C. Fyfe, A. Montenegro, and A. J. Weaver, 2010: Southern Ocean Response to Strengthening Winds in an Eddy-Permitting Global Climate Model. *Journal of Climate*, **23**, 5332–5343, doi:10.1175/2010JCLI3098.1.

Sprintall, J., S. E. Wijffels, R. Molcard, and I. Jaya, 2009: Direct estimates of the Indonesian Throughflow entering the Indian Ocean: 2004–2006. *Journal of Geophysical Research*, **114**, C07001, doi:10.1029/2008JC005257.

Srokosz, M., M. Baringer, H. Bryden, S. Cunningham, T. Delworth, S. Lozier, J. Marotzke, and R. Sutton, 2012: Past, Present, and Future Changes in the Atlantic Meridional Overturning Circulation. *Bulletin of the American Meteorological Society*, **93**, 1663–1676, doi:10.1175/BAMS-D-11-00151.1.

Steele, M., R. Morfley, and W. Ermold, 2001: PHC: A global ocean hydrography with high-quality Artic Ocean. *Journal of Climate*, **14**, 2079–2087.

Stramma, L., and R. G. Peterson, 1990: The South Atlantic Current. *Journal of Physical Oceanography*, **20**, 846–859, doi:10.1175/1520-0485(1990)020<0846:TSAC>2.0.CO;2.

Stramma, L., and J. R. E. Lutjeharms, 1997: The flow field of the subtropical gyre of the South Indian Ocean. *Journal of Geophysical Research*, **102**, 5513–5530.

Stramma, L., and M. England, 1999: On the water masses and mean circulation of the South Atlantic Ocean. *Journal of Geophysical Research*, **104**, 20863, doi:10.1029/1999JC900139.

Swallow, J., M. Fieux, and F. Schott, 1988: The boundary currents east and north of Madagascar: 1. Geostrophic currents and transports. *Journal of Geophysical Research*, **93**, 4951, doi:10.1029/JC093iC05p04951.

Swart, N. C., and J. C. Fyfe, 2012: Observed and simulated changes in the Southern Hemisphere surface westerly wind-stress. *Geophysical Research Letters*, **39**, 6–11, doi:10.1029/2012GL052810.

Taylor, K. E., R. J. Stouffer, and G. A. Meehl, 2012: An Overview of CMIP5 and the Experiment Design. *Bulletin of the American Meteorological Society*, **93**, 485–498, doi:10.1175/BAMS-D-11-00094.1.

The DRAKKAR Group, 2007: Eddy-permitting ocean circulation hindcasts of past decades. *CLIVAR Exchanges*, Vol. 12 of, 8–14.

Toggweiler, J. R., 2009: Climate change. Shifting westerlies. *Science*, **323**, 1434–1435, doi:10.1126/science.1169823.

Toggweiler, J. R., J. L. Russell, and S. R. Carson, 2006: Midlatitude westerlies, atmospheric CO 2 , and climate change during the ice ages. *Paleoceanography*, **21**, 1–15, doi:10.1029/2005PA001154.

Tréguier, A.-M., 1992: Kinetic energy analysis of an eddy resolving, primitive equation model of the North Atlantic. *Journal of Geophysical Research*, **97**, 687–701, doi:10.1029/91JC02350.

Tréguier, A.-M., I. M. Held, and V. D. Larichev, 1997: Parameterization of Quasigeostrophic Eddies in Primitive Equation Ocean Models. *Journal of Physical Oceanography*, **27**, 567–580, doi:10.1175/1520-0485(1997)027<0567:POQEIP>2.0.CO;2.

Tréguier, A.-M., O. Boebel, B. Barnier, and G. Madec, 2003: Agulhas eddy fluxes in a 1/6° Atlantic model. *Deep Sea Research*, **50**, 251–280, doi:10.1016/S0967-0645(02)00396-X.

Tsugawa, M., and H. Hasumi, 2010: Generation and Growth Mechanism of the Natal Pulse. *Journal of Physical Oceanography*, **40**, 1597–1612, doi:10.1175/2010JPO4347.1.

van Aken, H. M., A. K. van Veldhoven, C. Veth, W. P. M. de Ruijter, P. J. van Leeuwen, S. S. Drijfhout, C. P. Whittle, and M. Rouault, 2003: Observations of a young Agulhas ring, Astrid, during MARE in March 2000. *Deep Sea Research*, **50**, 167–195, doi:10.1016/S0967-0645(02)00383-1.

van Aken, H. M., H. Ridderinkhof, and W. P. M. de Ruijter, 2004: North Atlantic deep water in the south-western Indian Ocean. *Deep Sea Research*, **51**, 755–776, doi:10.1016/j.dsr.2004.01.008.

van Aken, H. M., J. R. E. Lutjeharms, M. Rouault, C. Whittle, and W. P. M. de Ruijter, 2013: Observations of an early Agulhas current retroflection event in 2001: A temporary cessation of inter-ocean exchange south of Africa? *Deep Sea Research*, **72**, 1–8, doi:10.1016/j.dsr.2012.11.002.

van der Sluijs, J. P., 2012: Uncertainty and Dissent in Climate Risk Assessment: A Post-Normal Perspective. *Nature and Culture*, **7**, 174–195, doi:10.3167/nc.2012.070204.

van der Werf, P. M., P. J. van Leeuwen, H. Ridderinkhof, and W. P. M. de Ruijter, 2010: Comparison between observations and models of the Mozambique Channel transport: Seasonal cycle and eddy frequencies. *Journal of Geophysical Research*, **115**, C02002, doi:10.1029/2009JC005633.

van Leeuwen, P. J., W. P. M. de Ruijter, and J. R. E. Lutjeharms, 2000: Natal pulses and the formation of Agulhas rings. *Journal of Fluid Mechanics*, **105**, 6425–6436.

van Sebille, E., and P. J. van Leeuwen, 2007: Fast Northward Energy Transfer in the Atlantic due to Agulhas Rings. *Journal of Physical Oceanography*, **37**, 2305–2315, doi:10.1175/JPO3108.1.

van Sebille, E., C. N. Barron, A. Biastoch, P. J. van Leeuwen, F. C. Vossepoel, and W. P. M. de Ruijter, 2009a: Relating Agulhas leakage to the Agulhas Current retroflection location. *Ocean Science*, **5**, 511–521, doi:10.5194/os-5-511-2009.

van Sebille, E., A. Biastoch, P. J. van Leeuwen, and W. P. M. de Ruijter, 2009b: A weaker Agulhas Current leads to more Agulhas leakage. *Geophysical Research Letters*, **36**, L03601, doi:10.1029/2008GL036614.

van Sebille, E., P. J. van Leeuwen, A. Biastoch, C. N. Barron, and W. P. M. de Ruijter, 2009c: Lagrangian validation of numerical drifter trajectories using drifting buoys: Application to the Agulhas system. *Ocean Modelling*, **29**, 269–276, doi:10.1016/j.ocemod.2009.05.005.

van Sebille, E., P. J. van Leeuwen, A. Biastoch, and W. P. M. de Ruijter, 2010a: Flux comparison of Eulerian and Lagrangian estimates of Agulhas leakage: A case study using a numerical model. *Deep-Sea Research*, **57**, 319–327, doi:10.1016/j.dsr.2009.12.006.

van Sebille, E., P. J. van Leeuwen, A. Biastoch, and W. P. M. de Ruijter, 2010b: On the fast decay of Agulhas rings. *Journal of Geophysical Research*, **115**, 1–15, doi:10.1029/2009JC005585.

van Sebille, E., L. M. Beal, and W. E. Johns, 2011: Advective time scales of Agulhas leakage to the North Atlantic in surface drifter observations and the 3D OFES model. *Journal of Physical Oceanography*, 110301132530083, doi:10.1175/2011JPO4602.1.

van Sebille, E., W. E. Johns, and L. M. Beal, 2012: Does the vorticity flux from Agulhas rings control the zonal pathway of NADW across the South Atlantic? *Journal of Geophysical Research*, **117**, C05037, doi:10.1029/2011JC007684.

Vianna, M. L., and V. V. Menezes, 2011: Double-celled subtropical gyre in the South Atlantic Ocean: Means, trends, and interannual changes. *Journal of Geophysical Research*, **116**, C03024, doi:10.1029/2010JC006574.

Visbeck, M., 2009: A Station-Based Southern Annular Mode Index from 1884 to 2005. *Journal of Climate*, **22**, 940–950, doi:10.1175/2008JCLI2260.1.

Visbeck, M., J. Marshall, T. Haine, and M. Spall, 1997: Specification of Eddy Transfer Coefficients in Coarse-Resolution Ocean Circulation Models. *Journal of Physical Oceanography*, **27**, 381–402, doi:10.1175/1520-0485(1997)027<0381:SOETCI>2.0.CO;2.

Walsh, J., 2013: Melting Ice: What is Happening to Arctic Sea Ice, and What Does It Mean for Us? *Oceanography*, **26**, doi:10.5670/oceanog.2013.19.

Watson, P. a. G., D. J. Karoly, M. R. Allen, N. Faull, and D. S. Lee, 2012: Quantifying uncertainty in future Southern Hemisphere circulation trends. *Geophysical Research Letters*, **39**, L23708, doi:10.1029/2012GL054158.

Weijer, W., W. P. M. de Ruijter, H. A. Dijkstra, and P. J. van Leeuwen, 1999: Impact of Interbasin Exchange on the Atlantic Overturning Circulation. *Journal of Physical Oceanography*, **29**, 2266–2284, doi:10.1175/1520-0485(1999)029<2266:IOIEOT>2.0.CO;2.

Weijer, W., W. P. M. De Ruijter, A. Sterl, and S. S. Drijfhout, 2002: Response of the Atlantic overturning circulation to South Atlantic sources of buoyancy. **34**, 293–311.

Weijer, W. and Coauthors, 2012: The Southern Ocean and Its Climate in CCSM4. *Journal of Climate*, **25**, 2652–2675, doi:10.1175/JCLI-D-11-00302.1.

Welch, B. L., 1947: The generalization of `Student's' problem when several different population variances are involved. *Biometrika*, **34**, 28–35, doi:10.1093/biomet/34.1-2.28.

Whitworth, T., 1983: Monitoring the Transport of the Antarctic Circumpolar Current at Drake Passage. *Journal of Physical Oceanography*, **13**, 2045–2057, doi:10.1175/1520-0485(1983)013<2045:MTTOTA>2.0.CO;2.

Wyrwoll, K.-H., B. Dong, and P. Valdes, 2000: On the position of southern hemisphere westerlies at the Last Glacial Maximum: an outline of AGCM simulation results and evaluation of their implications. *Quaternary Science Reviews*, **19**, 881–898, doi:10.1016/S0277-3791(99)00047-5.

Zahn, R., 2009: Climate change: Beyond the CO(2) connection. *Nature*, **460**, 335–336, doi:10.1038/460335a.

Zahn, R., J. Lutjeharms, A. Biastoch, I. Hall, G. Knorr, W. Park, and C. Reason, 2010: Investigating the Global Impacts of the Agulhas Current. *Eos, Transactions American Geophysical Union*, **91**, 109, doi:10.1029/2010EO120001.

Zalesak, S. T., 1979: Fully multidimensional flux corrected transport algorithms for fluids. *Journal of Computational Physics*, **31**, 335–362.

Zhai, X., and R. J. Greatbatch, 2007: Wind work in a model of the northwest Atlantic Ocean. *Geophysical Research Letters*, **34**, L04606, doi:10.1029/2006GL028907.

Zhai, X., H. L. Johnson, D. P. Marshall, and C. Wunsch, 2012: On the Wind Power Input to the Ocean General Circulation. *Journal of Physical Oceanography*, **42**, 1357–1365, doi:10.1175/JPO-D-12-09.1.

Zhang, D., R. Msadek, M. J. McPhaden, and T. Delworth, 2011: Multidecadal variability of the North Brazil Current and its connection to the Atlantic meridional overturning circulation. *Journal of Geophysical Research*, **116**, 1–9, doi:10.1029/2010JC006812.

Zharkov, V., and D. Nof, 2008: Agulhas ring injection into the South Atlantic during glacials and interglacials. *Ocean Science*, **4**, 223–237, doi:10.5194/os-4-223-2008.

# Reflections and Acknowledgements

*There is a time for everything,*
*and a season for every activity under the heavens:*

*…, a time to plant and a time to uproot,*
*…, a time to tear down and a time to build,*
*a time to weep and a time to laugh,*
*a time to mourn and a time to dance,*
*a time to scatter stones and a time to gather them,*
*…, a time to search and a time to give up,*
*a time to keep and a time to throw away,*
*…, a time to love and a time to hate,*
*a time for war and a time for peace.*

*What do workers gain from their toil?*

These wise words, excerpted from Ecc. 3:1–9, perfectly summarise my journey over the last three and half years. At the beginning, the foundations needed to be laid; sifting through the wealth of information, it was time to plant, build and search. Preconceived ideas and assumptions needed to be uprooted, torn down, and new concepts and hypotheses were put in place, ready to be investigated. The time spent constructing the machinery necessary to generate the data can be best described as a brawl between 'weeping and laughing', a tango between 'mourning and dancing'. Pass the jubilation of having gotten the machinery well-oiled and ready for production, the enormous dataset that was produced required thoughtful 'keep and throw away' (archive). Hours and hours spent thinking and digesting the vast amount of information produced … if only my couch had lips, if only my kettle could relate! What helped was to scatter the stones – dozens of graphs, charts, illustrations – and with the insightful and cheerful guidance of my advisor, gather them coherently, discarding the irrelevant. Making sense of it all, coming up with a premise, an opinion, making a stand and defending it … what a journey it's been! Giving up was never an option – Yes, the journey has redefined what it meant to 'love and hate' something at the same time; it showed what war of the mind and inner peace meant. The result of my toil – oh yes, a toil it was indeed – is this dissertation. The gain from it: clarity and understanding, furtherance and satisfaction, … and the privilege of being conferred a doctorate.

My heartfelt gratitude goes to my advisor, Arne Biastoch, whose steadfast support and guidance during the last three and half years have been essential. Arne, many thanks for having an open-door policy and for the readiness to listen to and discuss ideas. It has been a great honour and pleasure to work under your tutelage. Furthermore, I would like to acknowledge the entire Theory and Modelling group of GEOMAR. I benefited greatly from the experience within the group, especially while building the ORCA05 and INALT01 model configurations.

A note on the origin of the name 'INALT' is certainly warranted. When the global-nested configuration was established, I wanted to baptise it with a name that was at the same time meaningful and catchy. While brainstorming, I came across the word 'inaliti' in isiXhosa (2nd most common spoken language in South Africa), meaning 'needle'. That was very appropriate since 'Agulhas' is Portuguese for 'needles'. Dropping the last two i's, the name INALT emerged. Coincidentally, INALT can also be read as simply meaning INdian-AtLanTic, to designate its nested domain. The appended suffix, 01, refers to the horizontal resolution of the nest, 0.1 degree. And that's the story behind the name!

This work received funding from the European Community's Seventh Framework Programme FP7/2007-2013-Marie-Curie ITN, under grant agreement n°238512, GATEWAYS project. Being part of the GATEWAYS community was a privilege. The collaboration, exposure, collegial conversations, and intellectual network it fostered were paramount to the construction of this thesis. I particularly thank Ben Loveday of the University of Cape Town for making model data from AGIO and ARC available. Moreover, I acknowledge the exchange with the co-authors of the publications that resulted from the work presented in this dissertation.

Constructive comments obtained on drafts of this dissertation will not go without a note of appreciation. Dad, Isabelle, Severin, Erik, and Arne – thank you for providing a fresh pair of eyes and critically assessing my proses; Severin, Patrick and Erik for the German translation of the abstract. Finally, Figure 1.1 was meticulously produced by Markus.

September 2013.